DEF6 Aggregation is Linked to Active Translation and mRNA Turnover in T Cells

By

Kerry Louise Remon BSc

Thesis submitted to The University of Nottingham for the degree of Doctor of Philosophy

September 2016

Acknowledgements

I would like to begin by thanking my supervisors Professor Fred Sablitzky and Dr Peter Jones. Thank you both for your technical knowledge, guidance and support and for always having an open door. A special thanks to Fred for genuinely caring and motivating me to complete this thesis, you never doubted I could do it.

Thank you to the other members of the Sablitzky and Jones labs, including Tamil, Maha, Deniz, Tao, Chen, Eleanor and Maria for the help along the way and the friendship.

Thanks to Hannah and Ruth, both of which will have completed their theses with me, and I am grateful that we have shared this experience together and have become friends.

Finally, to my family I am extremely grateful for their patience and support, particularly my husband Guy and my mum, and I thank them for all their help throughout my PhD.

Abstract

Spatiotemporal responses to extracellular signals have been documented in a wide variety of cells, such as neuronal synapses, cytotoxic T lymphocytes, germ cells and during embryo development. Selective release of a key molecule allows a cell to respond at a given moment, and cells ensure that the response can be initiated instantly by pre-producing and packaging the molecule, often storing the molecule as a granule. Differentially Expressed in FDCP6 is a guanine nucleotide exchange factor, primarily expressed in T cells, which has been previously shown to form cytoplasmic aggregates when phosphorylated by ITK. DEF6 also translocates to the immunological synapse following phosphorylation by LCK in response to antigenic presentation. As a result, DEF6 is a likely candidate in mediating a spatiotemporal response to an extracellular signal in T cells. Data presented in this work suggest that endogenous DEF6 forms cytoplasmic granules in a variety of T cell states and the DEF6 mutant Y210EY222E, which mimics ITK phosphorylation, interacts with mRNA. Moreover, DEF6 is hypothesised to have two unconventional RNA binding domains; a feature which has also been described in the literature within proteins that catalyse glycolysis. DEF6 is also shown to be in close proximity to PABP and eIF4E, both of which are translation factors, as well as active translation in resting Jurkat T cells and the immunological synapse. Furthermore, endogenous DEF6 co-localises with 4E-T, a P-body marker which is involved with miRNA mediated decay, in resting and stressed Jurkat T cells. These data corroborate that of Hey et al. (2012) and suggests that DEF6 does indeed interact with P-bodies. Finally, translocation of DEF6 appears to occur in response to an extracellular signal alternative to the T cell receptor during T-T communication and that the translocation may occur in vesicle-like structures in close proximity to LFA-1. Consequently, these data identify a novel link between DEF6 and active translation as well as mRNA turnover and that the extracellular signal required for this spatial response is not antigen presenting cell specific but rather a response to LFA-1 stimulation.

Abbreviations

4E-T	Transporter of eIF4E
mAb	Monoclonal Antibody
ABCE1	ATP Binding Cassette Subfamily E Member 1
Ago	Argonaute Protein
APC	Antigen Presenting Cell
APS	Ammonium Persulphate
ARE	AU-Rich Element
ARP 2/3	Actin-Related Protein 2/3 complex
BSA	Bovine Serum Albumin
CCR4	C-C Chemokine Receptor 4
CCR4-NOT	CCR4-NOT complex
Cdc42	Cell Division Control Protein 42 homolog
CTL	Cytotoxic T Lymphocyte
DAG	Diacylglycerol
DAPI	4’,6 Diamidino-2-Phenylindole Dihydrochloride
DCP1	Decapping Enzyme 1
DCP2	Decapping Enzyme 2
DDX6	DEAD Box Helicase 6
DEF6	Differentially Expressed in FDCP6
DEPC	Diethylpyrocarbonate
DH	Dbl Homology Domain
DHL	Dbl Homology-Like Domain
DMEM	Dulbecco’s Modified Eagle’s Medium
DMSO	Dimethyl Sulfoxide

DSH	DEF6/SWAP70 Homology Like Domain
dsRED	*Discosoma species* Red Fluorescent Protein
EAE	Experimental Autoimmune Encephalitis
ECL	Enhanced Chemiluminescence
EDTA	Ethylenediaminetetraacetic acid
eIF	Eukaryotic Initiation Factor
eRF	Eukaryotic Release Factor
F-actin	Filamentous Actin
FBS	Foetal Bovine Serum
FISH	Fluorescent In Situ Hybridisation
FMRP	Fragile X Mental Retardation Protein
FRAP	Fluorescence Recovery After Photobleaching
GEF	Guanine nucleotide Exchange Factor
GFP	Green Fluorescent Protein
GST	Glutathione S-Transferase
GTPase	Guanosine Triphosphate Hydrolase
HS1	Haematopoietic-cell-Specific Protein 1
IBP	IRF4 Binding Protein (alternative name for DEF6)
ICAM-1	Intercellular Adhesion Molecule-1
InsP3	Inositol 3, 4, 5 Triphosphate
IP_3	Inositol Triphosphate
IP_3R_1	IP_3 Receptor 1
IRF4	Interferon Regulatory Factor 4
IS	Immunological Synapse
ITAM	Immunoreceptor Tyrosine-based Activation Motif

ITK	Interleukin-2 Inducible T cell Kinase
LAT	Linker for Activation of T cells
LC	Low Complexity Sequence
LCK	Lymphocyte-specific Protein Tyrosine Kinase
LFA-1	Lymphocyte Function Associated Antigen-1
mGluR	Metabotropic Glutamate Receptors
MHC	Major Histocompatibility Complex
mRNA	Messenger RNA
miRNA	Micro RNA
mRNP	Messenger Ribonuclear Proteins
pMHC	Epitope Presenting MHC
NCK	Non-Catalytic Region of Tyrosine Kinase
NES	Nuclear Export Signal
$NFAT_{c1/2}$	Nuclear Factor of Activated T cells
NK	Natural Killer cells
NKT	Natural Killer T cells
NLS	Nuclear Localisation Signal
NMD	Nonsense-Mediated mRNA Decay
PABP	Poly(A) Binding Protein
PATL1	PAT 1 Homolog 1
P-body	Processing Body
PBS	Phosphate Buffered Saline
PBST	Phosphate Buffered Saline with Tween-20
PFA	Paraformaldehyde
PH	Pleckstrin Homology Domain

PIP_3	Phophatidylinositol 3, 4, 5, Triphosphate
PLCγ1	Phospholipase Cγ1
PLCθ	Phospholipase Cθ
PMA	Phorbol Myristate Acetate
PMSF	Phenylmethylsulfonyl fluoride
PVDF	Polyvinylidene fluoride
eQTL	Cis-expression Quantitative Trait Loci
Rac1	Ras-Related C3 Botulinum Toxin Substrate 1
RASGRP	RAS Guanyl Releasing Protein
RISC	RNA-Induced Silencing Complex
ROCK	Rho Associated Protein Kinase
RPMI	Roswell Park Memorial Institute medium
RRM	RNA Recognition Motif
SDS	Sodium Dodecyl Sulphate
SDS-PAGE	Sodium Dodecyl Sulphate Polyacrylamide Gel Electrophoresis
SEA/B	*Staphylococcus aureus* enterotoxin A and B
SLAT	SWAP-70 Like Adapter of T cells (alternative name for DEF6)
SLE	Systemic Lupus Erythematous
SLP76	SRC homology-2 domain containing Leukocyte Protein of 76kDa
SMAC	Supramolecular Activation Cluster
cSMAC	Central Supramolecular Activation Cluster
dSMAC	Distal Supramolecular Activation Cluster
pSMAC	Peripheral Supramolecular Activation Cluster
SNP	Single Nucleotide Polymorphism

SSC	Saline Sodium Citrate
SWAP70	Switch-Associated Protein-70
TBS	Tris Buffered Saline
TBST	Tris Buffered Saline with Tween-20
TCR	T Cell Receptor
TEMED	Tetramethylethylenediamine
TIA-1	T-cell restricted Intracellular Antigen 1
TIA-R	TIA-1 Related protein
TGFβ1	Transforming Growth Factor β1
tRNA	Transfer RNA
VEGFA	Vascular Endothelial Growth Factor A
WASP	Wiskott–Aldrich Syndrome Protein
WAVE2	WASP-family Verprolin-homologous Protein-2
XRN1	5'-3' Exoribonuclease 1
YFP	Yellow Fluorescent Protein
ZAP-70	ζ-chain associated protein of 70kDa

List of Contents

List of Figures

List of Tables

Chapter 1 Introduction

1.1 Role of DEF6 in the Signal Transduction Cascade and Cytoskeletal Remodelling

1.1.1 T Cell Signalling in Response to Antigen Presentation

Signal propagation in T cells is a highly controlled event. The number of self-antigens greatly exceeds those of non-self-antigens therefore a T cell must be regulated to prevent an inappropriate response to a self-antigen. A T cell is highly motile and during 'scanning' of Antigen Presenting Cells (APC) it will encounter and assess several APCs per minute (Friedl and Gunzer, 2001). Each APC expresses MHC molecules which present processed peptides (pMHC), from antigens, to T cells. The motile T cell has a leading edge rich in invadosome-like protrusions containing filamentous actin (F-actin) and T Cell Receptors (TCR) which are able to probe APCs and facilitate TCR-pMHC contact for a short period of time (Sage et al., 2012). The motile T cell engages the APC if the TCR and pMHC are sufficiently complementary and are able to bind with a high affinity.

Sustained TCR signalling requires the T cell to reduce its motility by adhering to the APC. This is achieved using integrin based adhesion between lymphocyte function associated antigen-1 (LFA-1), expressed on the T cell, and intercellular adhesion molecule-1 (ICAM-1) which is primarily expressed on the APC (Stewart et al., 1996). Dustin and Springer (1989) demonstrated that LFA-1 adhesion occurs after the initial TCR-pMHC recognition. Moreover, LFA-1 increases the sensitivity of the TCR for pMHC resulting in a 100-fold decrease in the amount of antigen required (Bachmann et al., 1997). During scanning of APCs the T cell may encounter a presented epitope from the

same antigen expressed by multiple APCs. This pMHC may induce weak association with the TCR and the T cell may form a semi-motile synapse termed a kinapse (Dustin, 2008). A T cell is able to induce its tolerance to prevent an inappropriate response to a self-antigen or a frequent antigen (Zehn and Bevan, 2006). However, a rare or weak self-antigen may induce a response due to failure of tolerance induction and is speculated to result in autoimmunity (Dustin, 2009).

Figure 1.1-1 depicts the TCR signal cascade in response to the presentation of an epitope by a MHC II receptor. Specifically in terms of DEF6 activation, LCK is activated following CD4 co-receptor stabilisation of the TCR-pMHC II complex. LCK phosphorylates DEF6 at amino acid residues Y133 and Y144 which results in DEF6 activation (Becart et al., 2008a). DEF6 catalyses the GDP-GTP exchange for Cdc42 as well facilitating Vav1 in the activation of Rac1 resulting in the release of intracellular calcium (Tybulewicz and Henderson, 2009). An increase in intracellular calcium results in the activation of $NFAT_{c1/2}$ which translocates to the nucleus and promotes T cell activation and proliferation (Becart et al., 2007). Furthermore, the activation of Cdc42 and Rac1 results in the production of F-actin at the immunological synapse (IS) which forms filopodia and lamellipodia at the leading edge, increasing the surface area of the IS and stabilising the interaction between the T cell and APC (Billadeau et al., 2007).

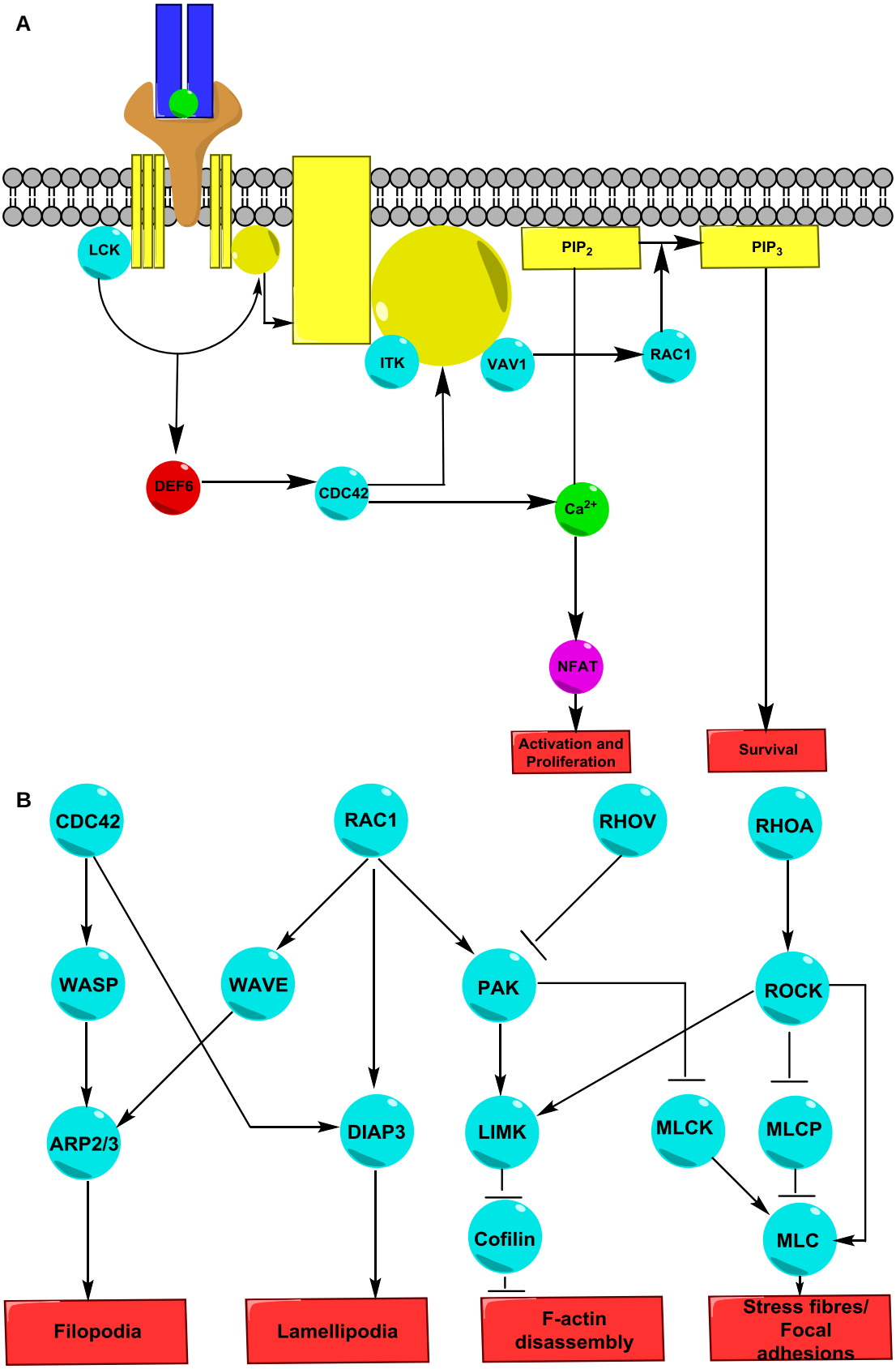
A
LCK
PIP2
PIP3
ITK
VAV1
RAC1
DEF6
CDC42
Ca2+
NFAT
Activation and Proliferation
Survival
B
CDC42
RAC1
RHOV
RHOA
WASP
WAVE
PAK
ROCK
ARP2/3
DIAP3
LIMK
MLCK
MLCP
Cofilin
MLC
Filopodia
Lamellipodia
F-actin disassembly
Stress fibres/ Focal adhesions

Figure 1.1-1 **A** - Signal transduction from the T cell receptor. Following the presentation of the epitope by the APC, the TCR-MHC II complex is stabilised by the co-receptor CD4. This activates LCK which phosphorylates tyrosine residues within the ITAM of the CD3 tails, amplifying the signal transduction. This leads to the activation of ζ-chain associated protein of 70kDa (ZAP-70) which phosphorylates and activates Linker for Activation of T cells (LAT) resulting in the recruitment of SRC homology-2 domain containing Leukocyte Protein of 76kDa (SLP76). Together, LAT and SLP76 provide a scaffold for the recruitment of Phospholipase Cγ1 (PLCγ1), Non catalytic region of tyrosine kinase (NCK) and ITK which recruits Vav1 (Billadeau et al., 2007). The recruitment and activation of PLCγ1 results in the hydrolysis of Phosphatidylinositol 4,5 bisphosphate to produce Inositol 3,4,5 triphosphate (InsP3) and Diacylglycerol (DAG). InsP3 production results in the release of intracellular calcium from the Endoplasmic Reticulum which activates Nuclear Factor of Activated T cells (NFAT) and results in the translocation of NFAT to the nucleus. DAG activates RAS Guanyl Releasing Protein (RASGRP) which activates RAS. RAS goes on to induce the RAF, MAPK/ERK Kinase and Extracellular Signal-Regulated Kinase cascade. DAG also activates Protein Kinase C θ which activates Nuclear Factor κβ. Activation of the above described transcription factors and cascade, promote activation and proliferation of the T cell. Activation of AKT by Phosphatidylinositol 3,4,5 triphosphate leads to the inhibition of the transcription factor Forkhead Box 01 promoting T cell survival along with NFκβ.
B – The regulation of F-actin polymerisation downstream of DEF6 and Vav1 activation. Cdc42 activates the Wiskott-Aldrich Syndrome Protein which associates with Actin-Related Protein 2/3 complex. Rac1 activates WASP-family verprolin homologous protein-2 (WAVE2 complex) which activates ARP2/3. ARP2/3 goes on to catalyse actin polymerisation. RhoA mediates Myosin Light Chain II formation by activating Rho Associated Coiled-coil containing protein Kinase. ROCK inhibits Myosin Light Chain Phosphatase and activates Lim Motif containing Kinase. Together, the inhibition of MLCP and Cofilin by LIMK results in MLC II formation catalysed by Myosin Light Chain Kinase. Cdc42 and Rac1 inhibit MLCK by activating p21 Activated Kinases indicating that Cdc42 and Rac1 oppose RhoA mediated MLC II formation. Adapted from Tybulewicz and Henderson (2009).

T cell activation requires rapid actin polymerisation and microtubule nucleation to form the IS and maintain TCR-pMHC signalling as described below. The induction of actin polymerisation occurs after the initial TCR-pMHC contact during APC scanning (Billadeau et al., 2007). In fact, signalling molecules in the TCR signal transduction cascade facilitate the catalysis of F-actin polymerisation. This allows the initial propagation of the TCR signal to feedback and result in the formation of the IS which maintains continued TCR-pMHC signalling and increases the T cell-APC contact area. The main proteins involved during this process include, but are not limited to: Vav1; Rac1; Cdc42; WASP-family verprolin-homologous protein-2 (WAVE2) complex; Actin-Related Protein 2/3 complex (ARP 2/3); Wiskott–Aldrich syndrome protein (WASP); Haematopoietic-cell-Specific Protein-1 (HS1) and Cofilin (Billadeau et al., 2007).

Current literature attributes the majority of Rac1 activation during T cell activation to Vav1, a GEF which catalyses the GDP-GTP exchange for Rac1 and Cdc42 (Tybulewicz, 2005; Billadeau et al., 2007; Tybulewicz and Henderson, 2009). Rac1 catalyses F-actin polymerisation via the WAVE2 complex which regulates and activates the ARP2/3 complex as shown in figure 1.1-1B (Nolz et al., 2006).

Cdc42 is another Rho family GTPase which has an important role in F-actin polymerisation: the activation of Cdc42 by Vav1 results in Cdc42 binding to WASP preventing the auto-inhibition of WASP to continue so that it can associate with ARP2/3 and catalyse F-actin polymerisation (Zeng et al., 2003). Again, current literature suggests that Vav1 is the main activator of Cdc42 during the process of F-actin polymerisation after TCR-pMHC recognition (Tybulewicz, 2005; Billadeau et al., 2007; Tybulewicz and Henderson, 2009). HS1 is activated by LCK and ZAP-70 which phosphorylate tyrosine residues resulting in the binding of HS1 to ARP2/3 and promoting stability of F-actin polymerisation (Gomez et al., 2006).

Although Vav1 is primarily attributed to Cdc42 and Rac1 activation, DEF6 is also able to catalyse the GDP-GTP exchange for Cdc42 and Rac1 (Mavrakis et al., 2004; Gupta et al., 2003a). As shown in figure 1.1-1B, the activation of Rac1 and Cdc42 will result in F-actin polymerisation via WAVE and WASP respectively. Therefore, activation of Rac1 and Cdc42 by DEF6 also results in the formation of lamellipodia and filopodia respectively (Mavrakis et al., 2004).

Furthermore, Fanzo et al. (2006) demonstrated that DEF6-deficient T cells resulted in a reduction in F-actin polymerisation and lamellipodia formation. The stabilisation and maturation of the IS was rescued following the introduction of constitutively activated Rac1 (Fanzo et al., 2006). This demonstrates that DEF6 also has an important role in the regulation of F-actin polymerisation.

As shown in figure 1.1-1A, NFAT is an important transcription factor activated following TCR-MHC II engagement resulting in differentiation and proliferation of the T cells. Becart et al. (2007) demonstrated that DEF6 is required for $NFAT_{c1/2}$ nuclear translocation due to the requirement for Cdc42 mediated intracellular calcium mobilisation. DEF6-deficient mice resulted in a reduction of Cdc42 dependent intracellular calcium release as the activation of Cdc42 requires DEF6 to catalyse the GDP-GTP exchange. This was quickly followed by the demonstration of the dependence of $NFAT_{c1/2}$ activation upon DEF6 translocation to the IS during T cell activation. The activation of $NFAT_{c1/2}$ was shown to require LCK phosphorylation of DEF6 at tyrosine residues 133 and 144. Furthermore, constitutively activated DEF6 (Y133-144D mutants) could not induce $NFAT_{c1/2}$ nuclear translocation alone, TCR stimulation was still required (Becart et al., 2008a). Nuclear translocation of $NFAT_{c1/2}$ is important during T cell activation as it results in proliferation and Interleukin-2 production which is impaired in DEF6 knockout mice. As a result, DEF6-deficient mice were unable to mount sufficient Th_2 or Th_1 cell responses and had a reduced number of peripheral T cells due to an arrest in T cell development at the double negative stage (Becart et al., 2007).

Due to the complex requirement of actin polymerisation and contractile activity, DEF6 may play a larger role in the cytoskeletal reorganisation following T cell-APC contact than is suggested by the current literature. DEF6 catalyses the GDP-GTP exchange for Rac1, RhoA and Cdc42 and although Rac1 and RhoA have opposing cellular responses, the activation of RhoA may be implicated in the enhancement of F-actin flow by contractile activity via myosin light chain II contraction. Polymerisation of myosin light chain II is induced via the ROCK pathway which is activated by RhoA as depicted by figure 1.1-1B.

1.1.2 Formation and Maintenance of the Immunological Synapse

The IS is a complex structure consisting of F-actin, microtubules and TCR associated signalling molecules. Although schematic representations give the impression of a single TCR engaging a single pMHC there are multiple TCR-pMHC complexes which are formed and recycled to maintain the propagated signal until the response is completed (Valitutti et al., 1995). The movement of TCR microclusters, complexes consisting of the T cell receptor, CD3 and associated signalling proteins, is achieved due to the centripetal flow of F-actin from the distal Supramolecular Activation Cluster (dSMAC) to the peripheral SMAC (pSMAC) as shown in figure 1.1-2 (Kaizuka et al., 2007). It is suggested that the polymerisation, depolymerisation and recycling of F-actin towards the central SMAC (cSMAC) creates a mechanical force which will be exerted on the TCR-pMHC complexes and cause disassociation if the force exceeds the affinity of the TCR for the pMHC (Kim et al., 2012). As a result, it is believed that the flow of F-actin and the resulting mechanical force provides another regulatory mechanism to reduce the risk of T cells propagating a response to self-antigens.

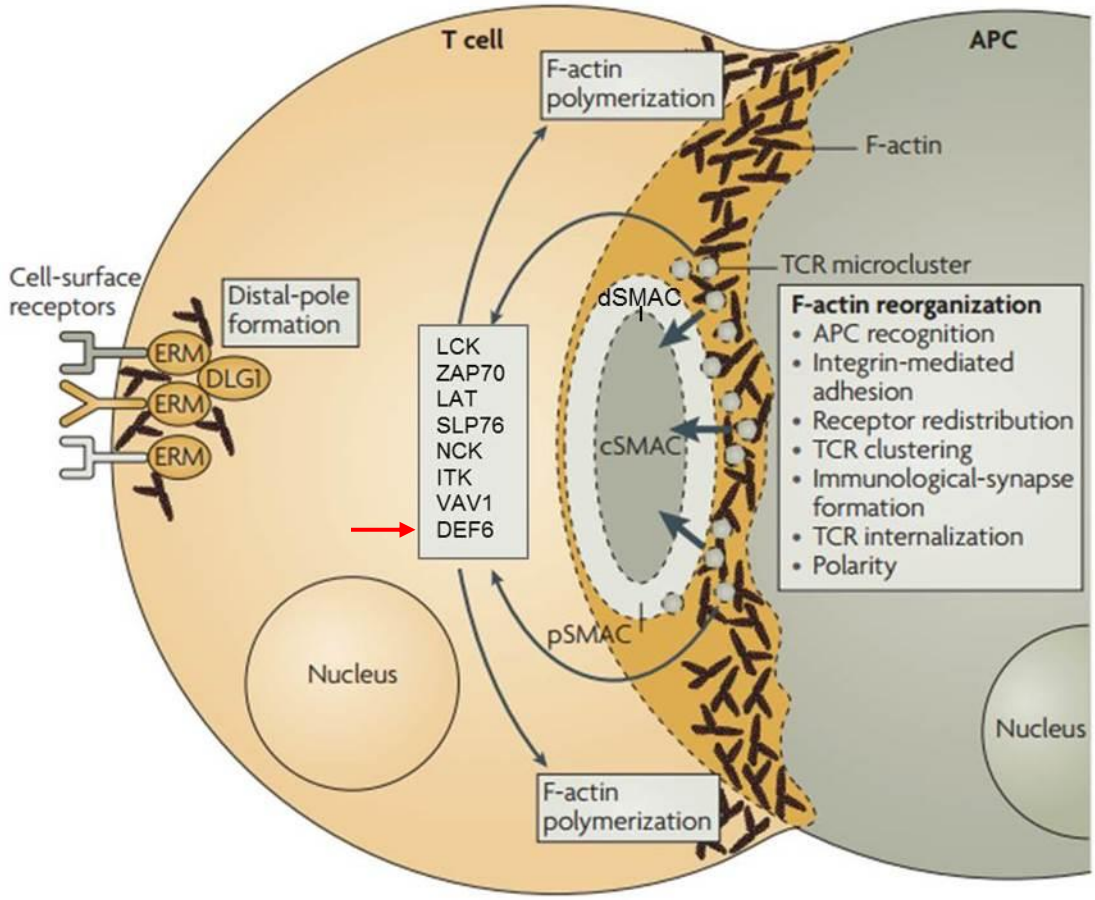

Figure 1.1-2 Formation of the immunological synapse between the T cell and the antigen presenting cell. Following initial TCR-pMHC recognition, binding is enhanced via LFA-1 and ICAM-1 association in the area immediately surrounding the central Supramolecular Activation Cluster. The polymerisation of F-actin increases TCR-APC contact due to the formation of lamellipodia in the distal SMAC. Signalling is maintained via TCR microclusters that translocate from the dSMAC to the peripheral SMAC due to centripetal flow of F-actin and myosin light chain II contraction indicated by the large arrows. The TCR are recycled once they reach the cSMAC via internalisation. The signalling molecules depicted are involved in the polymerisation of F-actin following TCR-pMHC recognition. Finally, formation of the immunological synapse results in distal polarity where the distal pole expresses receptors that are believed to be involved in the negative regulation of T cell activation and may cause signalling to end once the response has been completed. Adapted from Billadeau et al. (2007) with addition of the dSMAC and the substitution of IBP for DEF6 to maintain nomenclature.

As shown in figure 1.1-2, the dSMAC is an actin rich region of the IS where the TCR microclusters form and continue to signal during their translocation to the pSMAC. The pSMAC is rich in actomyosin and is a highly contractile region surrounding the cSMAC. The cSMAC is actin depleted but facilitates adhesion to the APC due to the ring of LFA-1 which encircles the cSMAC. The translocation of TCR microclusters is believed to be enhanced by the contractile activity of the pSMAC which may suggest that myosin light chain II contraction enhances the effect of the centripetal flow of F-actin (Yi et al., 2012).

1.2 Structure and Function of Differentially Expressed in FDCP 6 (DEF6)

1.2.1 Identification and Characterisation of DEF6

Differentially expressed in FDCP6 (DEF6) is a Rho family Guanine nucleotide Exchange Factor (GEF) primarily expressed in T cells. Switch-Associated Protein-70 (SWAP-70), a protein primarily expressed by B cells, is also a Rho family GEF but it is associated with B cell class switching (Masat et al., 2000). The expression of Def6 was first identified in mouse haematopoietic tissues (Hotfilder et al., 1999). The gene was identified as its expression was down regulated during the differentiation of FDCP-mix A4 cells towards the myeloid cell lineages (Hotfilder et al., 1999). DEF6 is also known as IRF4 Binding Protein (IBP) (Gupta et al., 2003a) and SWAP-70 Like Adapter of T cells (SLAT) (Tanaka et al., 2003) by the respective groups but shall be referred to as DEF6 throughout this work. The human DEF6 protein was identified using a human lymph node cDNA library during a screen for proteins which bind IRF4. The full ~2.3kb cDNA was isolated and translated to produce a 631 amino acid protein with a molecular weight of ~74kDa (Gupta et al., 2003b). The Altman group also investigated DEF6 cDNA isolated from transgenic mouse Th_2 cells expressing an AD10 T Cell Receptor (TCR) and the expression of DEF6 was described as being elevated in Th_2 cells in comparison to Th_1 cells. DEF6 was also shown to be expressed in human peripheral T cells, Jurkats, an established Th_2 cell clone and THP-1 cells (Tanaka et al., 2003).

1.2.2 DEF6 is a Guanine nucleotide Exchange Factor

DEF6 and SWAP-70 are members of the Dbl family of GEFs. DEF6 and SWAP-70 are 45% homologous and have a 65% similarity (Gupta et al., 2003b). Both proteins are proposed to consist of two calcium binding EF hands, a DEF6/SWAP70 Homology Domain (DSH), a Pleckstrin Homology (PH) domain and a Dbl-Homology Like domain (DHL) as shown in figure 1.2-1 (Gupta et al., 2003b; Mavrakis et al., 2004).

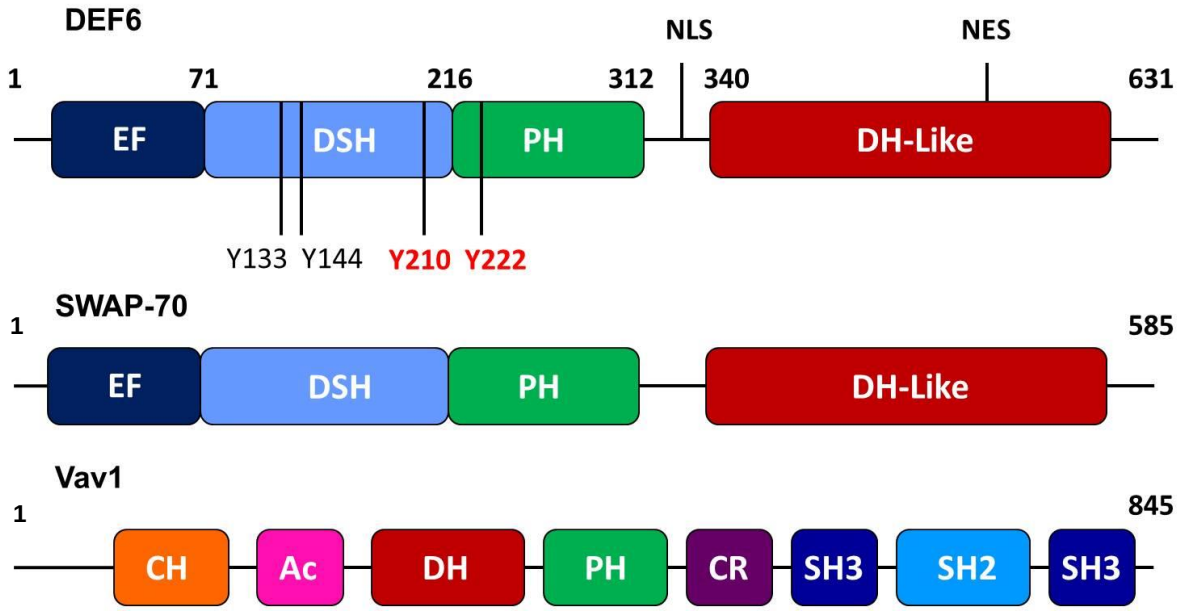

Figure 1.2-1 Schematic diagram comparing the domain structure of human DEF6 to SWAP-70 and Vav1. DEF6, SWAP-70 and Vav1 are Dbl family GEFs that all contain a Dbl Homology domain which catalyses the GDP-GTP exchange for GTPases. However, DEF6 and SWAP-70 have a structure which differs from the typical Dbl family GEF as the Dbl Homology domain is flanked at its N terminus by the Pleckstrin Homology domain rather than at its C terminus as depicted for Vav1. Abbreviations: EF – EF hand; DSH – DEF6/SWAP70 Homology domain; PH – Pleckstrin Homology domain; DH-like – Dbl Homology-like domain, CH – Calponin Homology domain; Ac – Acidic motif; DH - Dbl Homology domain; CR – Cysteine-rich Zinc finger; SH3 – SRC Homology 3 domain; SH2 – SRC Homology 2 domain; Y – tyrosine residue, black indicative of LCK phosphorylation and red indicative of ITK phosphorylation. Adapted from Hey (2011).

A ^{45}Ca overlay assay described by Fos et al. (2014) suggests that a GST-EF-ITAM fusion protein binds calcium and that deletion of the proposed calcium binding motifs at amino acid residues 19-30 and 57-68 substantially reduces binding of calcium. However, the ^{45}Ca signal bound to Calmodulin is substantially higher than the GST-EF-ITAM fusion protein even though the amount of Calmodulin present is substantially lower than the amount of GST-EF-ITAM protein. Moreover, the ^{45}Ca signal attributed to calcium bound by GST-EF-ITAM fusion proteins and their deletion mutants is not convincing. As a result, it has still not been confirmed that DEF6 consists of two EF hands at the N terminus, although the proposed function appears possible as the two potential EF hands show a 63% and 68% similarity with the EF hand consensus sequence (Mavrakis et al., 2004). The amino acids required for calcium binding described by the consensus sequence are substituted for polar, non-charged amino acids which decrease the affinity of the potential EF hands for calcium binding suggesting an alternative function for the N-terminus of DEF6 which shall be discussed in chapter 3.4.

Moreover, DEF6 and SWAP-70 differ from the typical Dbl family GEF, such as Vav1, as shown in Figure 1.2-1. The DH domain is typically flanked at the C-terminus by the PH domain as shown by the schematic representation of Vav1 (Tybulewicz, 2005). The DH domain catalyses the GDP-GTP exchange for Rho family GTPases and is shown to be flanked at the N-terminus by the PH domain for DEF6 and SWAP-70 suggesting another potential role for the DH domain which may require a position at the C terminus (Mavrakis et al., 2004; Masat et al., 2000).

The function of the DSH domain is not currently understood but it is present in DEF6 and SWAP70. The DSH domain contains an Immunoreceptor Tyrosine-based Activation Motif (ITAM) like region in the case of DEF6 and is the primary site of tyrosine phosphorylation (Becart et al., 2008a). LCK phosphorylates tyrosine residues 133 and 144 whereas ITK phosphorylates tyrosine residues 210 and 222 (Becart et al., 2008a; Hey et al., 2012) The PH domain binds phosphatidylinositols, including phosphatidylinositol 3,4,5 triphosphate, but the requirement for this binding for the function of DEF6 has not been fully confirmed (Gupta et al., 2003a). DEF6 also contains a Nuclear Localisation Signal (NLS) and a Nuclear Export Signal (NES) suggesting the ability of DEF6 to have a cytosolic and/or nuclear location.

Fos et al. (2014) have recently suggested that the EF hand domain and the PH domain of DEF6 directly and independently associate with IP_3 receptor 1, specifically amino acid residues 366-441, and simultaneous deletion of both domains significantly affects NFAT activation in Jurkat TAg cells which may reduce activation and proliferation. Moreover, DEF6 association with IP_3R_1 in the presence of $CaCl_2$ is independent of CD3 stimulation, using anti-CD3, and chelation of Ca^{2+}, using EGTA, is suggested to reduce DEF6 and IP_3R_1 association indicating a potential link between calcium binding and IP_3R_1 association (Fos et al., 2014).

1.3 Post-transcriptional Regulation of mRNA

1.3.1 Translation Initiation

Translation begins with the formation of the eukaryotic initiation factor 2 (eIF2) ternary complex which consists of: eIF2, a trimer of eIF2α, eIF2β and eIF2γ; Methionine associated initiator tRNA (Met-$tRNA_i^{Met}$) which recognises the AUG start codon; and GTP as depicted in figure 1.3-1. Next, the 40S ribosomal subunit is formed and consists of: eIF1; eIF1A; and eIF3. The 40S subunit associates with the eIF2 ternary complex to form the 43 pre-initiation complex. The mRNA is then activated by eIF4F; a trimer of eIF4A, eIF4E and eIF4G; and eIF4B which bind the mRNA cap and unwind the mRNA by hydrolysing ATP to form ADP and phosphate. The 43S pre-initiation complex then binds the activated mRNA and begins 5'-3' scanning of the mRNA. Once the Met associated initiator tRNA anti-codon reaches the AUG start codon, the AUG start codon is recognised and eIF2 hydrolyses GTP leading to the release of phosphate. This results in the formation of the 48S complex which changes to the closed conformation preventing further scanning. The closed conformation causes displacement of eIF1 and allows eIF5 mediated hydrolysis of GTP to produce GDP and phosphate which drives the association of the 48S and 60S ribosomal subunits. EIF5 then mediates the displacement of eIF2-GDP, eIF1, eIF3, eIF4B, eIF4F and eIF5. Hydrolysis of GTP by eIF5B results in the displacement of eIF1A and eIF5B-GDP with the release of phosphate to form the competent 80S ribosome.

Synthesis of the polypeptide occurs during elongation and termination and the termination complex ribosome is recycled by the displacement of eRF1 and eRF3 by eIF1, eIF1A, eIF3 and ABCE1 causing dissociation of the 60S and 40S subunits and the release of tRNA and mRNA (Jackson et al., 2010).

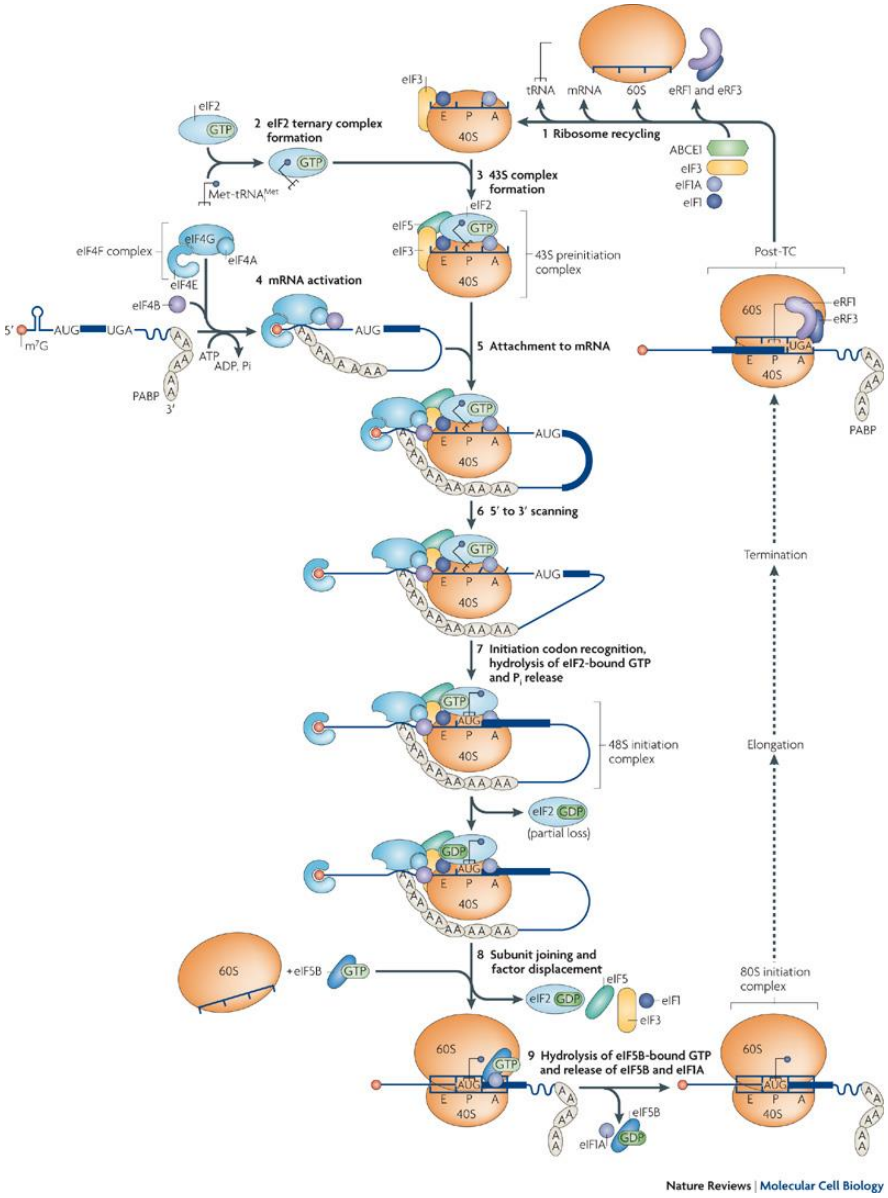

Figure 1.3-1 The canonical cap-dependent pathway of eukaryotic translation initiation. Translation initiation begins with the formation of the eIF2 ternary complex (2). The 40S ribosomal subunit is formed and associates with the eIF2 ternary complex to form the 43 pre-initiation complex (3). EIF4F and eIF4B bind the mRNA cap and activate the mRNA (4). The 43S pre-initiation complex then binds the activated mRNA and begins 5'-3' scanning of the mRNA (6). Recognition of the AUG start codon leads to eIF2 mediated GTP hydrolysis resulting in the formation of the 48S complex (7). The closed conformation causes displacement of eIF1 and allows eIF5 mediated association of the 48S and 60S ribosomal subunits. EIF5 then mediates the displacement of eIF2-GDP, eIF1, eIF3, eIF4B, eIF4F and eIF5 (8). Hydrolysis of GTP by eIF5B results in the displacement of eIF1A and eIF5B-GDP to form the competent 80S ribosome (9). Protein synthesis occurs during elongation and termination and the termination complex ribosome is recycled causing dissociation of the 60S and 40S subunits and the release of tRNA and mRNA (1) (Jackson et al., 2010).

PABP is also present during translation initiation, elongation and termination. It is hypothesised to circularise mRNA by binding eIF4E and eIF4G on the 5' mRNA cap as described by the mRNA closed loop model (Kahvejian et al., 2001). Although little *in vivo* evidence has been described, it is hypothesised that the binding of PABP to 5' mRNA cap proteins helps to regulate expression by promoting or repressing translation. *In vitro* translation studies allowed the visualisation by atomic force microscopy of closed loop structures following the mixing of eIF4E, eIF4G, PABP and mRNA (Wells et al., 1998). An *in vivo* study which appears to suggest that closed loops are formed during a particular phase of translation initiation was carried out by Archer et al. (2015). Yeast cells expressing tagged versions of eIF4E, eIF4G and PAB were grown to an exponential growth phase and cross-linked using formaldehyde to stabilise *in vivo* polysomes. Co-factor associated mRNA was isolated by immunoprecipitation and non-co-factor bound mRNA was digested by RNase I treatment. Quantification of the co-factor at the opposing end of the mRNA than is expected was assumed to corroborate the mRNA closed loop model. Archer et al. (2015) suggested that eIF4E/G was more often enriched at the 3' end than PAB at the 5' end and that this may suggest that the closed loop model was occurring during distinct phases of translation initiation.

1.3.2 Aggregate Formation and Intrinsically Disordered Proteins are Features of the mRNA cycle

The targeting of mRNA to specific cytoplasmic foci is highly dependent upon the ability of a protein to recognise the mRNA and to either shuttle the mRNA to the foci or to subsequently drive aggregation (Anderson and Kedersha, 2006). As shall be described below, mRNA can be targeted to many different areas including polysomes, stress granules and P-bodies. TIA-1 and TIA-R are ubiquitously expressed but are fundamental in Cytotoxic T Lymphocyte (CTL) granule mediated apoptosis as they drive nucleolysis in the target cell. Both proteins have 3 RNA Recognition Motifs (RRM) as well as a glutamine rich domain at their C-termini (Tian et al., 1991; Kawakami et al., 1992). Both proteins are able to bind mRNA via their RRMs as well as aggregate due to the glutamine rich region at their C-termini which results in bundling of the target mRNA and any associated pre-initiation factors to form stress granules.

However, P-body components drive aggregation individually due to the presence of glutamine/asparagine (Q/N) rich regions which are examples of low complexity sequences (LC). Q/N rich regions have been associated with prion proteins and are often described as prion-like domains due to their spontaneous ability to self-aggregate (Kato et al., 2012). However, Q/N rich regions are abundant in eukaryotes and are described as a new mechanism for protein-protein interactions due to the presence of polar side chains which would enable frequent hydrogen bonding (Michelitsch and Weissman, 2000). Specific binding of mRNA is facilitated by the presence of RRMs within the decapping enzymes, RNA helicases and exonucleases (Eulalio et al., 2007a).

1.3.3 The Role of Stress Granules and P-bodies in the regulation of mRNA

Following transcription, circumstances and cellular conditions may change before a particular transcript is translated. Following these new conditions the mRNA transcript may not be suitable and translation will result in inefficient energy expenditure. As a result, cells require a mechanism to regulate mRNA translation within the cytoplasm. This is achieved using the mRNA cycle which involves polysomes, stress granules and P-bodies as depicted in figure 1.3-2.

The mRNA cycle begins with the production of mRNA transcripts which are bound by nuclear proteins that facilitate the shuttling of mRNA from the nucleus to the cytoplasm (Buchan and Parker, 2009). As depicted in figure 1.3-2, the nascent transcripts can potentially be incorporated straight into P-bodies for decay, for example if the transcript is faulty or processing of pre-miRNA to produce miRNA and mediate further decay (Eulalio et al., 2009). Transcripts can also be exchanged with stress granules resulting in the dissociation of RNA degradation proteins, such as decapping enzymes 1 and 2 (DCP1/2) and RNA helicases, and the association of eukaryotic initiation factors which form pre-initiation complexes (Decker and Parker, 2012). The stress granules can dissociate into smaller modules which consist of the translation initiation complex and allow the formation of the ribosomal complex which further aggregate to form polysomes.

mRNA transcripts can undergo multiple rounds of translation to increase the protein expression before the ribosomal complex is displaced by the degradation machinery, promoting either deadenylation and 3'-5' exosomal decay or incorporation into P-bodies (Buchan and Parker, 2009). If expression of a protein is increased, the degradation machinery can be displaced by eukaryotic translation initiation factors to begin translation once again. If no further protein is required, DCP1 and 2 cause mRNA decapping and the mRNA undergoes 5'-3' mediated decay (Eulalio et al., 2007b). As the mRNA transcript can enter at multiple points within the process and is constantly replaced or degraded, the turnover of mRNA is referred to as a cycle (Buchan and Parker, 2009).

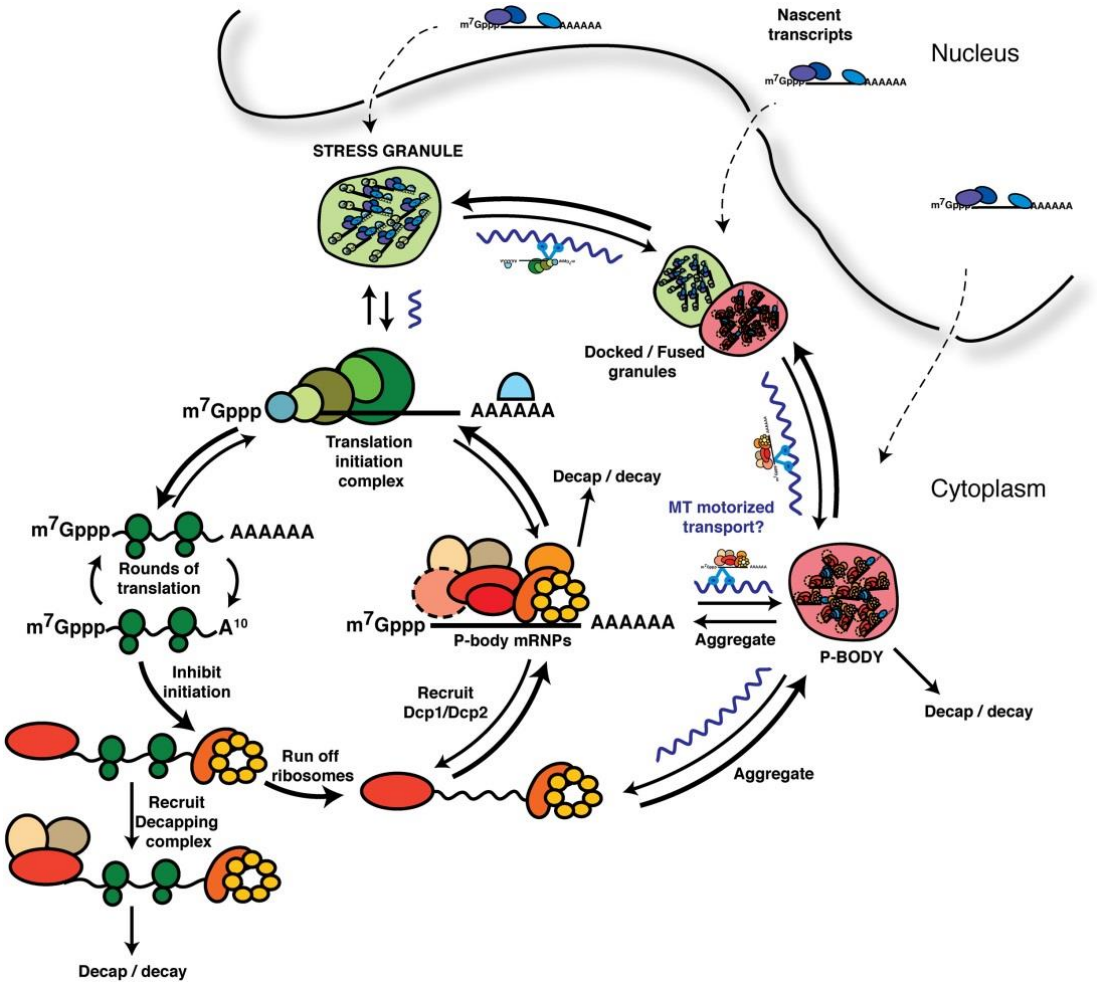

Figure 1.3-2 The regulation of translation via the mRNA cycle. mRNA can undergo multiple rounds of translation via polysomes resulting in the production of the target protein. Once the transcript is no longer required the mRNA can either be deadenylated and undergo 3'-5' degradation by the exosome or become incorporated within P-bodies. The incorporation of mRNA within P-bodies requires mRNPs, including the decapping machinery, which decap and degrade the mRNA. However, the mRNA may require storage or translocation in which case the P-body docks with a stress granule resulting in a change in the mRNP content and exchange of the mRNA. From stress granules or P-bodies, mRNA transcripts are able to re-enter translation. Transcripts may also be incorporated straight into stress granules or P-bodies directly from the nucleus for temporary storage before translation or decay (Buchan and Parker, 2009).

Stress granules are cytoplasmic aggregates consisting of messenger Ribonuclear Proteins (mRNPs) that are associated with translation initiation but are non-translating in their current state. Stress granules form following harsh cellular conditions, major examples include: glucose deprivation, heat shock, viral infection, amino acid deprivation, oxidative stress, hyperosmolarity and ultraviolet radiation (Anderson and Kedersha, 2002). Stress granules provide a concentrated cytoplasmic location that temporarily stores mRNA while harsh conditions render non-stress related protein translation undesirable. They form following eIF2α phosphorylation by the associated kinases which are PKR, PERK-PEK, GCN2 and HRI (Kedersha et al., 1999). These serine/threonine kinases phosphorylate eIF2α which increases the affinity of the heterotrimeric eIF2 for eIF2B. eIF2B catalyses the GDP-GTP exchange required for eIF2 to form the ternary complex consisting of eIF2, GTP and Met-tRNA. However, eIF2B is unable to catalyse the GDP-GTP exchange when eIF2α is phosphorylated. Moreover, the binding of eIF2B by phosphorylated eIF2α sequesters eIF2B so that it acts as a secondary regulatory feature during adverse cellular conditions (Kedersha et al., 1999). As the ternary complex cannot form, the pre-initiation complex fails to form (43S) as the ternary complex is required to bind to the 40S subunit. Stalled translation results in shuttling of the pre-initiation complexes towards stress granules via TIA-1 and TIAR (Kedersha et al., 2000). The mRNA is temporarily stored and sorted so that it can resume translation via polysomes (Kedersha and Anderson, 2002). However, if the adverse stimulus persists and the cell becomes damaged then mRNA is redirected towards decapping and degradation.

P-bodies are discreet cytoplasmic foci consisting of mRNA sequestered by aggregating mRNPs which include the decapping and degradation machinery (Sheth and Parker, 2003). P-bodies have been implicated in mRNA degradation, Nonsense-Mediated mRNA Decay (NMD) and translational repression (Sheth and Parker, 2003; Sheth and Parker, 2006; Teixeira et al., 2005). It has also been suggested that P-bodies contribute to gene expression control by aggregating mRNA following small interfering mRNA or miRNA gene silencing as inhibition of these pathways prevents P-body formation (Eulalio et al., 2007b). However, P-bodies are not essential for mRNA decay as inhibition of P-body formation by cycloheximide treatment does not prevent deadenylation and mRNA degradation in yeast (Hilgers et al., 2006).

In eukaryotes there are two major mRNA degradation pathways. Following deadenylation of the PolyA tail, the mRNA undergoes either 3'-5' degradation by the exosome or decapping followed by 5'-3' degradation by Xrn1 as depicted by figure 1.3-3 (Anderson and Parker, 1998; Muhlrad et al., 1994; Larimer et al., 1992). P-bodies consist of multiple protein components, including: the decapping enzymes DCP2 and DCP1; the 5'-3'exonuclease, Xrn1; the decapping activating Lsm1-7 complex; the translation initiation factor eIF4e and its transporter 4E-T (van Dijk et al., 2002; Bashkirov et al., 1997; Ingelfinger et al., 2002; Andrei et al., 2005; Ferraiuolo et al., 2005). However, this list is not exhaustive and there are many other P-body components (Eulalio et al., 2007a).

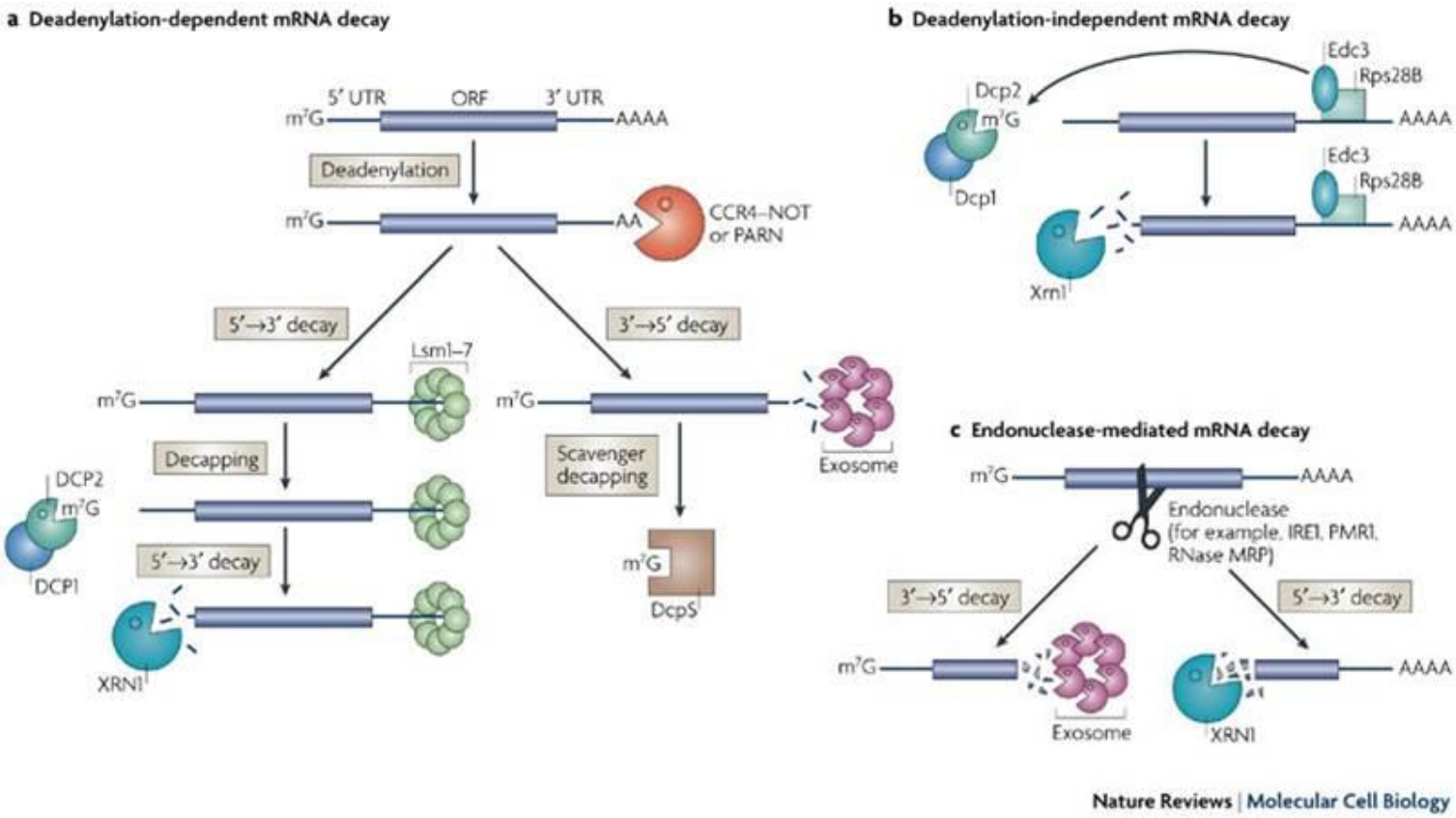
a Deadenylation-dependent mRNA decay
5′ UTR
ORF
3′ UTR
m7G
AAAA
Deadenylation
AA
CCR4–NOT or PARN
5′→3′ decay
3′→5′ decay
Lsm1–7
Decapping
DCP2
DCP1
Scavenger decapping
DcpS
Exosome
XRN1
b Deadenylation-independent mRNA decay
Edc3
Rps28B
Dcp2
Dcp1
Xrn1
c Endonuclease-mediated mRNA decay
Endonuclease (for example, IRE1, PMR1, RNase MRP)
Nature Reviews | Molecular Cell Biology

Figure 1.3-3 The major pathways of mRNA decay. **A** – Deadenylation-dependent mRNA decay. The Poly(A) is removed during deadenylation by the CCR4-NOT complex or PARN and results in either a 5'-3' or 3'-5' decay event. During 5'-3' decay, Lsm1-7 associates with the 3' end of mRNA and causes DCP1/2 to associate with the mRNA cap and cause decapping. Without the cap, mRNA is susceptible to exonuclease activity which is catalysed by Xrn1, a 5'-3' exonuclease. Alternatively, during 3'-5' decay, the exosome catalyses exonuclease activity at the 3' end of the mRNA and the remaining cap structure is hydrolysed by DcpS. **B** – In yeast the decay can deadenylation-independent as Rps28B associates with Ehancer of decapping-3 to recruit the decapping machinery. Following DCP1/2 removal of the 5' cap, Xrn1 begins 5'-3' exonuclease decay. C – Internal cleavage of the mRNA transcript by endonucleases results in unprotected fragments that either undergo 3' decay by the exosome or 5' decay by Xrn1 (Garneau et al., 2007).

The formation of P-bodies within eukaryotes is based upon a model derived from experimental evidence in yeast cells. It is believed that P-bodies only consist of un-translating mRNA unlike stress granules which consist of stalled pre-initiation complexes. The mRNA exits polysomes and translation is repressed upon the binding of P-body protein components to form small mRNPS. The proteins within the mRNP are able to interact with themselves and other P-body components and the mRNPs aggregate to form visible cytoplasmic granules (Jain and Parker, 2013). The aggregating proteins within the mRNPs have specific aggregation promoting domains such as the Q/N rich region in the C terminus of Lsm4. This prion like domain has been demonstrated to promote P-body assembly following removal of the self-interacting domain of Edc3 which acts as a scaffold protein during P-body assembly (Decker et al., 2007).

The formation of DEF6 aggregates to form granules may be associated with the role of DEF6 during T cell activation as the rapid polymerisation of actin and microtubule nucleation may provide a highly efficient transport network for the translocation of DEF6 granules to the IS. As DEF6 granules have been previously demonstrated to co-localise with P-bodies, this translocation may in fact induce the delivery of selective mRNAs, stored within the stress granule-P-body cycle to facilitate an efficient and selective response to T cell activation. The ability of DEF6 to catalyse actin polymerisation and potentially associate with the regulation of mRNA translation is an efficient dual role that requires further investigation.

1.3.4 Posttranscriptional Regulation of mRNA in $CD4^+$ T cells

In mammalian cells, posttranscriptional regulation of mRNA can occur through a variety of methods. For example, the poly(A) tail can be shortened through deadenylation to suppress translation of the transcript or lengthened by polyadenylation to promote translation. mRNA transcripts can also be bound by RBPs which prevent the association of the translation initiation complex and drive the transcript to P-bodies to suppress translation. Particular proteins, such as HuR and TTP, can bind AREs within the 3' UTR to suppress translation and target a transcript towards degradation. Finally, miRNAs can associate with complementary sequences on the mRNA transcript to suppress translation and allow association of the argonaut proteins and the formation of the RISC complex which drives the transcript towards degradation (Istomine et al., 2016).

Examples of miRNAs which have a role in controlling naïve $CD4^+$ T cell differentiation and proliferation include miR-17, miR-19a, let-7d, miR-21 and miR-466l. The miRNAs target cytokine production to determine the cell fate of the $CD4^+$ T cell and control the determined cell lineage and proliferation. miR-17 promotes a commitment to a Th_1 cell lineage as it represses the translation of TGFβ receptor 2 transcripts and reducing the sensitivity of the cell to TGFβ secretion which would promote Th_2 differentiation. miR-19a promotes the production of cytokines which induce Th_2 differentiation and proliferation (Istomine et al., 2016). Let-7f miRNA represses the translation of IL-23 receptor transcripts which reduces the ability of Th_{17} cells to sustain its activity due to a reduced sensitivity to IL-23 secretion (Li et al., 2011). miR-21 promotes a Th_{17} lineage due to repressing the translation of SMAD-7

transcripts so that the reduction in SMAD-7 expression leads to an increase in TGFβ expression (Murugaiyan et al., 2015). Treg cells secrete IL-10 to reduce IFNγ and IL-2 production in target effector T cells which results in a reduction in cell differentiation and proliferation. miR-466l binds IL-10 mRNA to increase stability as it prevents the binding of TTP to the corresponding 3'UTRs. This results in a reduction in IL-10 transcript deadenylation and degradation and increases the expression and secretion of IL-10 (Ma et al., 2010).

A general control of $CD4^+$ differentiation by miRNAs is achieved by the miRNA cluster 17-92 which represses the translation of PTEN transcripts and reduces the protein levels of PTEN (Jiang et al., 2011). A reduction in PTEN results in a reduction in AKT inhibition which increases the phosphorylation and subsequent activation of mTOR leading to the phosphorylation of eIF4E binding proteins. Phosphorylated eIF4E binding proteins dissociate from eIF4E increasing the availability of eIF4E for the formation of translation initiation complexes and increases the rate of translation. An increased rate of translation promotes $CD4^+$ T cell differentiation into effector T cell lineages and inhibits the expression of FOXP3 (Bjur et al., 2013).

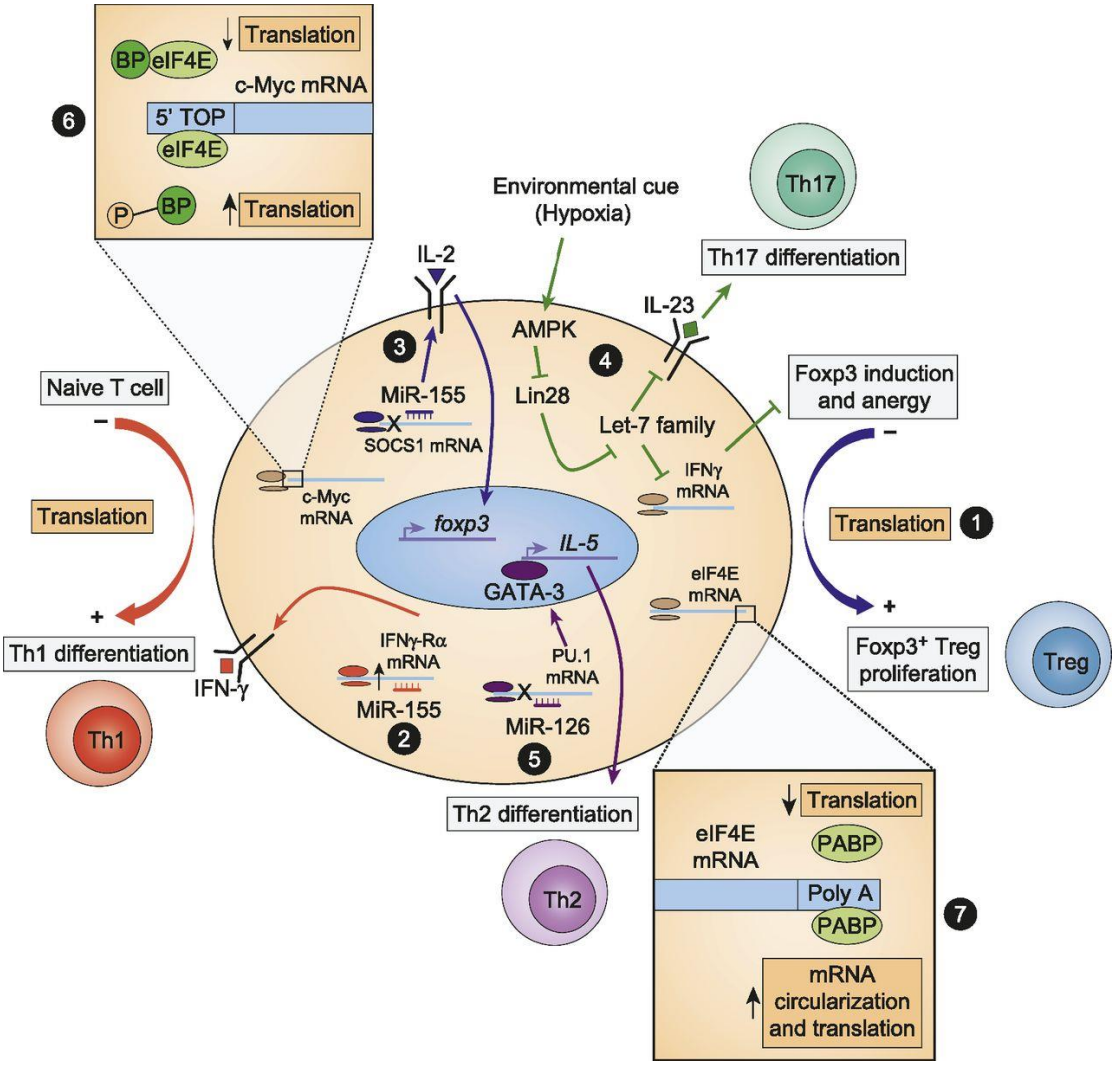

Figure 1.3.4 Examples of miRNA involved in the posttranscriptional regulation of cytokine and interleukin expression in naïve $CD4^+$ T cells. Differentiation and proliferation of naïve $CD4^+$ cells is regulated by the production and secretion of particular cytokines. TCR stimulation results in mTOR activation and phosphorylation of eIF4E binding proteins which dissociate from eIF4E and results in an increased rate of translation. Th_1 differentiation is achieved by IFNγ production which is regulated by miR-155. MiR-126 regulates GATA-3 and IL-5 production to promote Th_2 differentiation. IL-23 promotes Th_{17} differentiation which is regulated by the Let-7 family of miRNAs. Environmental stressors result in sequestering of eIF4E by eIF4E binding proteins and a reduction in translation causing a shift to FOXP3 expression and Treg differentiation (Istomine et al., 2016).

Treg cells are also able to regulate the posttranscriptional control of mRNA in the target cell due to the production and secretion of exosomes. These exosome contains miRNAs which transfect the target effector T cell and affect the translation of target transcripts to induce the desired cell response. For example, let-7d is secreted within exosomes and the miRNA suppresses the translation of IFNγ transcripts resulting in a reduction in IFNγ secretion by the target effector T cell and a reduction in differentiation and proliferation (Okoye et al., 2014).

1.4 Alternative characteristics of DEF6

1.4.1 Phosphorylation of DEF6 by ITK results in Aggregation of DEF6

DEF6 has been demonstrated to form cytoplasmic granules in Jurkat T cells and COS-7 cells. The N-terminus of the DHL domain contains a glutamine rich region which was demonstrated to form cytoplasmic aggregates when amino acids 311-501 were transfected into COS-7 cells (Hey et al., 2012). Moreover, the DHL domain of DEF6 has a high probability of containing a coiled-coil forming region which is characteristic of self-interacting and aggregating proteins (Fiumara et al., 2010). Hey et al. (2012) also investigated the effect of ITK phosphorylation at tyrosine residues 210 and 222 upon the cellular localisation of DEF6. GFP tagged Y210EY222E DEF6 is a mutant which mimics ITK phosphorylation of DEF6 due to the substitution of tyrosine residues 210 and 222 for glutamic acid as shown in figure 1.2-1. The Y210EY222E DEF6 mutant was found to form cytoplasmic granules in untreated and sodium pervanadate treated Jurkat T cells following stimulation using anti-CD2, CD3 and CD28 coated magnetic beads. Moreover, GFP tagged Y210EY222E DEF6 was also demonstrated to form cytoplasmic granules which co-localised with DCP1, a P-body marker, in untreated and sodium arsenite treated COS-7 cells (Hey et al., 2012). This suggests that DEF6 granules may be associated with P-bodies or perhaps stress granules which have been shown to dock with P-bodies.

1.4.2 The DHL domain drives DEF6 aggregation while the N-terminus targets the aggregate to P-bodies

Further investigation of the DHL domain has identified not only a high concentration of glutamine and asparagine residues but also an absence of proline in the same area which is indicative of P-body aggregating proteins (Mollett, 2014). The coiled-coil structure predicted by Hey (2011) was also corroborated using circular dichroism to distinguish singular alpha helices to interacting helices, a feature characteristic of coil-coil regions. Exogenous expression of the DHL domain in COS-7 cells resulted in spontaneous aggregation of the DHL domain to form cytoplasmic foci. The cytoplasmic foci did not co-localise with dsRED DCP1 granules, however some granules appear to cluster around the DCP1 granules without mixing.

Exogenous expression of DEF6-ΔC, a mutant lacking the 39 amino acids at the C–terminus, in COS-7 cells also resulted in spontaneous aggregation and the aggregates co-localised with dsRED DCP1. This suggested that the DHL domain is likely to drive the DEF6 protein into aggregates due to the intrinsic properties characteristic of P-body markers, and deletion of the C-terminus is insufficient to prevent targeting of the aggregates to P-bodies (Mollett, 2014).

Subsequent photo-bleaching of DEF6 granules demonstrated that the percentage recovery of fluorescence was low, indicative of a low rate of DEF6 turnover within granules, and the rate was comparable to structural aggregating markers of P-bodies. The granules also translocated within the cytoplasm and appeared to move with a velocity indicative of both actin and tubulin mediated transport. Moreover, endogenous DEF6 granules were also identified at the IS which may suggest movement of DEF6 granules to areas of cell-cell contact (Mollett, 2014).

1.4.3 DEF6 Co-Immunoprecipitates with Polysomes in Jurkat T Cells

Differential centrifugation of a Jurkat cell lysate led to the isolation of DEF6 associated polysomes. Dr Peter Jones (unpublished) used a sucrose cushion comprised of a density gradient to separate the Jurkat T cell lysates by ultracentrifugation. Smaller and less dense particles were able to sediment further in the increasing gradient before reaching equilibrium. Fractions were then isolated from the different sucrose concentrations, separated by SDS-PAGE and immunoblotted. Ribosomal protein L7a was used as a marker of ribosomes and is indicative of the 60S subunit (Uchiumi et al., 1980). Anti-DEF6 was used to detect the presence of DEF6 within each fraction.

Co-immunoprecipitation of DEF6 associated polysomes was also achieved following isolation of polysomes from Jurkat T cells by sucrose cushion ultracentrifugation. Polysomes were then incubated with anti-DEF6 or incubated in the absence of antibody before precipitating DEF6 using magnetic beads. The absorbance at 254nm was then calculated for the DEF6 precipitated and control samples.

The membrane and cytosolic polysomes were isolated using cellular fractionation to separate the membrane from the cytosolic fraction. The two fractions were then subjected to sucrose cushion ultracentrifugation to isolate the associated polysomes. Proteins were separated by SDS-PAGE and immunoblotted to detect the presence of ribosomal protein L7a and DEF6.

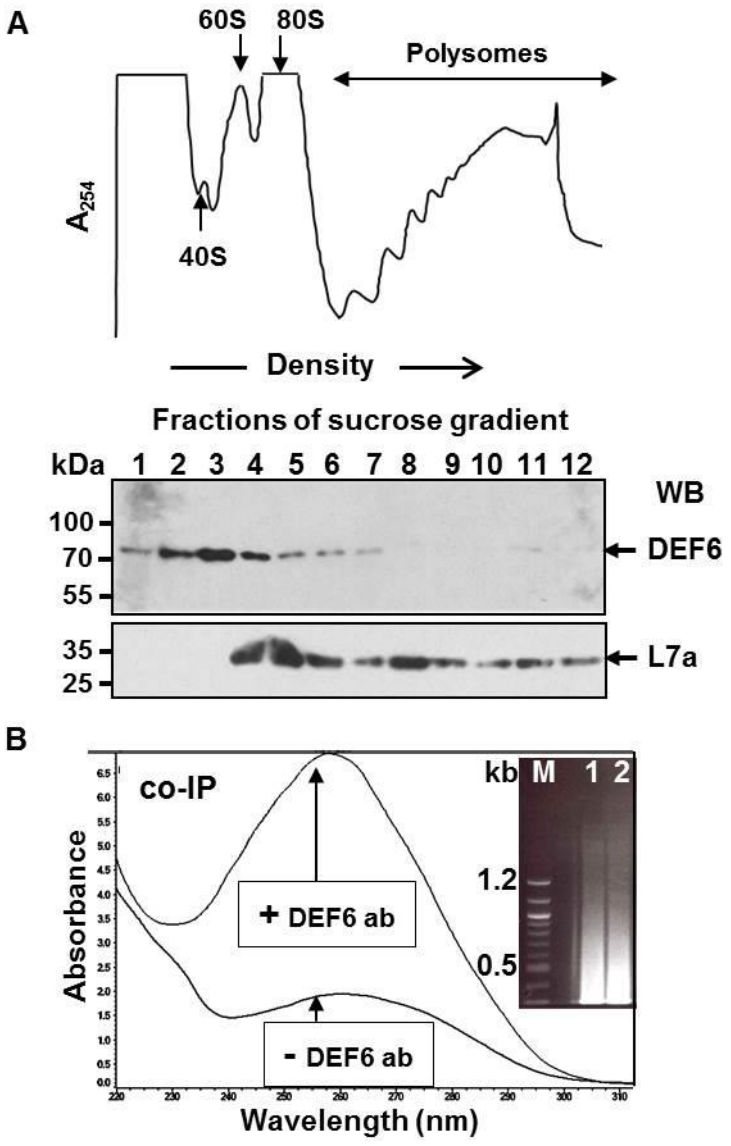
A
60S
80S
Polysomes
A_{254}
40S
Density
Fractions of sucrose gradient
kDa 1 2 3 4 5 6 7 8 9 10 11 12
WB
100
70
55
DEF6
35
25
L7a
B
co-IP
kb M 1 2
1.2
0.5
Absorbance
+ DEF6 ab
- DEF6 ab
Wavelength (nm)

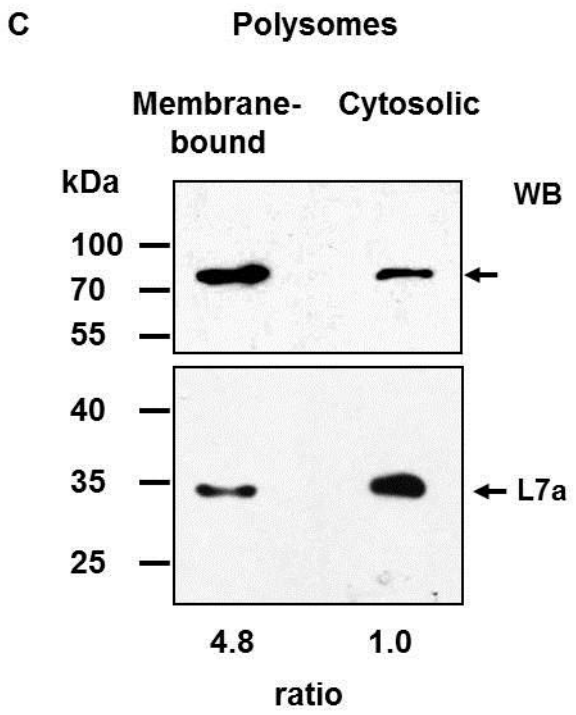

Figure 1.4-1 DEF6 is present in ribosomal subunit fractions following sucrose density gradient centrifugation and associates with membrane-bound and cytosolic polysomes. **A**- Jurkat T cells were lysed on ice and pre-cleared by centrifugation at 4°C. The supernatant was applied to a sucrose density gradient increasing in 10% intervals, with the most concentrated sucrose density at the base of the ultracentrifugation tube, and subjected to ultracentrifugation. Fractions were isolated from the varying sucrose concentrations and the relative absorbance was measured at 254nm. Smaller and less dense particles reached equilibrium further along the density gradient than larger and denser particles as indicated by the presence of ribosomal subunits in the earlier fractions isolated from the base of the tube. The isolated samples were then separated by SDS-PAGE and were immunoblotted using ribosomal protein L7a as a marker of the 60S subunit.
B – Polysomes from Jurkat T cells were isolated by sucrose cushion ultracentrifugation and were either incubated with anti-DEF6 or incubated in the absence of an antibody. Precipitation of DEF6 resulted in an increased absorbance at 254nm in comparison to the control sample. **C** – Polysomes were isolated based upon their cellular location by performing cellular fractionation to isolate the membrane versus the cytosol. Polysomes were then isolated by sucrose cushion ultracentrifugation and separated by SDS-PAGE followed by immunoblotting. The presence of polysomes is indicated by ribosomal protein L7a whilst anti-DEF6 was used to detect the presence of DEF6 in the different polysome fractions (P. Jones, unpublished).

Separation of the polysome fraction by differential centrifugation allows the fractionation of the 40S, 60S and 80S subunits along with polysomes of varying size as shown in figure 1.4-1A. Ribosomal protein 7a is part of the 60S subunit and is present within polysomes. Separation of the proteins by SDS-PAGE and immunoblotting identified DEF6 as a protein which co-sediments with the ribosome, with a significant DEF6 signal corresponding with the 40S subunit (1.4-1A). Immunoprecipitation of DEF6 increased the absorbance at 254nm indicating an increase in the presence of ribosomes in comparison to the control sample as shown in figure 1.4-1B. Separation of the membrane bound and cytosolic ribosomes by cellular fractionation and sucrose cushion ultracentrifugation identified an increased presence of DEF6 in the membrane-bound fraction with a 4.8 fold increase in DEF6 in comparison to the cytosolic fraction (1.4-1C). As a result, DEF6 was first linked to ribosomes and translation (P. Jones, unpublished), and led to the basis of this study.

1.5 Functions of Granules *in vivo*

Granules allow a cell to efficiently store molecules so that they can be transported, retained for future use or to prevent other interactions. This allows the regulation of when and where those particular molecules will continue their associated function. Two major examples of spatiotemporal regulation that utilise granules also involve synapses. Neuronal synapses and CTL synapses both utilise granules to regulate the location and the timing of the release of their corresponding cargo in response to an external signal.

1.5.1 Spatiotemporal Regulation of Translation in Neuronal Synapses

A key mediator of translation in neurons is Fragile X Mental Retardation Protein (FMRP). FMRP allows the selective translation of mRNA transcripts at synapses in response to activation of Gp1 metabotropic glutamate receptors (mGluRs) (Bassell and Warren, 2008). As a result FMRP allows the regulation of where and when an mRNA transcript will be translated. MGluRs are members of the C family of G protein coupled receptors that respond to L-glutamate (Niswender and Conn, 2010). The association of L-glutamate to the mGluR results in the activation of PP2A which dephosphorylates FMRP allowing translation of FMRP bound mRNA transcripts. Subsequent activation of mTOR by the Homer cascade results in phosphorylation of FMRP, preventing further translation of FMRP bound mRNA transcripts (Bassell and Warren, 2008).

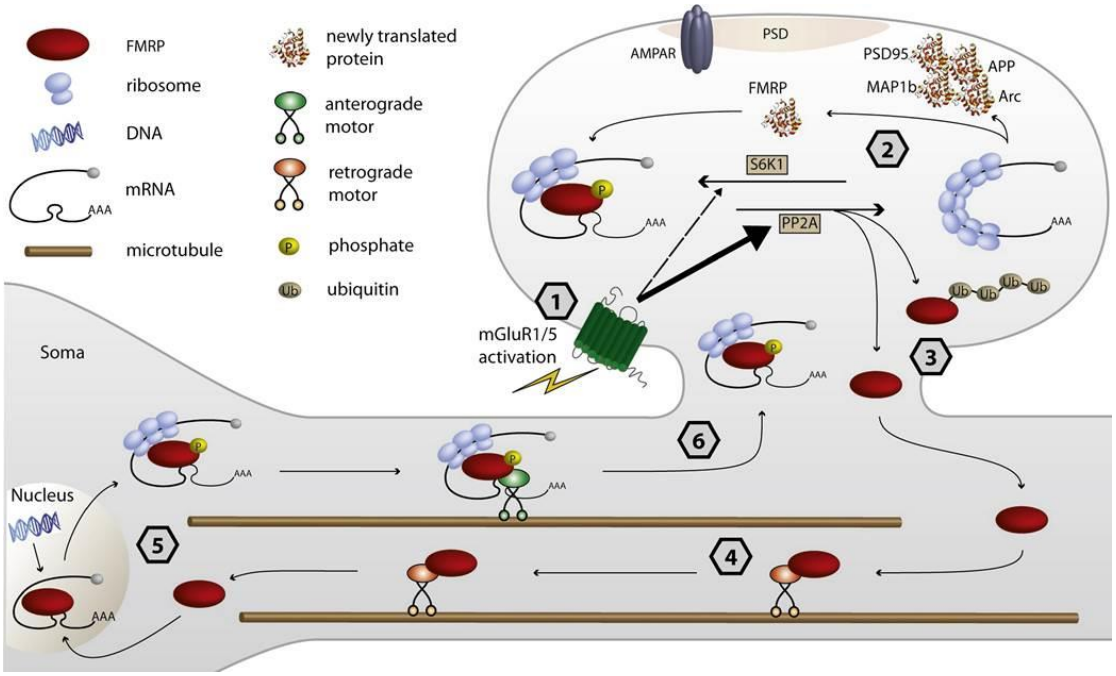

Figure 1.5-1 Hypothesis of Fragile X mental retardation protein aggregate translocation in response to mGluR activation. (1) MGluR activation results in PP2A activation and dephosphorylation of FMRP causing localised translation of proteins that affect AMPAR trafficking such as PSD-95, Arc, Map1b and APP (2). FMRP is then hypothesised to either be ubiquitinated for degradation to establish mGluR-Long Term Depression and reduce synaptic efficiency (3) or be transported to the nucleus by a retrograde motor (4). FMRP aggregates shuttle to nucleus and associate with specific target mRNA transcripts (5). FMRP-mRNA is shuttled out of the nucleus and the aggregates are transported along the axon by anterograde motors back to the synapse (6). FMRP is then phosphorylated by S6K1 which causes repression of the FRMP associated mRNA transcripts (2) (Bassell and Warren, 2008; Gladding et al., 2009).

The translation response to mGluR activation begins with translationally inactive FMRP-mRNA aggregates at the neuronal synapse as depicted in figure 1.5-1. MGluR activation results in PP2A activation and dephosphorylation of FMRP which causes derepression of the FMRP associated mRNA transcripts and localised translation at the synapse. FMRP is then hypothesised to either be ubiquitinated for degradation or transported to the nucleus by a retrograde motor. FMRP aggregates then shuttle to the nucleus and associate with specific target mRNA transcripts. Following shuttling of FMRP-mRNA to the cytoplasm, FMRP aggregates are transported along the axon by anterograde motors back to the synapse. FMRP is then phosphorylated by S6K1 which causes repression of the FRMP associated mRNA transcripts (Bassell and Warren, 2008).

1.5.2 Lytic Granule Secretion in $CD8^+$ Cytotoxic T Lymphocytes

The key immune cells involved in the lytic response include the $CD8^+$ CTLs, Natural Killer T cells (NKTs) and Natural Killer cells (NKs) (Angus and Griffiths, 2013). These cells store perforin and granzymes as cytotoxic granules which are released in a highly organised IS to cause lysis of the target cell and prevent damage to the surrounding area. The IS of CTLs and NKT cells follows the same arrangement as $CD4^+$ T cells as depicted in figures 1.1-2 and 1.5-2 below (Angus and Griffiths, 2013).

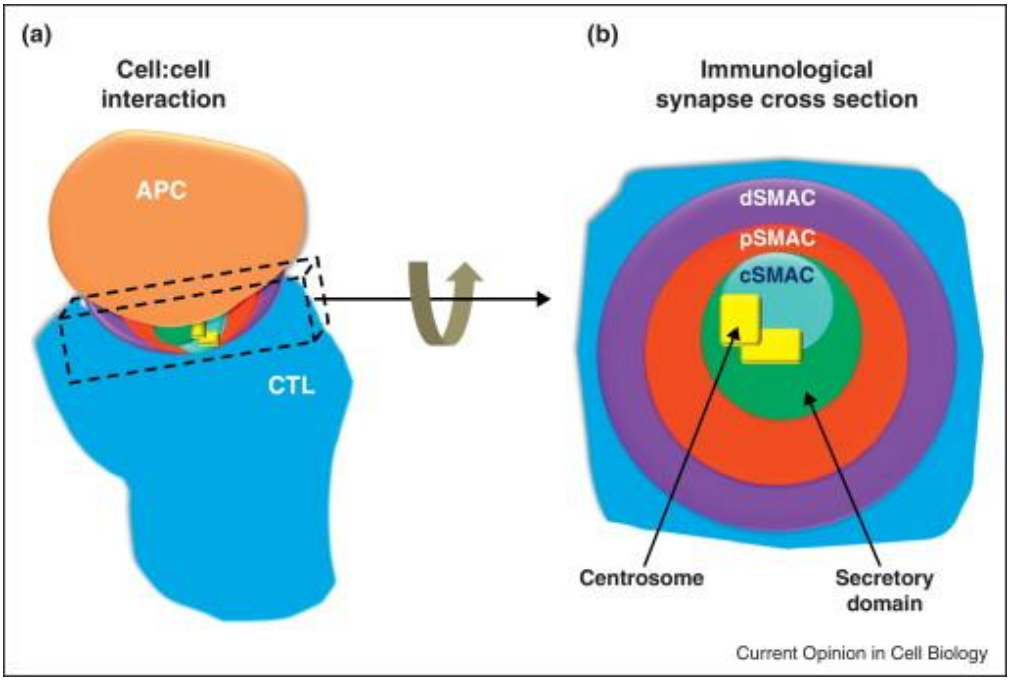

Figure 1.5-2 The immunological synapse in cytotoxic T lymphocytes. The IS is organised in distinct supramolecular activation clusters to form distal (dSMAC), peripheral (pSMAC) and central (cSMAC) concentric rings. The dSMAC is characterised by actin enrichment and the exclusion of CD45, the pSMAC by the enrichment of integrins, and the cSMAC by TCR microclusters. The centrosome is positioned directly beneath the cSMAC to direct polarised secretion of cytotoxic granules which are secreted through the secretory domain located at the centre of the cSMAC (Angus and Griffiths, 2013).

A viral-infected or cancerous cell will present an antigen to the CTL via the MHC class I receptor. The pMHC receptor is recognised by the TCR and the co-factor CD8 stabilises this interaction. An IS is then formed between the APC and the CTL which results in a polarity being established which ensures that the cytotoxic granules are secreted towards the APC (Dieckmann et al., 2016).

Figure 1.5-2 depicts the formed IS and the concentric rings which are produced. Each ring is a distinct SMAC: the dSMAC is actin enriched and provides stability to the IS; the pSMAC consists of LFA-1 which associates with ICAM-1 on the APC to further stabilise the TCR-pMHC interaction and prevents premature dissociation of the APC or CTL; and the cSMAC which consists of LAT and TCR microclusters and the secretory domain (Angus and Griffiths, 2013; Dieckmann et al., 2016). Following the pMHC recognition by the TCR, LCK phosphorylates the intracellular CD3 domains which results in the activation of ZAP-70 (Dieckmann et al., 2016). The subsequent cascade activates Indian Hedgehog resulting in Hedgehog signalling and the activation of Rac1. Rac1 facilitates actin remodelling at the IS which is necessary for centrosome translocation to the cSMAC (de la Roche et al., 2013). Consequently, centrosomal translocation enables targeted secretion of the cytotoxic granules towards the cSMAC and the target cell. This reduces the risk of lysis to the CTL and improves the efficiency of the immune response as the cytotoxic granules are quickly shuttled to the IS along the microtubules.

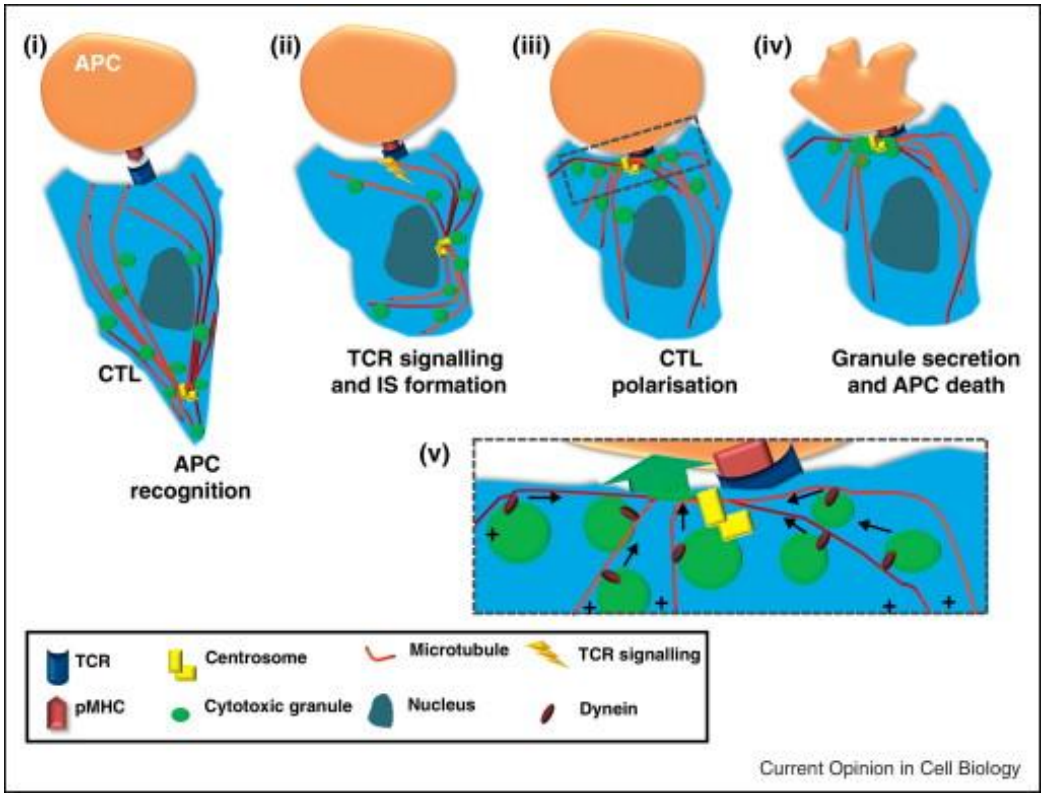

Figure 1.5-3 Establishing cell polarity during immunological synapse formation. The centrosome is located at the uropod opposite to the site of TCR-pMHC recognition and cytotoxic granules are distributed along the microtubules throughout the cytoplasm (i). TCR-pMHC recognition and the formation of the IS results in the translocation of the centrosome to the IS in response to TCR signalling (ii). A polarity at the APC-CTL contact site is established and cytotoxic granules are transported along the microtubules towards the cSMAC (iii and iv). Cytotoxic granules are secreted at the cSMAC causing APC death (v) (Angus and Griffiths, 2013).

Following the translocation of the centrosome from the uropod, a plasma membrane protrusion based at the distal side of the CTL, cytotoxic granules are transported towards the cSMAC. Figure 1.5-3 depicts the movement of cytotoxic granules along the microtubules by dynein towards the secretory domain due to a polarity which is established by the centrosome. The cytotoxic granules contain perforin and granzymes which perforate the APC plasma membrane and cause degradation of the cell leading to cell death. The cytotoxic granules are secreted via the secretory domain and reach the target cell within the confines of the IS to prevent damage to the surrounding environment (Angus and Griffiths, 2013).

1.6 Role of DEF6 in the onset of autoimmunity

1.6.1 DEF6 is linked to Systemic Lupus Erythematous

Canonigo-Balancio et al. (2009) investigated the role of Def6 in the onset of Experimental Autoimmune Encephalitis (EAE) by producing Def6-deficient mice of a C57BL/6 background using insertion of a retroviral cassette into ES cells to cause a single intronic mutation event between exons 1 and 2. The ES cells were then injected into C57BL/6 blastocysts to produce Def6-deficient mice. They compared Def6 expressing $CD4^+$ T cells to $Def6^{-/-}$ T cells and found that $Def6^{-/-}$ T cells had a reduced ability to proliferate and produce IL-2. Moreover, there was a reduction in Interferon-γ and Interleukin-17 production. As a result, $Def6^{-/-}$ mice appeared to resist central nervous system inflammation due to a reduction in Th_1 and Th_{17} infiltration, both of which are characteristic of EAE.

However, this opposes work carried out by Fanzo et al. (2006) and Chen et al. (2008). The Pernis group also described a gene trap method using retroviral insertion which was used to independently produce DO11.10 TCR transgenic Def6 deficient mice of a C57BL/6 background. Fanzo et al. (2006) found that $Def6^{trap/trap}$ mice spontaneously developed systemic lupus erythematous which was further corroborated by Chen et al. (2008) who found that $Def6^{trap/trap}$ developed rheumatoid arthritis and large vessel vasculitis. DEF6 has been shown to bind and sequester Interferon Regulatory Factor 4 (IRF4) and the binding of IRF4 prevents the promotion of IL-17 and -21 expression (Gupta et al., 2003b; Chen et al., 2008). As a result, it was believed that DEF6 could reduce the onset of autoimmunity, to a certain extent, due to the regulation of IRF4 and the differentiation into the Th_{17} subset (Chen et al., 2008). Recently,

the Pernis group has suggested that the regulation of IRF4 is in fact due to phosphorylation by ROCK, a serine/threonine kinase which is activated by RhoA following DEF6 activation of RhoA (Biswas et al., 2010; Isgro et al., 2013).

Sun et al. (2016) have recently identified rs10807150, an intronic Single Nucleotide Polymorphism (SNP), close to the DEF6 gene which occurs in Asian individuals suffering from systemic lupus erythematous. The SNP correlates with another cis-expression quantitative trait loci, rs8205, in the promoter of ZFN76. Together these intronic SNPs alter expression of ZFN76 and DEF6, although the exact mechanism of alteration is unknown. As an intronic SNP, the polymorphism may affect alternative splicing, production of miRNA, or binding of transcription factors etc.

Although the link between DEF6 and autoimmunity has been investigated to some degree, there may be another link yet to be established. Current observations have suggested that the aggregation of DEF6 into granules may be linked to the control of mRNA translation via the mRNA cycle and that this relationship may be linked to cytoskeletal reorganisation following T cell activation which is the focus of this work.

1.7 Research Hypothesis

DEF6 displays characteristics of an aggregating protein involved in mRNA regulation and turnover. DEF6 is hypothesised to form aggregates in a variety of T cell states and that these aggregates will co-localise with translation factors and a P-body marker as well as mRNA itself.

1.8 Research Aims and Objectives

1. Investigate a potential link between DEF6 aggregation and mRNA turnover in T cells, particularly in relation to P-bodies.
    a. Determine whether DEF6 forms aggregates in resting Jurkat T cells as well as in response to chemical activation or stress using IF and confocal microscopy.
    b. Determine the effect of chemical activation and stress upon DEF6 protein expression in Jurkat T cells using western blot analysis and densitometry
    c. Use of IF and a PLA imaged using confocal microscopy to determine whether DEF6 is in close proximity to 4E-T, a P-body marker, in response to chemical activation and stress.
    d. Use of FISH to determine whether exogenously expressed WT-DEF6 and Y210E and Y222E phosphomimic-DEF6 aggregates co-localise with mRNA in COS-7 cells using confocal microscopy.
2. Investigate whether DEF6 co-localises with active translation and translation factors in T cells, and whether active translation is present at sites of DEF6 enrichment at the IS.
    a. Determine whether DEF6 co-localises with active translation using the puromycylation method and investigate whether DEF6 and

active translation are in close proximity using a PLA and imaged by confocal microscopy.

b. Use of IF and a PLA to determine whether DEF6 is in close proximity to translation factors, particularly eIF4E and PABP, in response to chemical activation and stress.
c. Use of IF to determine whether the DEF6 and PABP distribution matches the distribution of puromycin incorporation during active translation and whether PABP co-localises with DEF6.
d. Determine whether active translation co-localises with DEF6 enrichment at the IS following Raji B cell SEA/B antigen presentation using IF and confocal microscopy.

3. Investigate the mode of DEF6 translocation to the immunological synapse and to determine whether translocation occurs in response to T cell receptor engagement alone.
    a. Investigation of DEF6 translocation in response to chemical activation, C305 Jurkat TCR antibody mediated activation and Raji B cell SEA/B mediated activation using IF and confocal microscopy.
    b. Use of IF and confocal microscopy to determine whether DEF6 enrichment occurs at T-T cell junctions.
    c. Investigation of CD81, LFA-1 and ICAM-1 as potential receptors which mediate APC independent DEF6 translocation to the synapse using IF, a PLA and co-immunoprecipitation analysed by western blotting.
    d. Use of the puromycylation method and IF to preserve fixation sensitive processes to determine whether preservation of trafficking and active translation has an effect on DEF6 and receptor proximity in Jurkat T cells.

Chapter 2 Materials and Methods

2.1 Cell Culture Materials

2.1.1 Cell Lines

Jurkat T cells: Jurkat E6.1 human leukaemic T cell lymphoblasts (ECACC #88042803).

HuT78 T cells: HuT78 human T cell lymphoma cells (ECACC #88041901).

Raji B cells: Raji human B cell lymphoblasts (Sigma #85011429).

2.1.2 Cell Culture Media and Solutions

RPMI-1640: RPMI 1640 (Sigma #R8758) supplemented with L-Glutamine, 10% (v/v) FBS (Sigma #F9665) and 1% (v/v) Penicillin and Streptomycin and stored at 4°C.

Dulbecco's Modified Eagle's Medium (DMEM): DMEM (Sigma #D6429) supplemented with 4500mg/L glucose, 110mg/L Sodium Pyruvate, L-Glutamine, 10% (v/v) FBS and 1% (v/v) Penicillin and Streptomycin and stored at 4°C.

10x Trypsin/EDTA: 10x filter sterilised solution containing 5g Porcine Trypsin and 2g EDTA (Sigma #T4174) diluted 1:9 in sterile 1x PBS.

Sterile Phosphate Buffered Saline: 10x Phosphate buffered saline prepared (1.37M NaCl, 27mM KCl, 100mM NA_2HPO_4 and 20mM KH_2PO_4 pH7.4) and diluted 1:9 in distilled water before being autoclaved and stored at 4°C.

Freezing mix: 10% (v/v) DMSO in FBS.

10x Penicillin and Streptomycin: 10,000 units Penicillin and 10mg Streptomycin per ml (Sigma #P0781) diluted 1:9 in sterile 1x PBS.

Puromycin: Puromycin Dihydrochloride (Calbiochem #540411) dissolved in DMSO (18mM stock solution).

Cycloheximide: Cycloheximide (Calbiochem #239763) dissolved in DMSO (771mM stock solution).

Phorbol-12-myristate-13-acetate: PMA (Calbiochem #524400) dissolved in DMSO (1.6mM stock concentration).

Ionomycin: *Streptomyces conglobatus* ionomycin calcium salt (Calbiochem #407952) dissolved in DMSO (1.3mM stock concentration).

Sodium arsenite: 50mM stock solution (Sigma #35000).

2.2 Buffers and Solutions

2.2.1 General Solutions

Phosphate Buffered Saline: 10x Phosphate buffered saline prepared (1.37M NaCl, 27mM KCl, 100mM NA_2HPO_4 and 20mM KH_2PO_4 pH7.4) and autoclaved. Stock buffer was diluted 1:9 in distilled water to give a 1x working buffer.

Tris Buffered Saline: 10mM Tris and 150mM NaCl pH8.0

2.2.2 Co-immunoprecipitation Buffers

Lysis Buffer: 150mM NaCl, 50mM Tris pH7.5, 0.1% (v/v) NP40, 80nM Sodium O-Vanadate and 1.5mM PMSF and stored at 4°C.

Wash Buffer: 150mM NaCl, 50mM Tris pH7.5, 80nM Sodium O-Vanadate and 1.5mM PMSF and stored at 4°C.

2.2.3 Sodium Dodecyl Sulphate Polyacrylamide Gel Electrophoresis Buffers and Solutions

1x SDS Loading Buffer: 50mM Tris HCl pH6.8, 4% (w/v) SDS, 20% (v/v) glycerol, 10% (v/v) β-mercaptoethanol in autoclaved distilled water with the addition of sufficient bromophenol blue to produce a dark blue solution.

Resolving Gel Buffer (10%): 4ml distilled water, 3.3ml 30% (v/v) bis acrylamide, 2.5ml 1.5M Tris pH 8.8, 100µl 10% (w/v) SDS, 100µl 10% (w/v) APS and 8µl TEMED.

Stacking Gel Buffer (5%): 3.4ml distilled water, 830µl 30% (v/v) bis acrylamide, 630µl 1M Tris pH6.8, 50µl 10% (w/v) SDS, 50µl 10% (w/v) APS and 8µl TEMED.

10x Running Buffer: 1.87M glycine, 250mM Tris and 0.1% (w/v) SDS diluted 1:9 to give a 1x working buffer.

Coomassie Blue Stain: 50% (v/v) methanol, 10% (v/v) acetic acid and 3mM Coomassie Brilliant Blue R (Sigma #B7920).

Coomassie Blue De-stain solution: 30% (v/v) methanol and 10% (v/v) acetic acid.

2.2.4 Western Blotting Buffers and Solutions

Transfer Buffer: 30mM Tris, 240mM glycine and 25% (v/v) methanol.

Ponceau S Stain: 0.5% (w/v) Ponceau S and 10% (v/v) acetic acid.

Blocking Solution: 1x PBS and 5% marvel milk powder.

Antibody Incubation Solution: 1x PBS and 3% (w/v) marvel milk powder.

Wash Solution: 10x PBS diluted 1:9 in distilled water and 0.01% (v/v) tween-20.

2.2.5 Immunofluorescence Solutions

Fixing Solution: 4% (w/v) PFA in 1x TBS with 10mM NaOH and heated to 60°C until dissolved.

Permeabilisation Solution: 0.02% (v/v) Triton X-100 in 1x PBS.

Blocking Solution: 5% (w/v) BSA in 1x PBS or 3% (w/v) BSA in 1x PBS where stated. For the use of goat primary antibodies, 5% donkey serum in 1x PBS was used.

2.2.6 RNA Fluorescent In Situ Buffers and Solutions

Diethylpyrocarbonate treated distilled water: 1ml of DEPC per 1L of distilled water and heated to 42°C overnight before autoclaving.

20x SSC: 3M NaCl, 300mM Sodium Citrate pH7.

10x PBS: 1.37M NaCl, 27mM KCl, 100mM NA_2HPO_4 and 20mM KH_2PO_4 pH7.4 dissolved in DEPC treated and autoclaved water.

Permeabilisation Solution: 70% ethanol in DEPC treated distilled water.

Rehydration Solution: 2x SSC and 10% (v/v) formamide.

Hybridisation solution: 2x SSC, 10% (w/v) dextran sulphate, 2mM vanadylribonucleoside complex, 0.02% (v/v) RNase free BSA, 10% (v/v) formamide, 1µg/µl *Escherichia coli* tRNA and 11µM Oligod(T) 5' Cy5 probe (Genelink #26-4421-02).

Wash Solution: 2x SSC, 10% (v/v) formamide.

2.2.7 Puromycylation Buffers

Labelling Medium: 208μM emetine and 91μM puromycin added to complete RPMI 1640.

1x Polysome Buffer: 50mM Tris HCl pH7.5, 5mM $MgCl_2$, 25mM KCl, 0.2M sucrose, 100μg/ml cycloheximide, 3% (w/v) PFA and 0.015% (w/v) digitonin. 10U/ml RNase inhibitor and 1.5mM PMSF were added immediately before use.

Staining Buffer: 0.05% (w/v) saponin, 5% (v/v) FBS and 10mM glycine in DEPC treated 1x PBS.

2.2.8 Proximity Ligation Assay Buffers and Solutions

Wash Buffer A: 1 packet of powder added to 700ml distilled water. Once dissolved, buffer was topped up to 1L and stored at 4°C (Sigma Aldrich #DUO82047).

Wash Buffer B: 1 packet of powder added to 700ml distilled water. Once dissolved, buffer was topped up to 1L and stored at 4° (Sigma Aldrich #DUO82048).

Blocking Buffer: 1x blocking buffer (Sigma Aldrich #DUO82014).

Antibody diluent: 1x antibody diluent (Sigma Aldrich #82015).

Phosphate Buffered Saline: DEPC treated 10x PBS diluted 1:9 in DEPC treated distilled water.

Probes: Donkey anti-rabbit plus (Sigma Aldrich #DUO92002), donkey anti-mouse minus (Sigma Aldrich #DUO92002) and donkey anti-goat minus (Sigma Aldrich #DUO92006) were diluted 1:4 in 1x antibody diluent.

Ligation buffer: 5x ligation buffer (Sigma Aldrich #DUO82016) diluted 1:4 in DEPC treated distilled water with the addition of ligase (1:39) (Sigma Aldrich #DUO82029).

Amplification Buffer: 5x amplification buffer (Sigma Aldrich #DUO82018) diluted 1:4 in DEPC treated distilled water with the addition of polymerase (1:79) (Sigma Aldrich #DUO82030).

Mountant: Duolink mounting medium with DAPI (Sigma Aldrich #DUO82040).

2.3 Cell Culture Methods

2.3.1 Cell Thawing

9ml of appropriate media was added to either a T25cm^2 flask or a sterile cell culture dish (Corning) for suspension cells or adherent cells respectively. The flask or dish was placed in the incubator overnight so that the media could acclimatise and to determine whether the media was contaminated. 1x10^7 cells in a cryogenic vial (Corning) were removed from liquid nitrogen and placed in dry ice before being warmed quickly to 37°C in a water bath. Once thawed, the cells were centrifuged at 1500rpm for 5 minutes and the supernatant removed. The cell pellet was re-suspended in 1ml of complete RMPI and immediately added to the flask or dish. The cells were cultured at 37°C 5% CO_2 and a maintained humidity until they had reached a density of 1x10^6 cells/ml before being passaged.

2.3.2 Passaging of Adherent Cell Lines

COS-7 cells were cultured using DMEM in sterile culture dishes at 37°C, 5% CO_2 and a maintained humidity. Once the cells had reached 80% confluency, the DMEM was aspirated and the cells were washed with 10ml sterile 1x PBS. The sterile 1x PBS was aspirated and 1.5ml of 1x trypsin EDTA in PBS was added to the dish. The excess 1x trypsin EDTA in PBS was removed and the dish incubated at 37°C, 5% CO_2 with a maintained humidity for 3 minutes. The dish was removed from the incubator and the sides of the dish were gently tapped to encourage the cells to detach. Cell detachment was determined by microscopy and if cells still appeared to be adherent the dish was placed in the incubator for an additional 2 minutes. The COS-7 cells were re-suspended in 10ml of DMEM and diluted in a new sterile cell culture dish 1:4 before being incubated at 37°C, 5% CO_2 and a maintained humidity.

2.3.3 Passaging of Suspension Cell Lines

Jurkat T cells, HuT-78 T cells and Raji B cells were cultured using RPMI-1640 in T75cm^2 flasks at 37°C, 5% CO_2 and a maintained humidity. Cell density was maintained at approximately 1x10^6 cells/ml by diluting the cells 1:4 using RPMI as required.

2.3.4 Cell Counting

10µl of suspended cells were added to the haemocytometer and covered using a coverslip. Cells were counted in the 5x5 centre grid including the cells overlapping the bottom and right edges. The number of cells were multiplied by 10,000 to give the number of cells per ml.

2.3.5 Cryopreservation

Cells were centrifuged at 1500rpm for 5 minutes and re-suspended in the appropriate volume of freezing mix to give a density of $1x10^7$ cells/ml. 1ml of re-suspended cells were aliquoted into cryogenic vials before being placed on ice. The cryogenic vials were transferred to the -80°C freezer overnight before being transferred to liquid nitrogen for storage.

2.3.6 Transfection of Adherent Cell Lines

COS-7 cells were trypsinised and diluted to achieve a cell density of $1x10^5$ cells/ml as described previously. $2x10^5$ cells were seeded onto sterile baked coverslips in a 6 well plate 24 hours prior to transfection to achieve 50-60% confluency.

2µg of DNA was diluted 9:1 in 2M NaCl and 80µl of ice cold 100% ethanol and incubated at -20°C for 10 minutes. DNA was centrifuged for 5 minutes at 4°C and 14000rpm and the supernatant was discarded. 500µl of ice cold 70% ethanol was added to the DNA pellet before being centrifuged for 5 minutes at 4°C and 14000rpm. Once inside the Class II tissue culture hood the ethanol was aspirated and the pellet was briefly air dried. The 2µg of ethanol precipitated DNA was diluted in 100µl of serum free DMEM and 6µl of Genejuice (Novagen) (1:3) and added to the corresponding coverslip. Cells were incubated at 37°C, 5% CO_2 and a maintained humidity for 24 hours.

2.3.7 T Cell Treatments

Chemical T cell activation: $1x10^6$ cells/ml were incubated with PMA (50nM) and ionomycin (1µM) for 30 minutes at 37°C, 5% CO_2 and a maintained humidity.

Activation of receptors: $1x10^5$ cells were pelleted (1600rpm, 5min) and re-suspended in 100µl of complete RPMI before adding 1µl of C305 anti-TCR monoclonal antibody or anti-CD81 and incubated for 1 hour at 37°C, 5% CO_2 and a maintained humidity.

Induce cellular stress: Sodium arsenite (1mM) was added to $1x10^6$ cells/ml and incubated for 30 minutes at 37°C, 5% CO_2 and a maintained humidity.

2.3.8 Immunological Synapse Formation

Immunological synapses were formed using super-antigen loaded Raji B cells and Jurkat T cells. $6.6x10^6$ Raji B cells were stained using 1µg/ml of Calcein Blue or Green for 20 minutes at 37°C, 5% CO_2 and maintained in the dark. Cells were washed with sterile PBS and incubated with *Staphylococcus aureus* enterotoxin A (1.5µg/ml) and *S. aureus* enterotoxin B (1.5µg/ml) for 30 minutes at 37°C and 5% CO_2 before being re-suspended in 250µl of RPMI. $3.3x10^6$ Jurkat T cells were re-suspended in 250µl of RPMI, added to the super-antigen loaded Raji B cells and incubated at 37°C and 5% CO_2 for 1 hour. Cells were diluted 1:2 in 3% BSA PBS and added to Poly-L-Lysine coated coverslips for 10 minutes. Cells were washed using 3% BSA PBS and fixed using 4% PFA for 10 minutes. 0.2% Triton X-100 PBS was used to permeabilise cells before washing using 3% BSA PBS. Immunological synapses were immunostained as described below.

2.4 Protein Based Methods

2.4.1 Preparation of Protein Samples

$1x10^6$ cells/ml were centrifuged at 1500rpm for 5 minutes and the supernatant discarded. The pellet was gently washed using 1x PBS on ice. The pellet was re-suspended in 1x SDS loading buffer, vortexed and sonicated for 10 seconds. The samples were heated to 95°C for 5 minutes and stored at -20°C.

2.4.2 Co-immunoprecipitation

$1x10^6$ Jurkat cells were lysed in 1ml of lysis buffer, vortexed and sonicated for 10 seconds before centrifugation at 14,000g, 4°C for 10min. The supernatant was transferred to a new Eppendorf and primary antibodies were added at a concentration of 2µg/ml to all supernatants except for the negative control. Supernatants were incubated overnight at 4°C with end-over-end rotation. 300µg of Protein G Dynabeads were added to each supernatant and incubated at room temperature with end-over-end rotation for 30min. Dynabeads were pelleted using a magnetic Eppendorf holder and the supernatants removed. Pellets were washed using wash buffer (Lysis buffer without NP-40) for 5min at room temperature with end-over-end rotation. Beads were pelleted and the supernatants removed before being re-suspended in 1x SDS loading buffer with 4M urea and heated to 95°C for 5min.

2.4.3 Sodium Dodecyl Sulphate Polyacrylamide Gel Electrophoresis

10% SDS polyacrylamide gels were prepared using the BioRad gel casting frame. A 1.5mm backing plate and front plate were inserted into the casting frame and the resolving gel buffer was added. Water saturated butanol was added to the top of the resolving gel buffer to remove air bubbles and create an air tight seal for polymerisation. Once the resolving gel had polymerised, the stacking gel buffer was added and a 1.5mm BioRad comb was inserted between the glass plates. Once the gel had fully polymerised the plates were removed from the casting frame and inserted into the BioRad tetra system either as a pair of gels or with a buffer plate. 1x running buffer was added to the tetra system and equal amounts of protein were loaded into the wells. 2µl of protein ladder (Thermoscientific) was also added. The samples were separated by electrophoresis at 35mA for approximately 1 hour or until fully resolved.

2.4.4 Protein Staining

SDS-PAGE gels were submerged in coomassie blue overnight with gentle agitation. The coomassie blue stain was removed and the gel was incubated with de-stain solution until the excess coomassie blue had been removed. Bands were imaged using the white light setting of a transilluminator.

2.4.5 Western Blotting

Proteins were transferred by semi-dry transfer using Whatman sponges soaked in transfer buffer. An 8cmx6cm PVDF membrane (GE Healthcare) was activated for 10 seconds using methanol, washed for 10 minutes using autoclaved distilled water and acclimatised for 10 minutes using transfer buffer. A soaked sponge was placed onto the semi-dry transfer machine

followed by the PVDF membrane, the SDS-PAGE gel and finally another soaked Whatman sponge. Air bubbles and excess transfer buffer were removed by pressing on the sponges and the proteins transferred at 15v for 1 hour. Protein transfer to the PVDF membrane was confirmed using Ponceau S staining and gentle agitation for 10min and removed by distilled water. Membranes were blocked using 5% BSA TBS or 5% marvel PBS at room temperature for 1 hour. Membranes were incubated with the primary antibody diluted at the appropriate dilution in either 3% BSA TBS or 3% marvel PBS for 1 hour at room temperature or overnight at 4°C. Membranes were washed 3 times for 5 minutes using wash buffer before being incubated with secondary antibodies (1/2000) diluted in 3% BSA TBS or 3% marvel PBS. Membranes were washed again, 3 times for 5 minutes before being incubated with ECL solution (1:1) (Thermoscientific) for 2min. Membranes were blotted dry and visualised using X-ray film exposure which was developed for approximately 1 minute and fixed for approximately 1 minute.

2.4.6 Re-probing of PVDF Membranes

PVDF membranes were re-activated using methanol for 1 minute. The membrane was then washed for 10 minutes using autoclaved distilled water and a further 10 minutes using either 1x PBST or TBST. The western blotting procedure then continued as described above.

2.5 Fluorescent Cell Staining Methods

2.5.1 Fluorescent In Situ Hybridisation

24 Hours post-transfection, the media was aspirated from the wells and the COS-7 cells were washed using 1x PBS. The cells were then fixed for 10 minutes using 4% PFA, washed twice using 1x PBS and then permeabilised using 70% ethanol overnight at 4°C. Cells were incubated for 5 minutes at room temperature in rehydration solution followed by incubation in hybridisation solution overnight at 37°C with a maintained humidity. Cells were washed twice for 30min using wash buffer before being mounted using Prolong Gold® (Molecular Probes).

2.5.2 Immunofluorescence

Suspension cells lines were added to Poly L-Lysine coated coverslips for 10 minutes before excess media was aspirated. Cells were washed once with sterile 1x PBS before being fixed using 4% PFA for 10 minutes at room temperature. After fixation, cells were washed twice with 1x PBS and permeabilised using 0.2% Triton X-100 PBS for 10 minutes at room temperature. 3% BSA PBS solution was added for 1 hour at room temperature to block the coverslips. Primary antibodies were diluted in 3% BSA PBS and cells were incubated for 1 hour at room temperature. Coverslips were washed 3 times for 5 minutes using 1x PBS and secondary antibodies were diluted in 3% BSA PBS. Cells were incubated in secondary antibody diluents for 1 hour at room temperature in the dark. Cells were washed 3 times for 5 minutes followed by incubation with 1µg/ml Hoechst 33258 diluted in 3% BSA PBS for 5 minutes to stain the nuclei. Coverslips were washed twice using 1x PBS before being mounted using Prolong Gold®.

2.5.3 Puromycylation and Immunofluorescence

The puromycylation method has been previously described by David et al. (2012) and was adapted for use with Jurkat T cells and Immune synapses. Sodium arsenite (500μM) was added to $1x10^6$ cells/ml and incubated for 15 minutes at 37°C and 5% CO_2. As a result, translation was inhibited prior to the addition of labelling medium and was used to produce a negative control. Cells were added to Poly-L-Lysine coated coverslips and incubated with labelling medium (208μM emetine and 91μM puromycin in complete RPMI 1640) for 5 minutes at 37°C and 5% CO_2. The cells were washed once with nuclease free 1x PBS, transferred to ice and then incubated in 1x polysome buffer for 20 minutes. Cells were permeabilised and blocked for 15 minutes using staining buffer and incubated with primary antibodies diluted in staining buffer for 1 hour at room temperature. Cells were washed 3 times using 1x PBS and incubated with goat anti-rabbit 568 and goat anti-mouse 488 diluted in staining buffer for 1 hour at room temperature. Cells were again washed 3 times using 1x PBS, incubated with 1μg/ml Hoechst 33258 diluted in staining buffer for 5 minutes and washed again using autoclaved distilled water. Coverslips were mounted using Prolong Gold.

2.5.4 Proximal Ligation Assay

The Duolink In Situ Red kit (Sigma DUO92101) was used to carry out the proximal ligation assay according to the manufacturers' instructions as depicted in figure 2.1-1.

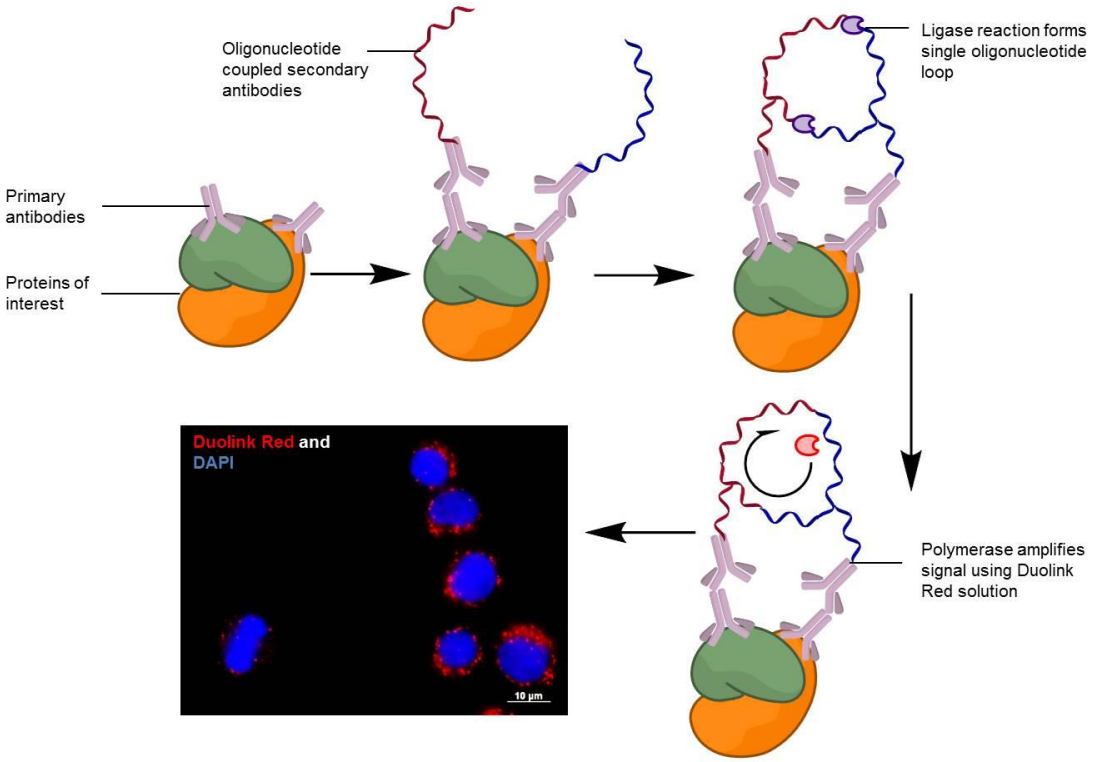

Figure 2.1-1 Stages of the proximal ligation assay. Cells were incubated with the corresponding primary antibodies of different species which bound the target proteins. The species A-plus and species B-minus oligonucleotide conjugated secondary antibodies associated with the corresponding primary antibodies. If the secondary antibodies were within a 40nm range, a ligase ligated the plus and minus oligonucleotides to form one nucleotide ring. A polymerase and amplification red solution amplified the signal of the complex to produce a red dot visible by fluorescence microscopy (Soderberg et al., 2006).

Cells were applied to poly-L-lysine coated coverslips, unless stated in a previous step, and blocked overnight at 4°C by inverting the coverslip on 200µl of 1x blocking solution. The blocking solution was applied to parafilm within a large, foil lined petri dish with DEPC-treated distilled water moistened blue tissue to maintain humidity. Cells were incubated with the primary antibodies diluted in 50µl of 1x antibody diluent per coverslip for 1 hour at room temperature. Coverslips were transferred to a 24 well plate and cells were washed twice using 200µl of nuclease free 1x PBS for 5 minutes with orbital shaking. The oligonucleotide conjugated secondary antibodies: anti-rabbit plus; anti-mouse minus; or anti-goat minus; were diluted 1:4 in 50µl of 1x antibody diluent per coverslip and applied to parafilm within the petri dish. Coverslips were inverted on the antibody diluent and incubated for 1 hour at 37°C. Coverslips were transferred to the 24 well plate and cells were washed twice for 5 minutes using 200µl of 1x wash buffer A with orbital shaking. The ligase was diluted in 50µl of 1x ligation buffer per coverslip and applied to the parafilm. Coverslips were inverted upon the ligation buffer and incubated for 30 minutes at 37°C. Coverslips were transferred to the 24 well plate and cells were washed twice for 2 minutes using 200µl of 1x wash buffer A with orbital shaking. The polymerase was diluted in 50µl of 1x amplification buffer per coverslip and applied to the parafilm. The coverslips were inverted upon the amplification buffer and cells were incubated for 100 minutes at 37°C in the dark using foil. Coverslips were transferred to the foil covered 24 well plate and cells were washed twice for 10 minutes using 200µl 1x wash buffer B with orbital shaking and again for 1 minute using 200µl 0.01x wash buffer B before being mounted using Duolink mountant with DAPI.

2.5.5 Antibodies

A comprehensive list of the antibodies used including their species and isotype, place of purchase and catalogue number is described in the appendix (pages 174-6).

2.6 Imaging Methods

2.6.1 Fluorescence Microscopy

Images were acquired using either a Zeiss AxioSkop MOT or a Zeiss Imager M2 and a 63x Plan-Apochromat Ph3 (NA 1.4) oil immersion objective.

2.6.2 Confocal Microscopy

Confocal images were acquired using a Zeiss LSM710 laser scanning microscope with a 63x Plan-Apochromat Ph3 (NA 1.4) oil immersion objective. Channel images were obtained sequentially using UV, 488, 561 and 633nm lasers. Pinhole diameter was set to 1 Airy unit and an optimal slice thickness of 0.43µm was used.

2.6.3 Analysis of Images

Images were analysed using the Fiji Version of ImageJ (Schindelin et al., 2012). Images were separated by channel colour using the split channel function and the average pixel size of the cells was calculated and used to set the rolling ball radius, beyond which the background was subtracted. Channel intensity was adjusted using the brightness and contrast function in an equal adjustment across all channels. To create representative Z stack images, Z stacks were compressed into single images using the maximum intensity setting of the Z project function. For quantitative PLA analysis, single red dots

were manually marked and counted using the ROI manager and “analyse particle” function.

2.7 Computational Methods

2.7.1 DEF6 Protein Sequence Alignment

DEF6 amino acid sequences were retrieved using UniProt and the FASTA sequences were aligned by T-Coffee using the default M-Coffee settings (Notredame et al., 2000; Wallace et al., 2006; Moretti et al., 2007). M-Coffee was used because it utilises a number of multiple sequence alignment methods, including Clustal and Muscle analysis, to align a protein sequence without a definitive tertiary structure.

2.7.2 RNA Bind R Analysis

The Homo sapien DEF6 amino acid sequence was analysed using RNA Bind R to determine the likelihood of each amino acid binding mRNA in the context of the adjacent amino acids. An amino acid likely to bind mRNA in its current context was awarded 1.0 if it scored >0.5 and amino acids unlikely to bind mRNA scored ≤0.5 (Terribilini et al., 2007).

2.7.3 Statistical Analysis

Statistical analyses were carried out using GraphPad Prism. To compare multiple test samples to one another, an ordinary one-way ANOVA was used to determine a significant difference between the groups. Further analysis was carried out if the standard deviations of the groups were not significantly different. Tukey's multiple comparisons test was then used to determine which groups were significantly different from one another. If the sample spread was unlikely to have a binomial distribution then a non-parametric Kruskal-Wallis one-way ANOVA was used. The comparison of multiple treatment groups to a control was carried out using a multiple comparison t-test which used the Holm-Sidak method and a significance level of 5%.

2.8 Summary of Granules and the Treatment Effects

Table 2.8-1 Summary of the key granules and the treatment effects within this work.

Granule Type	Example Markers	Induced by	Inhibited by	Expression	Role
Polysomes	PABP EIF4E	Puromycin and Emetine	Sodium arsenite	Ubiquitous	Enrichment of ribosomes to increase the efficiency of protein synthesis. Multiple ribosomes translocate along a transcript and synthesise multiple peptides concurrently.
Stress Granules	PABP EIF4E G3BP	Sodium arsenite	Puromycin	Ubiquitous	Stalled pre-initiation complexes complete with mRNA transcripts. Allows temporary storage of the transcripts and key translation factors until cellular conditions improve.
P-bodies	4E-T DCP1 DCP2	Puromycin	Cycloheximide	Ubiquitous	Enriched areas of mRNA degradation machinery and self-aggregating proteins. Allows efficient de-capping and degradation of mRNA transcripts that are no longer required or are incorrect. Provides a focus for posttranscriptional changes to expression by miRNA and the RISC complex.
Vesicle-like structures	DEF6 Sphingolipids Triacylglycerols Cholesterol	Puromycin and Emetine	Unknown	Currently Jurkat T cells	Structures visible within the Jurkat T cell that are stained using Nile red. Nile red selectively stains sphingolipids, cholesterols and triacylglycerols indicating a lipid rich environment. The vesicle-like structures also appear to have an enrichment of DEF6.

Chapter 3 Results

3.1 DEF6 aggregation is linked to mRNA turnover in T cells

3.1.1 DEF6 forms aggregates in different T cell states

As described previously by Hey et al. (2012), DEF6 is able to form cytoplasmic granules in response to cellular stress. However, the presence of endogenous cytoplasmic granules in other T cells states was not investigated. For example, does DEF6 form aggregates during T cell activation and are those aggregates present in the resting state prior to activation or stress?

To test this, Jurkat T cells were re-suspended in fresh RMPI 1640 and either remained untreated (a) or were treated with PMA and ionomycin (b) or sodium arsenite (c) in suspension at 37°C for 30 minutes. Cells were applied to poly-L-lysine coated coverslips and DEF6 was stained using rabbit anti-DEF6 and goat anti-rabbit 568.

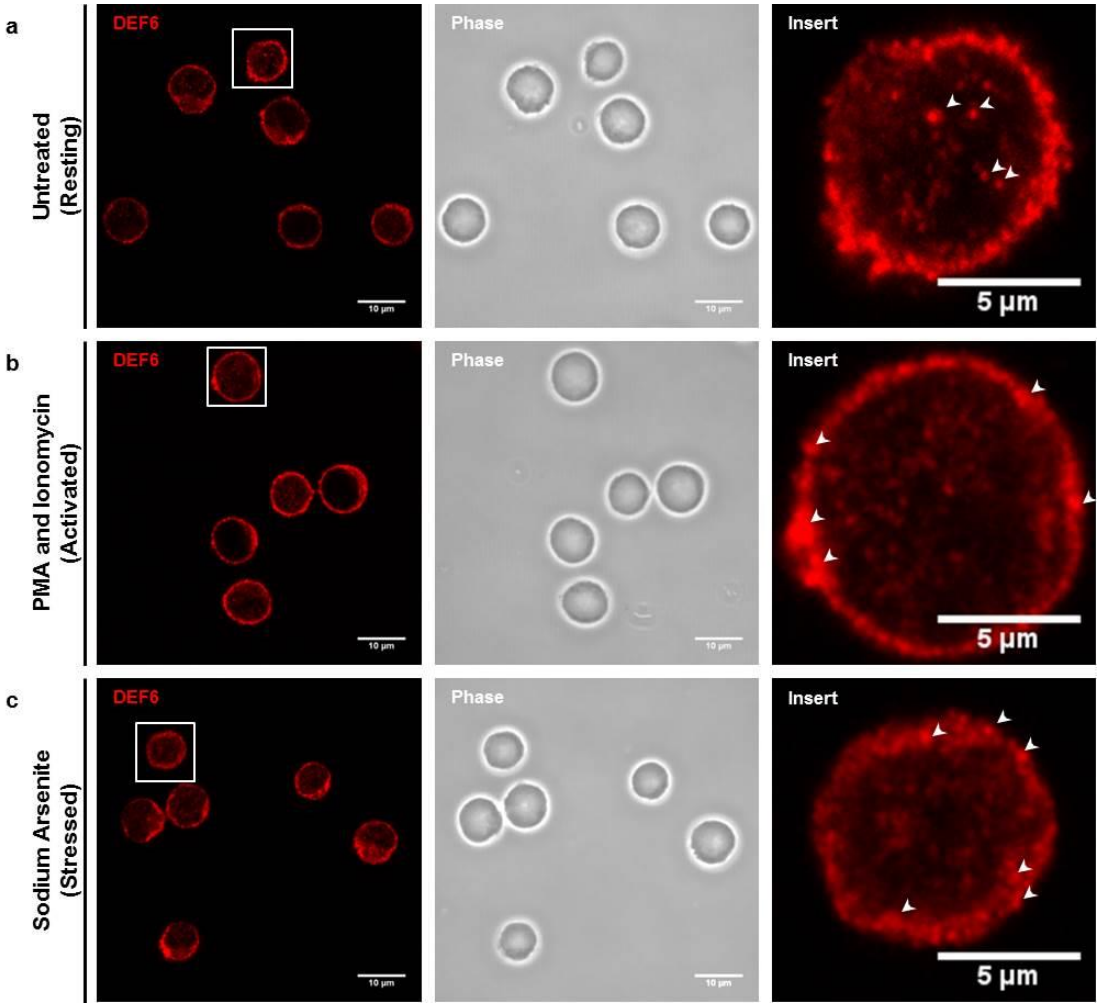

Figure 3.1-1 DEF6 forms aggregates in resting, activated and stressed states. Jurkat T cells were either left untreated (**a**), activated using PMA and ionomycin (**b**) or stressed using sodium arsenite (**c**) for 30 minutes at 37°C. DEF6 was stained using rabbit anti-DEF6 and goat anti-rabbit 568 before cells were imaged using confocal microscopy. Images are of a single z plane at 63x magnification. Arrow heads highlight areas of aggregation within the cell.

As shown in figure 3.1-1, DEF6 forms aggregates in resting (a), chemically activated (b) and stressed (c) Jurkat T cells. A high proportion of DEF6 is present at the plasma membrane in all 3 states however aggregation can also be seen within the cytoplasm. Representative images also show that in the stressed state, more cells display DEF6 aggregation within the cytoplasm however resting and activated states appear to have a similar number of cells displaying DEF6 aggregation.

3.1.2 DEF6 protein levels increase in response to activation

A general observation that a higher number of stressed Jurkat T cells appeared to display DEF6 aggregation in comparison to resting T cells led to an investigation of DEF6 protein expression in response to chemical activation and stress.

To test this, Jurkat T cells were re-suspended in fresh RPMI 1640 and either remained untreated (resting) or were treated with PMA and ionomycin (activated) or sodium arsenite (stressed) in suspension at 37°C for 30 minutes. Jurkats were pelleted and separated by SDS-PAGE before being immunoblotted using anti-DEF6 and anti-β actin. β-actin was used as a loading control to normalise DEF6 densitometry values in comparison to the untreated sample to reduce the effect of protein loading on the sample densitometry (3.1-2A). The mean adjusted relative values for three independent repeat experiments were compared using the non-parametric Kruskal-Wallis one-way ANOVA to determine whether there was a significant difference in the level of DEF6 protein expression in comparison to untreated Jurkat T cells as shown in figure 3.1-2B.

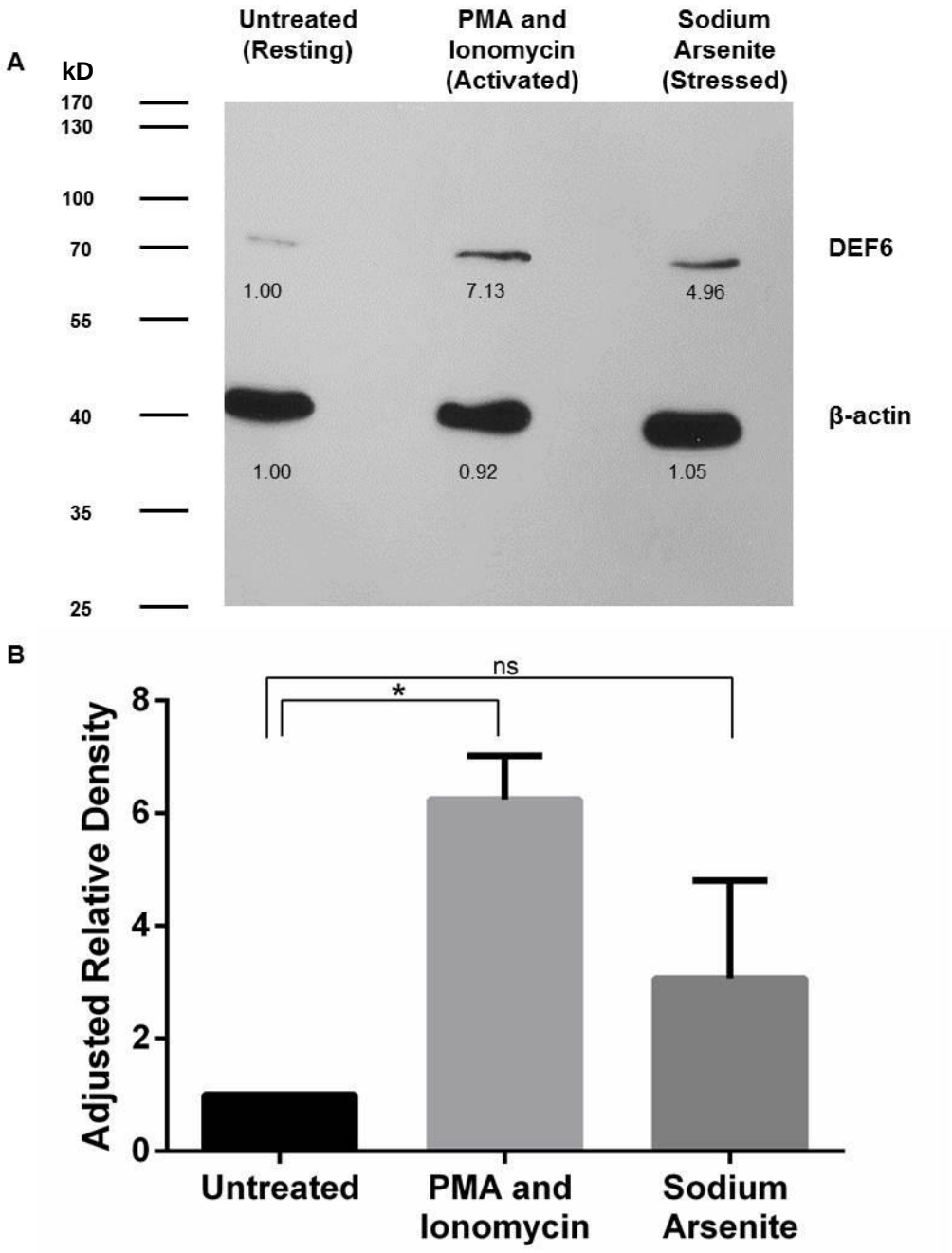

Figure 3.1-2 DEF6 expression in activated Jurkat T cells is increased in relation to untreated cells. Jurkat T cells were either left untreated, activated using PMA and ionomycin or stressed using sodium arsenite for 30 minutes at 37°C. **A** - Cell lysates were separated by SDS-PAGE and immunoblotted. β-actin was used as a loading control and to normalise DEF6 density values. **B** – Mean adjusted relative values for three independent repeat experiments were compared using the non-parametric Kruskal-Wallis one-way ANOVA. Error bars represent the standard deviation, * $p \leq 0.05$ and ns is not significant.

In response to chemical activation using PMA and ionomycin, DEF6 protein expression increased to a normalised density value of 7.13 in comparison to untreated Jurkats which is significantly higher ($p \leq 0.05$). Moreover, stressing of Jurkats using sodium arsenite also resulted in an increase in DEF6 protein expression to a normalised density value of 4.96 in comparison to untreated cells however the increase is not significantly different as shown in figure 3.1-2.

3.1.3 DEF6 is in close proximity to 4E-T in resting and stressed T cells

As demonstrated by Hey et al. (2012), exogenous DEF6 aggregates co-localise with DCP1 in COS-7 cells in response to stress. However, investigation of endogenous DEF6 aggregates and a P-body marker was not investigated. The transporter of eIF4E, known as 4E-T, is a P-body specific marker which is universally expressed (Ferraiuolo et al., 2005). To confirm a link between DEF6 and P-bodies, an association between DEF6 and 4E-T was investigated using co-localisation and a proximal ligation assay (PLA).

Jurkat T cells were re-suspended in RMPI 1640 and were either left untreated (resting) or treated with PMA and ionomycin (activated) or sodium arsenite (stressed) in suspension at 37°C for 30 minutes. Cells were applied to poly-L-lysine coated coverslips and DEF6 was stained using rabbit anti-DEF6 and donkey anti rabbit-568 whilst 4E-T was stained using goat anti-4E-T and donkey anti-goat 488. Nuclei were stained using Hoechst 33258 and cells were imaged using confocal microscopy (3.1-3A).

Quantitative analysis of the granules was achieved by counting the aggregates which had a red, green or yellow signal for each of the treatment states. Aggregate signals were isolated by adjusting the colour threshold to remove the general cytoplasmic signal based upon the resting images. Red aggregates were isolated by adjusting the brightness to between 200-255, green aggregates had a brightness between 140-255 and yellow aggregates had a hue of 30-50 and a brightness of 70-255. The analyse particles function was used to count the aggregates which retained a signal and preliminary data from a single culture (n=6) was analysed using a two-way ANOVA and Tukey's multiple comparison as shown in figure 3.1-3B.

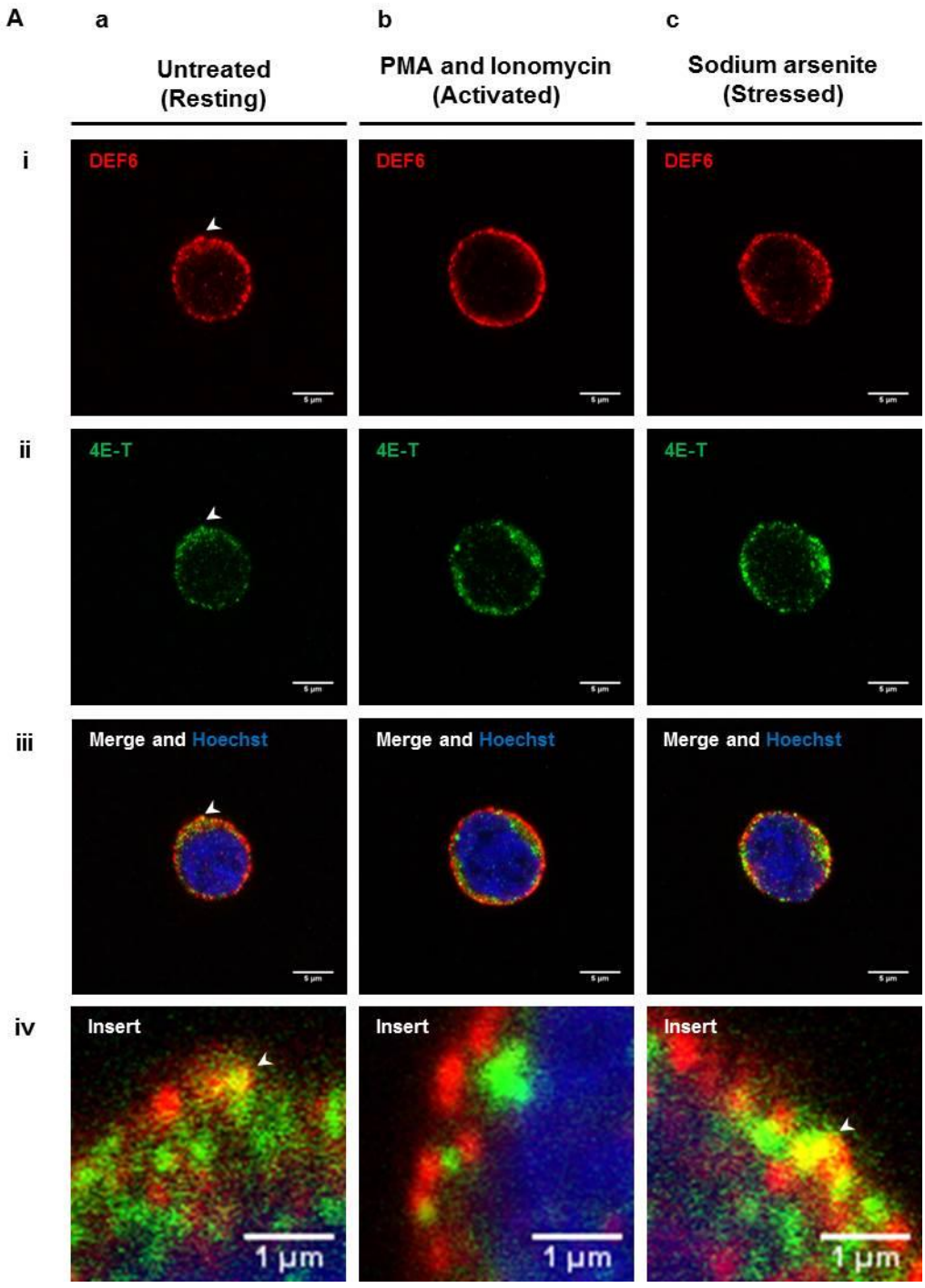
A
a
b
c
Untreated (Resting)
PMA and Ionomycin (Activated)
Sodium arsenite (Stressed)
i
DEF6
ii
4E-T
iii
Merge and Hoechst
iv
Insert
1 µm

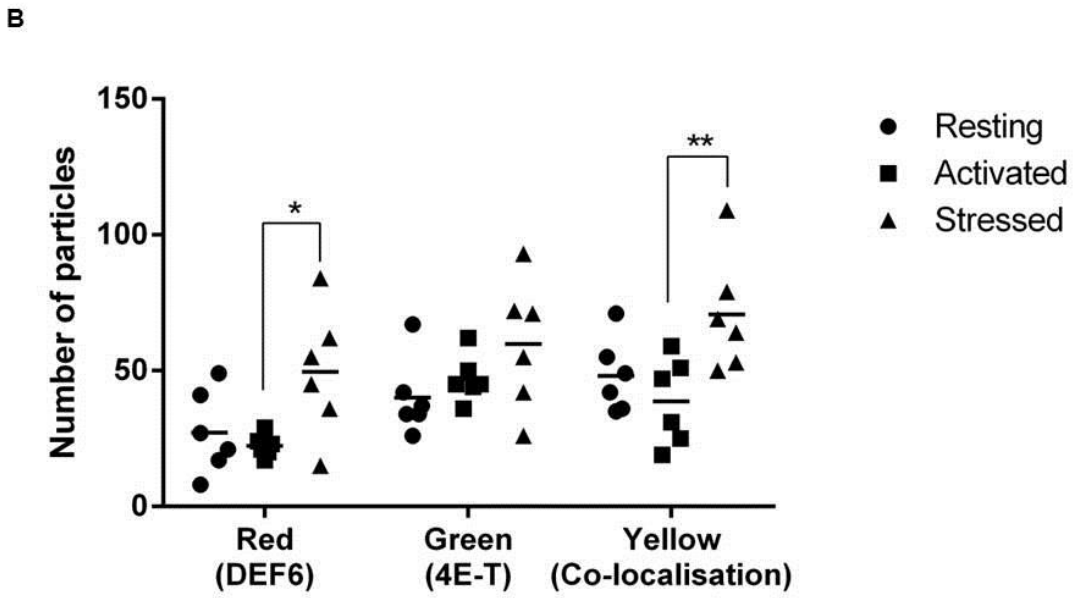

Figure 3.1-3 DEF6 and 4E-T co-localise in untreated (resting) and sodium arsenite treated (stressed) cells. **A** - Jurkat T cells were either left untreated, chemically activated using PMA and ionomycin or stressed using sodium arsenite for 30 minutes at 37°C. Cells were then applied to Poly-L-Lysine coated coverslips, fixed, and stained using rabbit anti-DEF6 and goat anti-4E-T. Primary antibodies were then labelled using donkey anti-rabbit 568 and donkey anti-goat 488 respectively. Images are of a single z plane at 63x magnification taken using a Zeiss LSM710 confocal microscope. White arrowheads indicate co-localisation. **B** – Particles were counted in the red, green and yellow hues by adjusting the colour threshold to isolate the aggregate signals. DEF6 aggregates were indicated by red signals with a brightness between 200-255, 4E-T aggregates were indicated by green signals with a brightness between 140-255 and co-localised aggregates were indicated by a yellow signal with a hue between 30-50 and a brightness between 70-255. Particles were then automatically counted within these thresholds using the analyse particles function in Fiji. Results are from a single Jurkat cell culture that was aliquoted and subjected to the stated treatments (n=6). Preliminary statistical analysis used a two-way ANOVA and Tukey's multiple comparison to compare the varying treatments for each aggregate type.

In preparation for the PLA, Jurkat T cells either remained untreated (resting), treated with PMA and ionomycin (activated) or sodium arsenite (stressed) as described above. Cells were again applied to poly-L-lysine coated coverslips and DEF6 was labelled using rabbit anti-DEF6 whilst 4E-T was labelled using goat anti-4E-T. The primary antibodies were labelled using oligonucleotide coupled secondary antibodies, donkey anti-rabbit plus and donkey anti-goat minus labelled anti-DEF6 and anti-4E-T respectively. A ligase reaction was used to couple the two oligonucleotide probes if they were within a 40nm range of one another and a polymerase reaction was used to amplify the signal of the ligated oligonucleotide using the red amplification buffer. Nuclei were labelled with DAPI within the duolink mountant and cells were imaged by confocal microscopy (3.1-4A).

The mean number of duolink red signals per cell was calculated however a small sample size prevents a statistical comparison between the different treatment states as $2 \leq n \geq 6$ as shown in figure 3.1-4B.

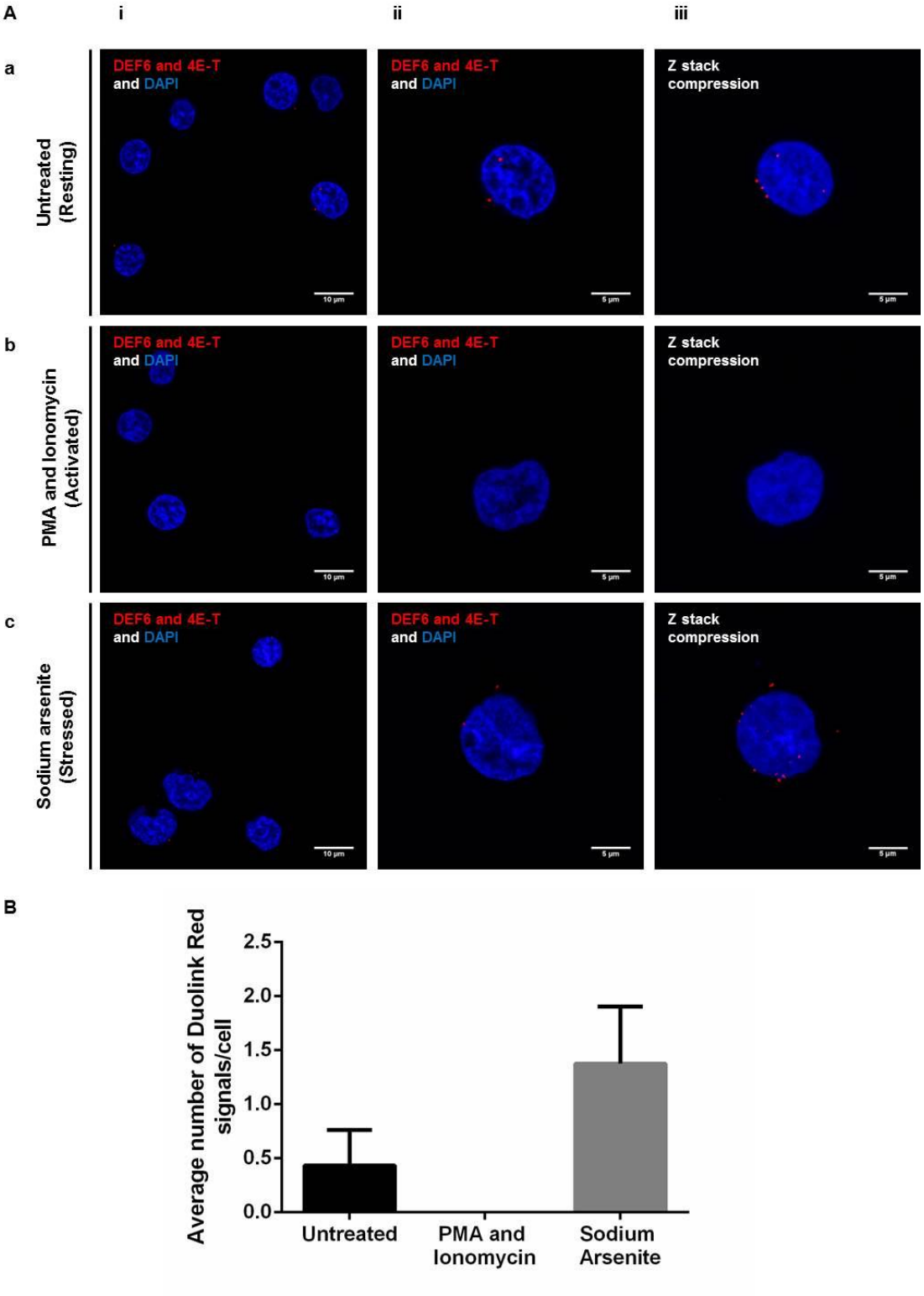
A
i
ii
iii
a
Untreated (Resting)
DEF6 and 4E-T and DAPI
DEF6 and 4E-T and DAPI
Z stack compression
b
PMA and Ionomycin (Activated)
DEF6 and 4E-T and DAPI
DEF6 and 4E-T and DAPI
Z stack compression
c
Sodium arsenite (Stressed)
DEF6 and 4E-T and DAPI
DEF6 and 4E-T and DAPI
Z stack compression
B
Average number of Duolink Red signals/cell
2.5
2.0
1.5
1.0
0.5
0.0
Untreated
PMA and Ionomycin
Sodium Arsenite

Figure 3.1-4 DEF6 is in close proximity to 4E-T in Resting and stressed Jurkat T cells. **A** - Cells were applied to Poly-L-Lysine coated coverslips, fixed, and labelled using rabbit anti-DEF6 and goat anti-4E-T. Proteins in close proximity were detected using Duolink Red (Sigma) according to the manufacturer's instructions. Images are of a single z plane at a 63x magnification and either a 2x zoom (**i**) or a 4x zoom (**ii**). Images to the right represent the entire cell following compression of the corresponding z-stack into a single image (**iii**). The number of dots per cell for each of the 1x zoom images were counted using nuclei to define a single cell and the mean number of dots per cell was calculated. **B** - Preliminary data suggests that more DEF6 may be in close proximity to 4E-T in sodium arsenite treated cells in comparison to untreated cells and PMA and Ionomycin activated cells. PMA and Ionomycin activation results in an abolishment of DEF6 and 4E-T being in close proximity to one another. Bars indicate the mean of two replicates and the standard deviation is represented as error bars where $2 \leq n \geq 6$.

As shown in Figure 3.1-3A, fluorescent microscopy appears to show co-localisation between DEF6 and 4E-T in the untreated (Aa) and sodium arsenite treated (Ac) states. Images Aa-iv and Ac-iv show representative examples of co-localisation between DEF6 and 4E-T, within aggregates that appear to be at the plasma membrane, in the resting and stressed states respectively. Moreover, there appears to be more co-localisation between DEF6 and 4E-T in response to sodium arsenite treatment with more aggregates displaying co-localisation, as indicated by the white arrow heads in images Ac-i, ii and iii, in comparison to the resting state (Aa). However, chemical activation of Jurkats using PMA and ionomycin appears to reduce DEF6 and 4E-T co-localisation (Ab) as the 4E-T distribution remains within the cytoplasm and does not appear to quite reach the plasma membrane (Ab-iv). Quantification of the aggregates in the varying hues also appears to show an increase in co-localisation between DEF6 and 4E-T following sodium arsenite treatment as shown in figure 3.1-3B. Preliminary statistical analysis shows that there was significantly more yellow aggregates following sodium arsenite treatment in comparison to chemical activation ($p \leq 0.01$).

To further corroborate these data, DEF6 appears to be in close proximity with 4E-T in untreated and stressed Jurkat T cells (Figure 3.1-4Aa and Ac respectively). However, chemical activation using PMA and ionomycin completely abolishes the proximal signal (Ab). Preliminary data suggests that there is an increase in the number of DEF6 and 4E-T proximal signals in response to sodium arsenite treatment in comparison to untreated cells, with an average PLA signal density of 1.5 signals/cell in comparison to 0.5 signals/cell, as shown in figure 3.1-4B.

To determine whether the abolishment of DEF6 and 4E-T proximity was due to an absence of P-bodies, a PLA was carried out using DDX6 and 4E-T. Both DDX6 and 4E-T are key components of P-bodies and are specific markers.

Cells were treated as above and again applied to poly-L-lysine coated coverslips. DDX6 was labelled using rabbit anti-DDX6 whilst 4E-T was labelled using goat anti-4E-T. The primary antibodies were labelled using oligonucleotide coupled secondary antibodies, donkey anti-rabbit plus and donkey anti-goat minus labelled anti-DDX6 and anti-4E-T respectively. A ligase reaction was used to couple the two oligonucleotide probes if they were within a 40nm range of one another and a polymerase reaction was used to amplify the signal of the ligated oligonucleotide using the red amplification buffer. Nuclei were labelled with DAPI within the duolink mountant and cells were imaged by confocal microscopy (3.1-5A). The mean number of PLA signals per cell was calculated and compared using multiple t-tests with untreated as the comparative control (3.1-5B).

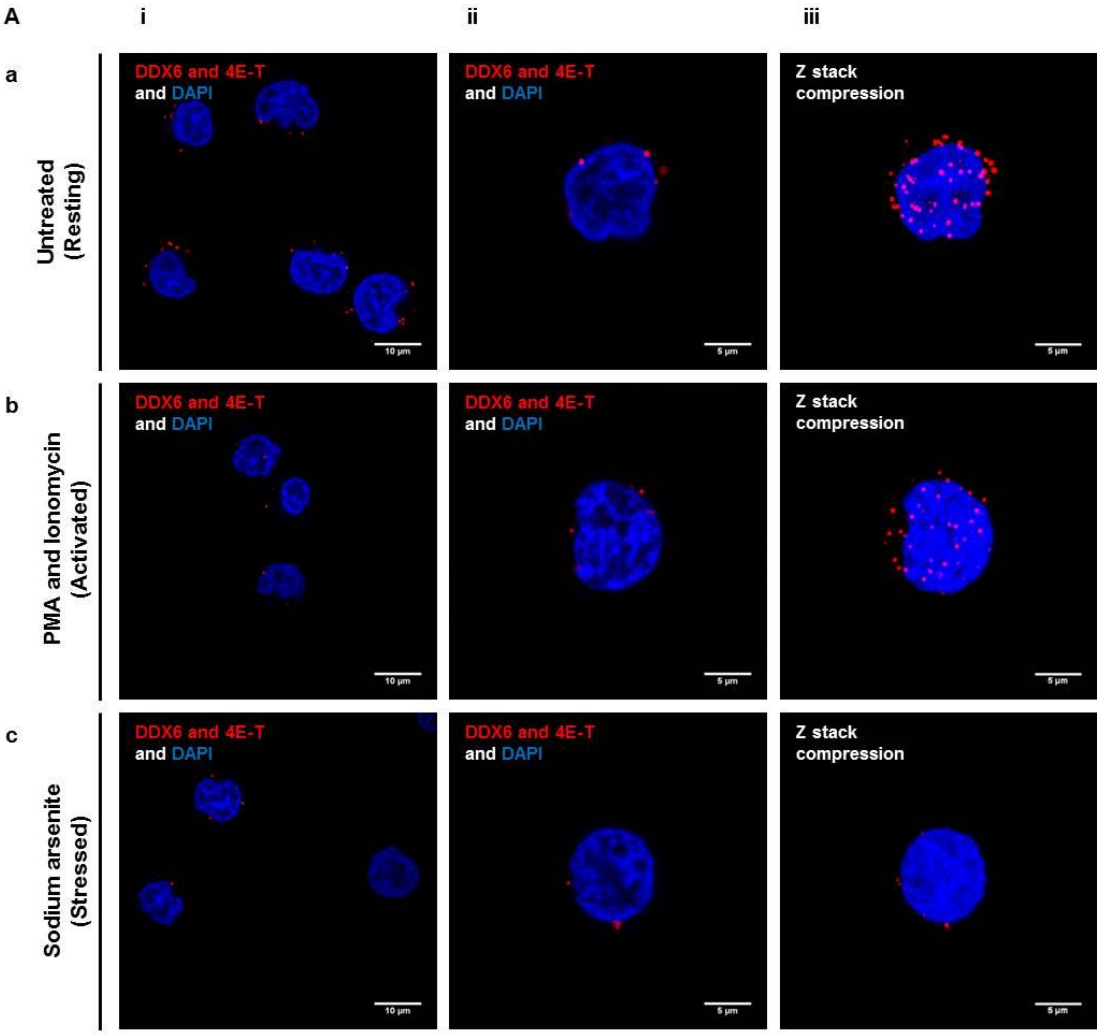
A
i
ii
iii
a
Untreated (Resting)
DDX6 and 4E-T and DAPI
DDX6 and 4E-T and DAPI
Z stack compression
b
PMA and Ionomycin (Activated)
DDX6 and 4E-T and DAPI
DDX6 and 4E-T and DAPI
Z stack compression
c
Sodium arsenite (Stressed)
DDX6 and 4E-T and DAPI
DDX6 and 4E-T and DAPI
Z stack compression
10 µm
5 µm

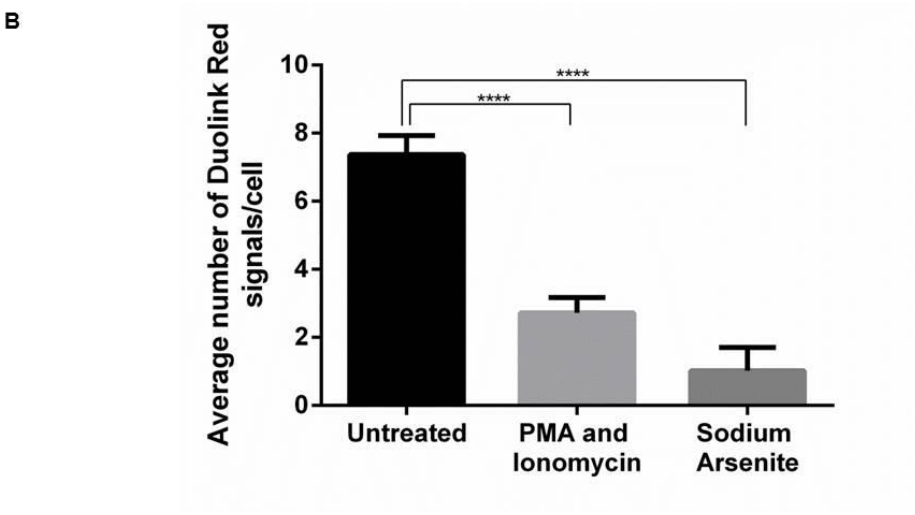
B
Average number of Duolink Red signals/cell
10
8
6
4
2
0
****
****
Untreated
PMA and Ionomycin
Sodium Arsenite

Figure 3.1-5 DDX6 is in close proximity to 4E-T when T cells are resting, chemically activated or stressed. Jurkat T cells were either left untreated, chemically activated using PMA and Ionomycin or stressed using sodium arsenite for 30 minutes at 37°C. Cells were then applied to Poly-L-Lysine coated coverslips, fixed, and labelled using rabbit anti-DDX6 and goat anti-4E-T. Proteins in close proximity were detected using Duolink Red (Sigma) according to the manufacturer's instructions. **A** - Images are of a single z plane at a 63x magnification and either a 2x zoom (**i**) or a 4x zoom (**ii**). Images to the right represent the entire cell following compression of the corresponding z-stack into a single image (**iii**). The number of dots per cell for each of the 1x zoom images were counted using nuclei to define a single cell and the mean number of dots per cell was calculated. **B** - More DDX6 is in close proximity to 4E-T in untreated cells in comparison to chemically activated or stressed Jurkat T cells. The average number of Duolink Red signals per cell was calculated and compared using multiple t-tests using untreated as the comparative control. For each staining condition $20<n>40$ with 3 replicates. Error bars represent the standard deviation and **** $p \leq 0.0001$.

Chemical activation of Jurkat T cells using PMA and ionomycin does not prevent P-body formation but does significantly reduce the number of DDX6 and 4E-T proximal signals suggesting fewer P-bodies. For example, the average number of PLA signals in untreated cells is around 7.5 signals per cell which is significantly higher than the activated state which has an average of 3 PLA signals per cell ($p \leq 0.0001$) as shown in figure 3.1-5B. Inducement of stress in Jurkat T cells using sodium arsenite also significantly reduces the number of DDX6 and 4E-T proximal signals resulting in 1 PLA signal per cell in stressed cells in comparison to 7.5 PLA signals per cell in untreated cells ($p \leq 0.0001$).

3.1.4 DEF6 granules co-localise with mRNA

As DEF6 forms aggregates regardless of the T cell state and these aggregates appear to be linked to mRNA turnover, DEF6 aggregates were investigated using FISH to determine whether they contain or co-localise with mRNA. To ensure that the aggregates were sufficiently large for the labelled mRNA to be visualised using confocal microscopy, exogenous DEF6 aggregates were used in COS-7 cells. To further the work of Hey et al. (2012), the phosphomimic Y210EY222E DEF6 mutant was used to mimic phosphorylation of DEF6 by ITK. YFP DCP2 was used as a positive control as DCP2 is a core component of P-bodies and can also self-aggregate to provide the necessary scaffold for endogenous proteins (Eulalio et al., 2007a). mRNA was labelled using a Cy5 coupled Oligod(T) which hybridised to the poly(A) tail of endogenous mRNA allowing visualisation by confocal microscopy.

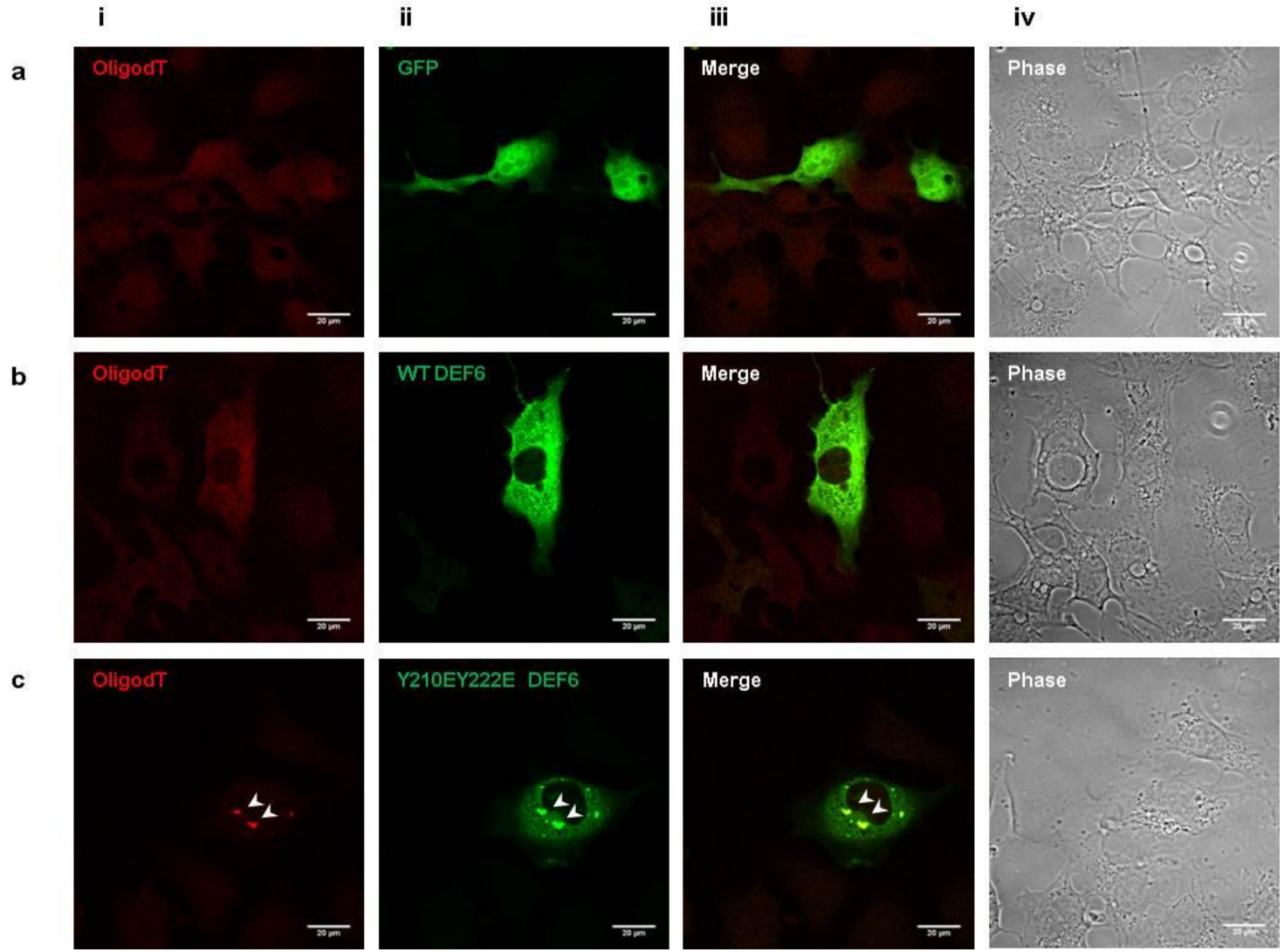
i
ii
iii
iv
a
OligodT
GFP
Merge
Phase
b
OligodT
WT DEF6
Merge
Phase
c
OligodT
Y210EY222E DEF6
Merge
Phase

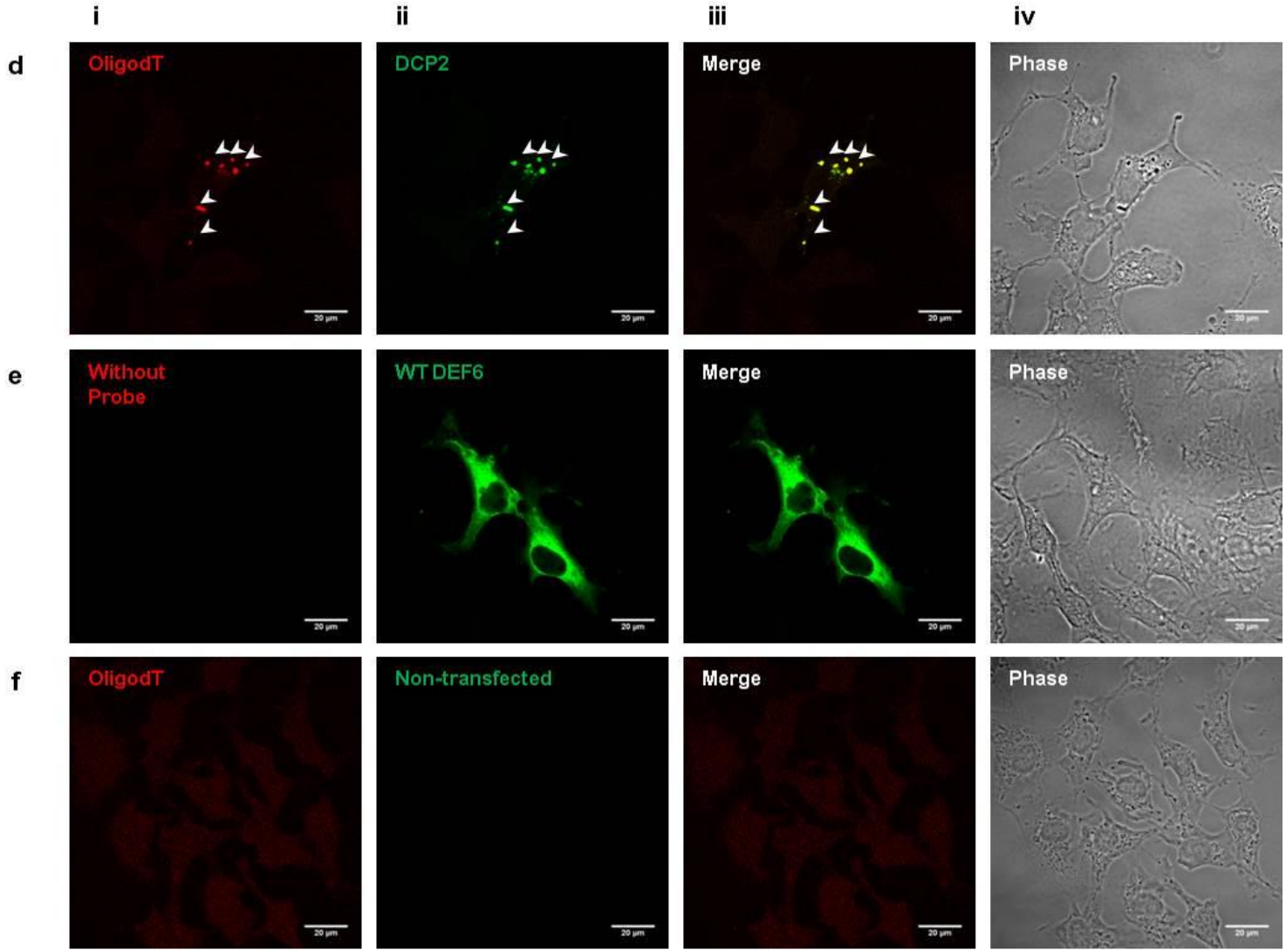
i
ii
iii
iv
d
OligodT
DCP2
Merge
Phase
e
Without Probe
WT DEF6
Merge
Phase
f
OligodT
Non-transfected
Merge
Phase

Figure 3.1-6 Exogenously expressed DEF6 aggregates co-localise with mRNA in COS-7 cells. GFP labelled wild type DEF6; phosphomimic Y210EY222E DEF6; DCP2; and GFP alone; were exogenously expressed in COS-7 cells for 24 hours. Cells were fixed, permeabilised using 70% ethanol overnight and rehydrated prior to incubation with the Cy5 conjugated oligod(T) probe. To ensure the specificity of the technique, COS-7 cells exogenously expressing wild type DEF6 were subjected to the same procedure in the absence of the oligod(T) probe and cells transfected in the absence of plasmid were also labelled using the oligod(T) probe. Images are of a single z plane at a 63x magnification taken using a Zeiss LSM710 confocal microscope. White arrow heads indicate areas of aggregation that co-localise with enrichment of mRNA.

In response to Y210EY222E DEF6 expression, mRNA is aggregated and co-localises with the phosphomimic aggregates as indicated by the white arrow heads in figure 3.1-6c i-iii. Expression of YFP DCP2 also causes mRNA aggregation and co-localisation indicating that this is a specific result (di-iii). Moreover, expression of GFP alone does not affect the localisation of mRNA demonstrating that the GFP label of the phosphomimic DEF6 has no effect on the mRNA (ai and aiii). Interestingly, image bi shows that wild type DEF6 does not affect mRNA localisation as it remains diffuse as previously described (Hey et al., 2012). To further demonstrate the specificity, the absence of the Oligod(T) probe does not result in a residual background red signal nor does the transfection of COS-7 cells affect the mRNA distribution within the cell (images ei-iii and fi-iii respectively). Consequently, DEF6 may be directly or indirectly associated with mRNA.

3.1.5 Summary of main findings

- DEF6 forms aggregates in Jurkat T cells regardless of cell treatment and chemical activation results in an increase of cellular DEF6.
- DEF6 is in close proximity to 4E-T and preliminary data suggests that the number of proximal signals increases in response to sodium arsenite treatment however the number of P-bodies containing DDX6 decreases.
- Phosphomimic Y210EY222E DEF6 aggregates co-localise with mRNA indicating DEF6 may be directly or indirectly associated with mRNA.

3.2 DEF6 is in close proximity to active translation and translation factors

Previous work in the laboratory, carried out by Dr Peter Jones (unpublished), has highlighted a potential link between DEF6 and active translation as DEF6 was co-precipitated with polysomes in Jurkat T cells as described in chapter 1.4.3. New research suggests that other proteins with a well-established metabolic role may in fact be involved with active translation as well. For example, proteins imperative to the process of glycolysis and the Krebs cycle may also regulate the translation of the respective partner proteins of these processes in response to the availability of glucose (Beckmann et al., 2015). This new hypothesis adds another complex layer to the regulation of protein synthesis within the cell, and allows efficient regulation in response to multiple different stimuli in a selective manner. As a result, identification of potential new translation regulators with established roles within cell signalling and metabolism is essential to further understand how cells regulate such a complex process and the consequences when this regulation is insufficient.

3.2.1 DEF6 co-localises with active translation in Jurkat T cells

To visualise polysomes engaged in active translation by confocal microscopy, the puromycylation method was used. Briefly, puromycin is incorporated into the synthesised polypeptide chain, anti-puromycin is used to label the polypeptide chain itself. The use of emetine in conjunction with puromycin prevents the dissociation of the ribosomal complex and the release of the puromycin incorporated polypeptide chain. Subsequently, a fluorescently labelled secondary antibody is used to visualise the complete ribosomal

complex and indicates sites of active translation prior to fixation using ribosome stabilising buffers (David et al., 2012).

To do this, Jurkat T cells were re-suspended in fresh RPMI and negative control cells were pre-incubated with sodium arsenite, to prevent activate translation, in suspension at 37°C for 15 minutes. Jurkats were applied to poly-L-lysine coated coverslips and were either left untreated or incubated with puromycin and emetine for 5 minutes at 37°C. Cells were fixed with polysome stabilisation buffers containing 3% PFA whilst on ice. DEF6 was stained using rabbit anti-DEF6 and goat anti-rabbit 568 whilst puromycin was stained using mouse anti-puromycin and goat anti-mouse 488. Nuclei were stained using Hoechst 33258 and cells were imaged by confocal microscopy.

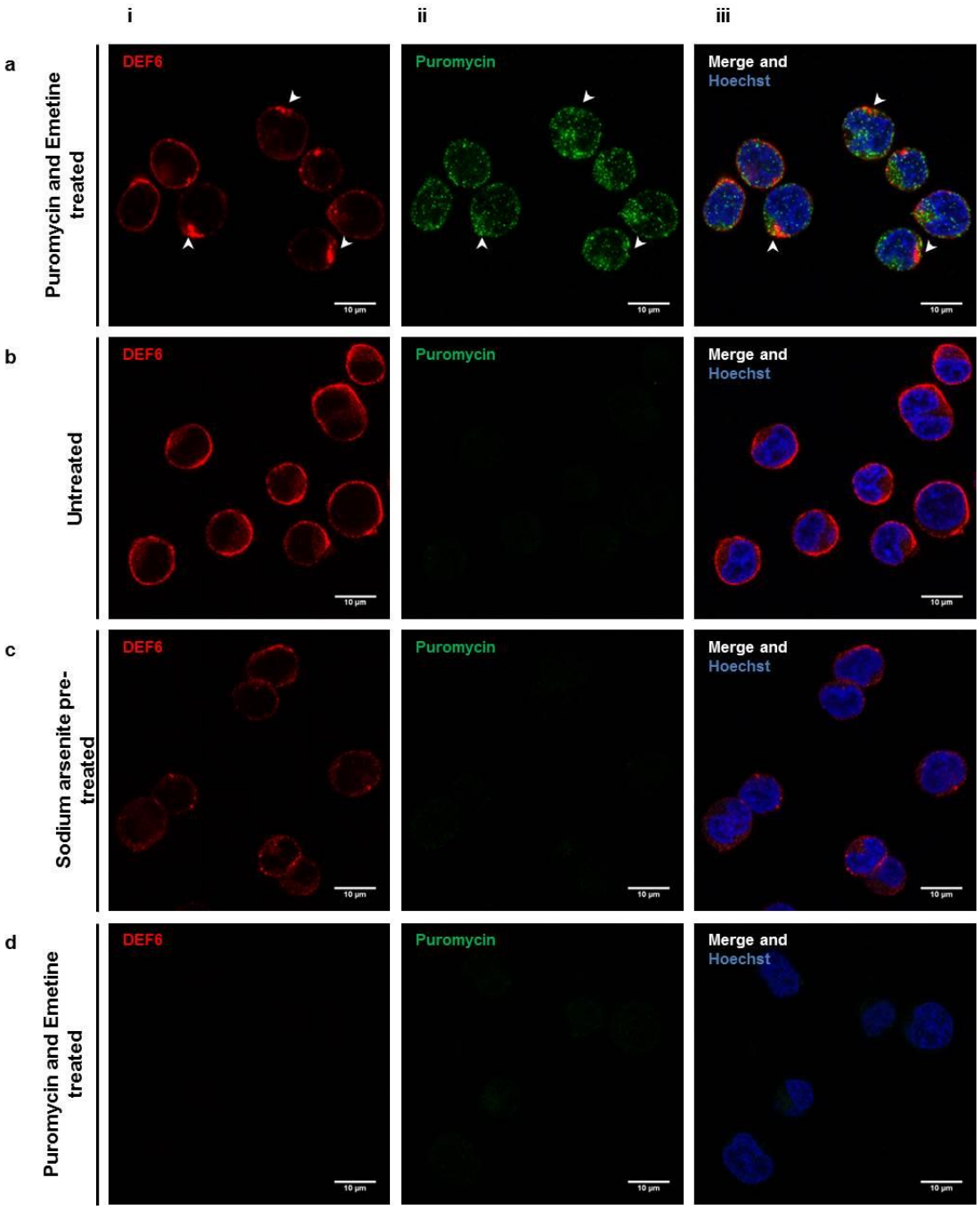
i
ii
iii
a
Puromycin and Emetine treated
DEF6
Puromycin
Merge and Hoechst
b
Untreated
DEF6
Puromycin
Merge and Hoechst
c
Sodium arsenite pre-treated
DEF6
Puromycin
Merge and Hoechst
d
Puromycin and Emetine treated
DEF6
Puromycin
Merge and Hoechst

Figure 3.2-1 DEF6 co-localises with active translation in Jurkat T cells. Cells were applied to Poly-L-Lysine coated coverslips and incubated with Puromycin and Emetine at 37°C for 5 minutes. The negative control cells were pre-incubated with sodium arsenite for 15 minutes prior to the puromycin and emetine treatment. Cells were maintained on ice using polysome stabilisation buffer to preserve active translation and 3%PFA was used to fix the cells. Staining buffer was used to permeabilise and block the cells before incubation with rabbit anti-DEF6 and mouse anti-puromycin. Primary antibodies were labelled using goat anti-rabbit 568 and goat anti-mouse 488 respectively, and nuclei were stained using Hoechst 33258. Specificity of the primary antibodies is demonstrated in the bottom row as the puromycin and emetine incubated cells were stained in the absence of primary antibodies. Images were acquired at a 63x magnification and 2x zoom using a Zeiss LSM710 confocal microscope.

Figure 3.2-1 shows that puromycin and emetine treatment resulted in a strong puromycin signal (aii) which co-localised with DEF6 in resting Jurkat T cells as indicated by the white arrow heads in image aiii. The absence of puromycin did not result in a signal nor did the use of sodium arsenite prior to the introduction of puromycin and emetine, which inhibited active translation, demonstrating the specificity of anti-puromycin (3.2-1b and c respectively). The use of fluorescently labelled secondary antibodies alone also did not result in a signal (3.2-1d).

Co-localisation between DEF6 and active translation was further investigated at a 4x zoom and 63x magnification as shown in figure 3.2-2. Overlap between DEF6 aggregates and active translation was viewed in the ZY and ZX planes to determine if co-localisation was truly visible from the side and top-down angles.

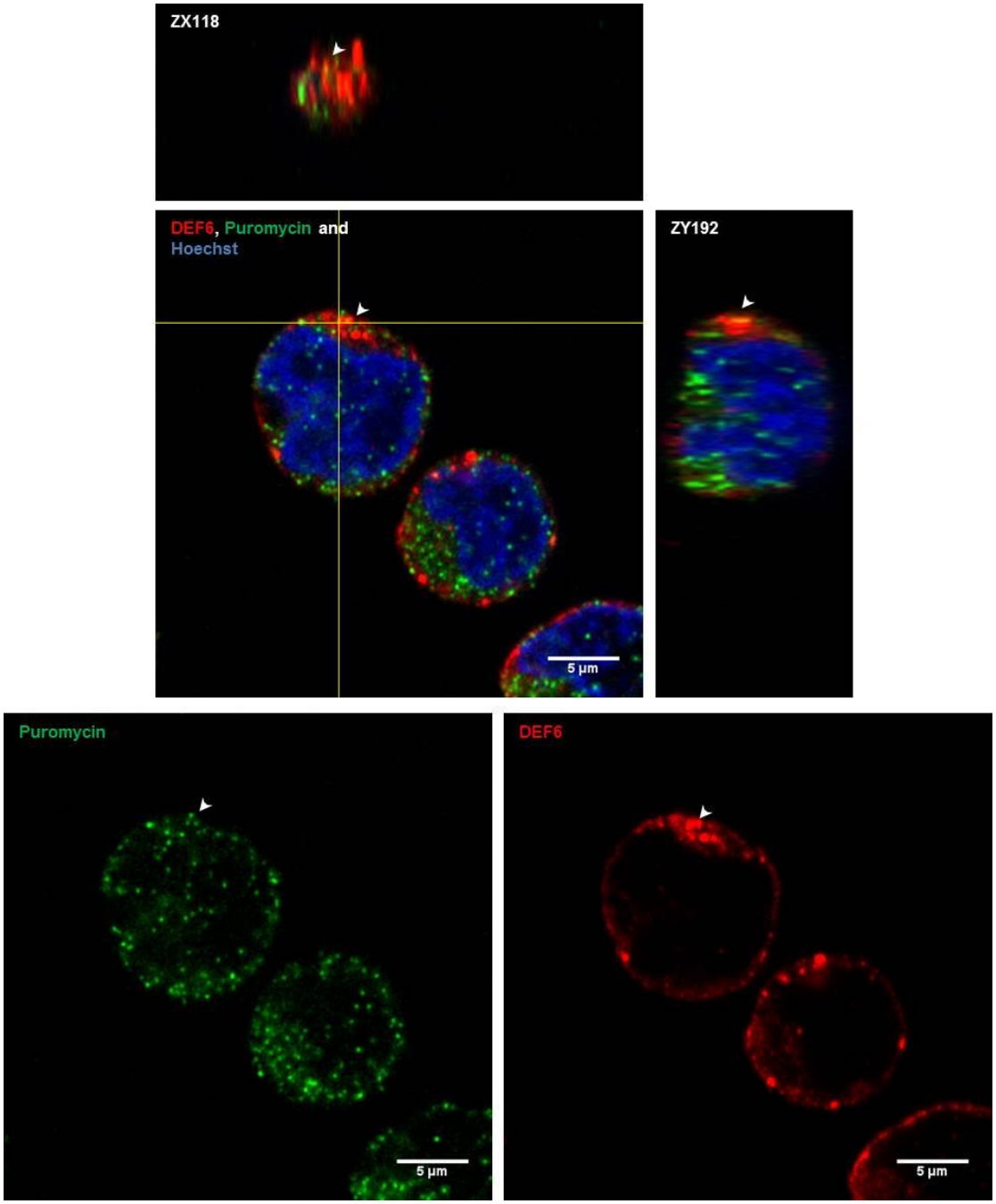

Figure 3.2-2 DEF6 aggregates co-localise with active translation in Jurkat T cells. Image shows a representative example of DEF6 aggregates at a 63x magnification and 4x zoom. Orthogonal viewpoints from the ZY and ZX perspective have been included to further highlight co-localisation with active translation which is indicated by the white arrowheads.

In resting Jurkat T cells there appears to be multiple areas of co-localisation between DEF6 aggregates and active translation as shown in figure 3.2-2. A side viewpoint determines that the DEF6 aggregate is large and appears to consist of multiple smaller aggregates within a ring and active translation co-localises with the top of this structure. A top-down view actually identifies multiple areas of co-localisation within different DEF6 aggregates which appear as a larger structure from the XY and ZY axis as indicated by the white arrow heads. Co-localisation was analysed using the coloc 2 function in Fiji. The background was subtracted in both channels and the Costes randomisations was set to 10 whilst the point spread function was 3. The Spearman's rank correlation value when analysing both complete cells was 0.435 but this increased to 0.561 when the area of increased granule density shown in figure 3.2-2 was used. Although the images show areas of co-localisation between DEF6 and active translation, it is not a significant level of co-localisation but it does indicate that there is an increase in co-localisation within the granules indicated by figure 3.2-2.

3.2.2 DEF6 is in close proximity to active translation

To further corroborate the finding that DEF6 co-localises with active translation, a PLA was used to determine whether DEF6 is within a 40nm range.

Jurkat T cells were re-suspended in fresh culture medium and negative control cells were pre-incubated with sodium arsenite in suspension at 37°C for 15 minutes. Jurkats were applied to poly-L-lysine coated coverslips and were either left untreated, or incubated with puromycin and emetine for 5 minutes at 37°C. Cells were fixed on ice using polysome stabilising buffers and DEF6 was labelled using rabbit anti-DEF6 whilst puromycin was labelled using mouse anti-puromycin. Oligonucleotide coupled secondary antibodies were used to label their respective primary antibodies: donkey anti-rabbit plus labelled DEF6 whilst donkey anti-mouse minus labelled puromycin. If the oligonucleotide probes were within 40nm, a ligase reaction was used to ligate the oligonucleotides and the signal was amplified using a polymerase and red amplification buffer. Nuclei were stained using DAPI within the mountant and cells were imaged by confocal microscopy.

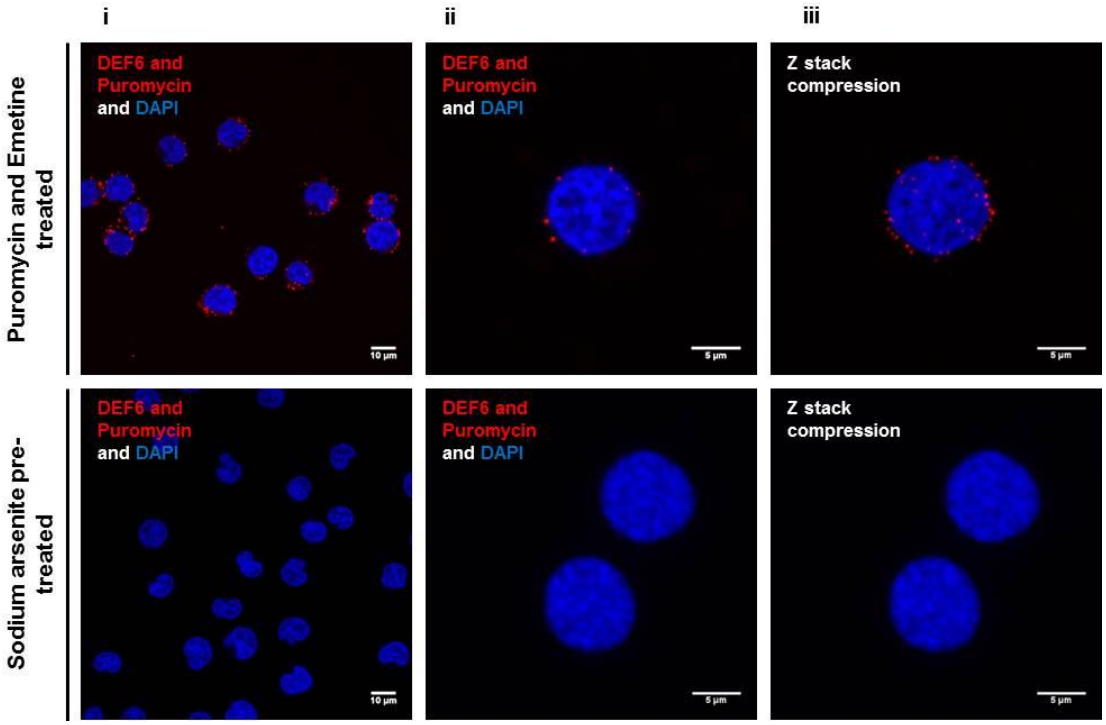

Figure 3.2-3 DEF6 is in close proximity to active translation in Jurkat T cells. Cells were applied to Poly-L-Lysine coated coverslips and incubated with puromycin and emetine at 37°C for 5 minutes. Negative control cells were pre-treated with sodium arsenite for 15 minutes prior to puromycin and emetine treatment. Cells were maintained on ice using polysome stabilisation buffer to preserve active translation and fix the cells. Staining buffer was used to permeabilise the cells and blocking buffer was used to block the cells. DEF6 and puromycin were labelled using rabbit anti-DEF6 and mouse anti-puromycin and close proximity was visualised using a PLA accordingto the manufacturer's instructions. Images are of a single z plane at a 63x magnification and either a 1x zoom (**i**) or 4x zoom (**ii**) and taken using a Zeiss LSM710 confocal microscope. A Z stack of the corresponding cells was compressed to a single image to represent the entire cell (**iii**).

Following treatment with puromycin and emetine, DEF6 is in close proximity to active translation in resting Jurkat T cells as shown in figure 3.2-3. The PLA signal between DEF6 and active translation appears to be evenly distributed throughout the Jurkat T cell cytoplasm (iii) and there are numerous PLA signals in all of the cells shown in the representative 1x zoom image (i). Prior treatment with sodium arsenite has resulted in no PLA signal as active translation was inhibited prior to the introduction of puromycin so that puromycin was not incorporated into the elongating polypeptide chain.

3.2.3 DEF6 co-localises with translation factors in Jurkat T cells

As DEF6 appears to be linked to active translation and can be co-precipitated with polysomes, as described in chapter 1.4.3, further investigation into a possible association between DEF6 and translation factors was carried out. Figure 3.1-4 has shown that DEF6 is in close proximity to 4E-T in resting and stressed Jurkat T cells. 4E-T is an eIF4E binding protein and sequesters eIF4E to P-bodies during mRNA degradation (Ferraiuolo et al., 2005). As a result, eIF4E was selected as an appropriate translation factor to determine a potential association between DEF6 and translation factors.

eIF4E is a translation factor which binds to the mRNA cap and facilitates the formation of the pre-initiation complex during translation initiation (Jackson et al., 2010). To look at a broader snapshot of translation, PABP was selected as another translation factor which may interact with DEF6 as it is bound to the Poly(A) tail during translation (Jackson et al., 2010).

Jurkat T cells were re-suspended in fresh RMPI 1640 and were either left untreated, treated with PMA and ionomycin or treated with sodium arsenite in suspension at 37°C for 30 minutes. Cells were applied to poly-L-lysine coated coverslips and DEF6 was stained using rabbit anti-DEF6 and goat anti-rabbit 568 whilst eIF4E was stained using mouse anti-eIF4E and goat anti-mouse 488. Nuclei were stained using Hoechst 33258 and cells were imaged using confocal microscopy. Inserts of areas of interest were produced in ImageJ (3.2-4A iv).

In preparation for the PLA, Jurkat T cells were treated as described above and primary antibodies were labelled using the corresponding oligonucleotide coupled secondary antibodies: donkey anti-rabbit plus labelled DEF6 whilst donkey anti-mouse minus labelled eIF4E. Nuclei were stained using DAPI within the mountant and cells were imaged by confocal microscopy. The mean number of PLA signals per cell was calculated and compared using multiple t tests with an untreated control.

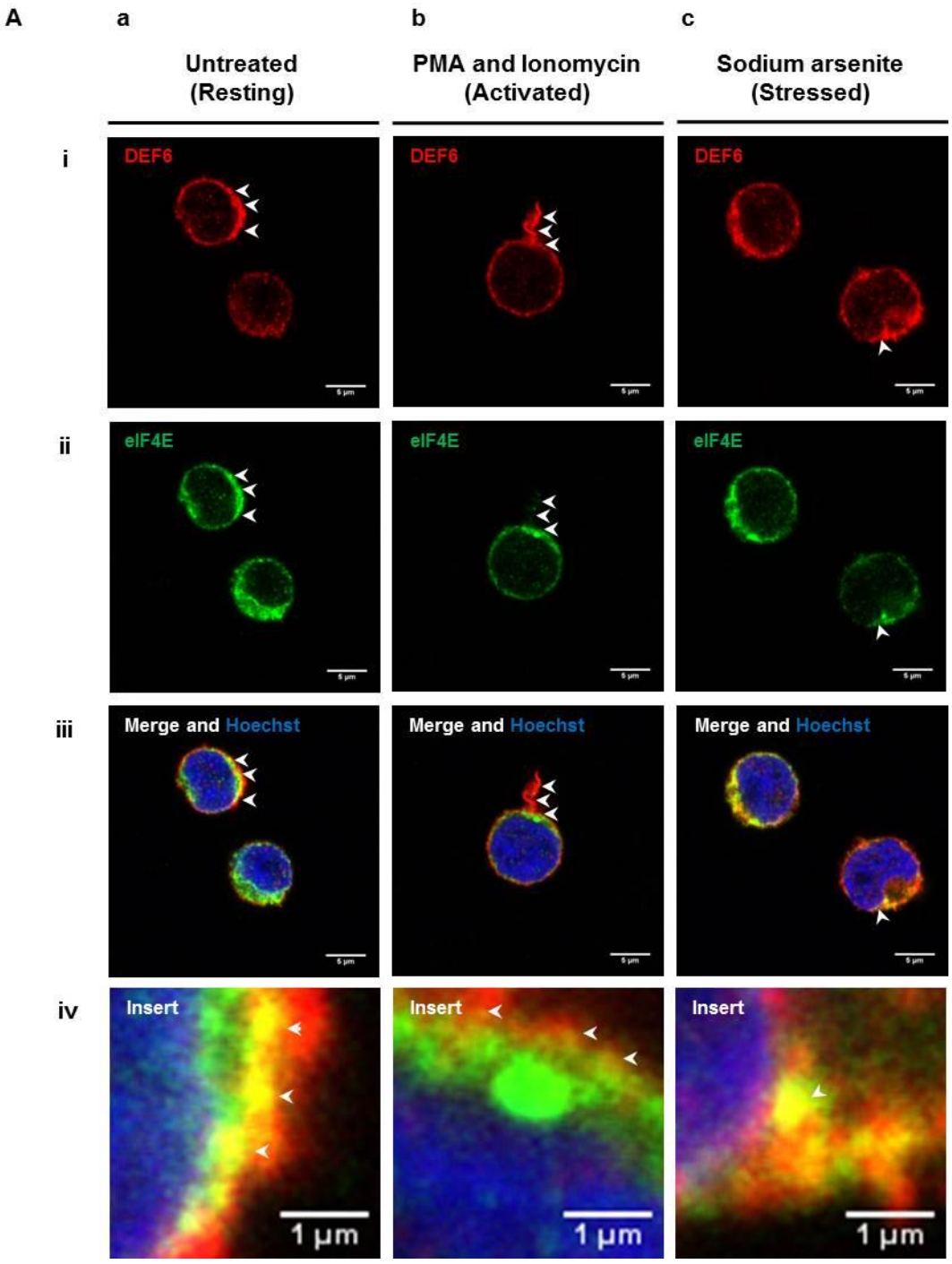
A
a
b
c
Untreated (Resting)
PMA and Ionomycin (Activated)
Sodium arsenite (Stressed)
i
DEF6
ii
eIF4E
iii
Merge and Hoechst
iv
Insert
1 µm

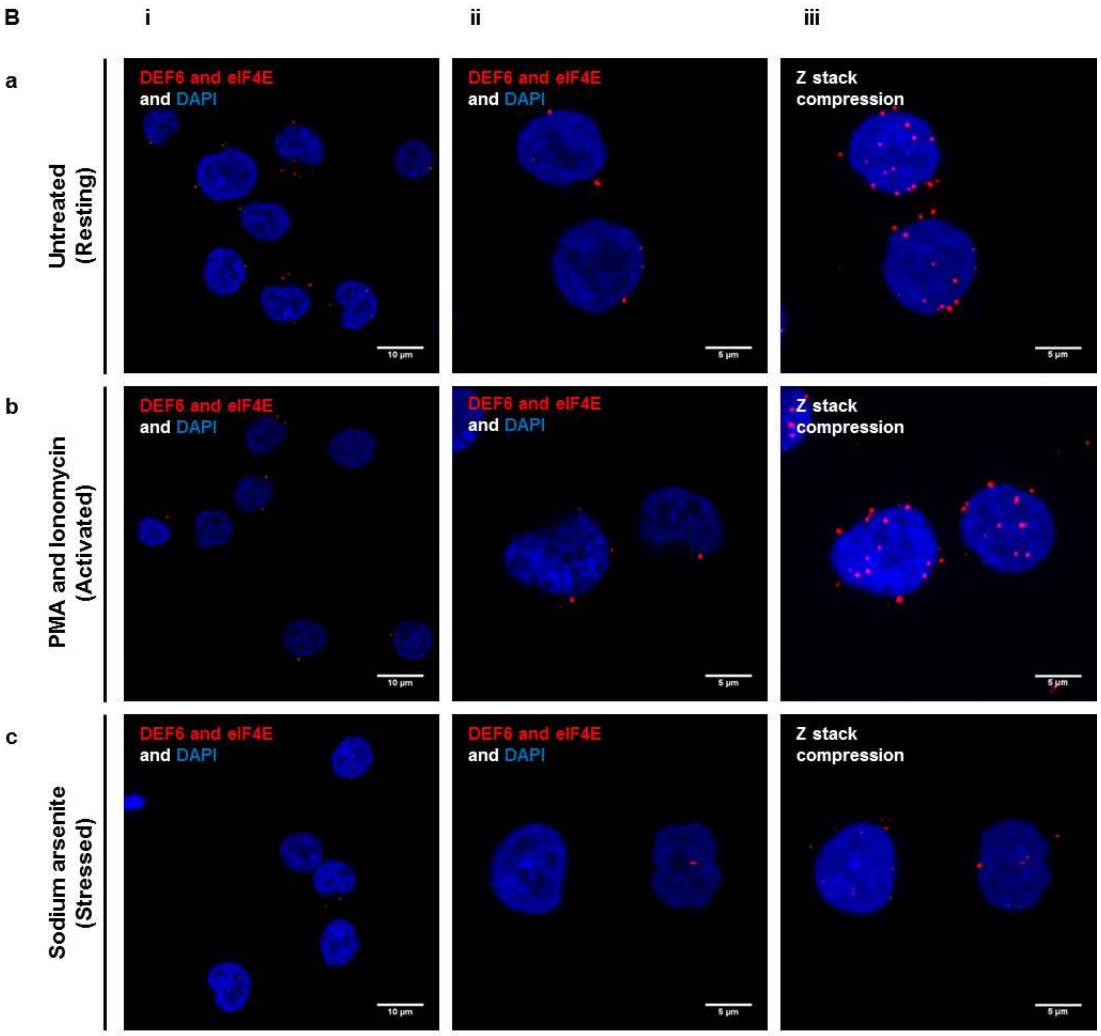
B
i
ii
iii
a
Untreated (Resting)
DEF6 and eIF4E and DAPI
DEF6 and eIF4E and DAPI
Z stack compression
b
PMA and Ionomycin (Activated)
DEF6 and eIF4E and DAPI
DEF6 and eIF4E and DAPI
Z stack compression
c
Sodium arsenite (Stressed)
DEF6 and eIF4E and DAPI
DEF6 and eIF4E and DAPI
Z stack compression
10 µm
5 µm

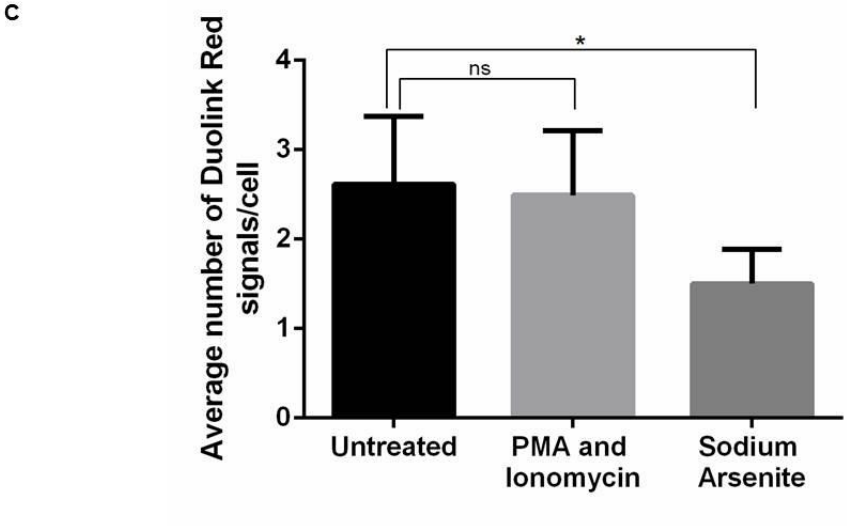
C
Average number of Duolink Red signals/cell
0
1
2
3
4
ns
*
Untreated
PMA and Ionomycin
Sodium Arsenite

Figure 3.2-4 DEF6 co-localises with eIF4E in all 3 states but more DEF6 is in close proximity to eIF4E in resting and activated Jurkat T cells. Jurkat T cells were either left untreated, chemically activated using PMA and Ionomycin or stressed using sodium arsenite for 30 minutes at 37°C. **A** - Cells were then applied to Poly-L-Lysine coated coverslips, fixed, and stained using rabbit anti-DEF6 and mouse anti-eIF4E. Primary antibodies were then labelled using goat anti-rabbit 568 and goat anti-mouse 488 respectively. Images are of a single z plane at 63x magnification taken using a Zeiss LSM710 confocal microscope. White arrowheads indicate co-localisation. **B** - Cells were then applied to Poly-L-Lysine coated coverslips, fixed, and labelled using rabbit anti-DEF6 and mouse anti-eIF4E. Proteins in close proximity were detected using Duolink Red (Sigma) according to the manufacturer's instructions. Images are of a single z plane at a 63x magnification and either a 2x zoom (**i**) or a 4x zoom (**ii**). Images to the right represent the entire cell following compression of the corresponding z-stack into a single image (**iii**). The number of dots per cell for each of the 1x zoom images were counted using nuclei to define a single cell and the mean number of dots per cell was calculated. **C** - More DEF6 is in close proximity to eIF4E in untreated cells in comparison to sodium arsenite treated cells. PMA and ionomycin activation had no significant effect on DEF6 and eIF4E complex formation in comparison to untreated cells. The average number of Duolink Red signals per cell was calculated and compared using multiple t-tests using untreated as the comparative control. For each staining condition $20<n>40$ with 3 replicates. Error bars represent the standard deviation, * $p \leq 0.05$ and ns is not significant.

Figure 3.2-4 shows that DEF6 is in close proximity to eIF4E in resting, chemically activated and stressed Jurkat T cells. Moreover, immunofluorescence shows that DEF6 and eIF4E have large areas of co-localisation (3.2-4A). In particular, untreated Jurkats have extensive regions of co-localisation between the cytoplasm and plasma membrane as shown by representative image Aa iv. Chemical activation using PMA and ionomycin appears to result in more eIF4E aggregation in comparison to untreated Jurkats, however there is still co-localisation between DEF6 and eIF4E at the plasma membrane (Ab iv). Interestingly, the Jurkat T cell shown in images Ab i-iv has an extensive filopodial protrusion that also has eIF4E aggregates which co-localise with DEF6, as indicated by the white arrow heads. Stressing of the Jurkat T cells results in more DEF6 aggregation that also appears to co-localise with eIF4E within the cytoplasm (Ac iv).

Comparison of the average number of PLA signals per cell following chemical activation and stress shows that there is a reduction in the number of PLA signals between DEF6 and eIF4E from around 2.5 signals per cell to 1.5 signals per cell as shown in figure 3.2-4C ($p \leq 0.05$). However, chemical activation of Jurkat T cells using PMA and ionomycin has no significant effect on the average number of PLA signals per cell, maintaining an average number of around 2.5 signals per cell (3.2-4C).

Investigation of an association between DEF6 and PABP was carried out as described above but mouse anti-PABP was used instead of mouse anti-eIF4E.

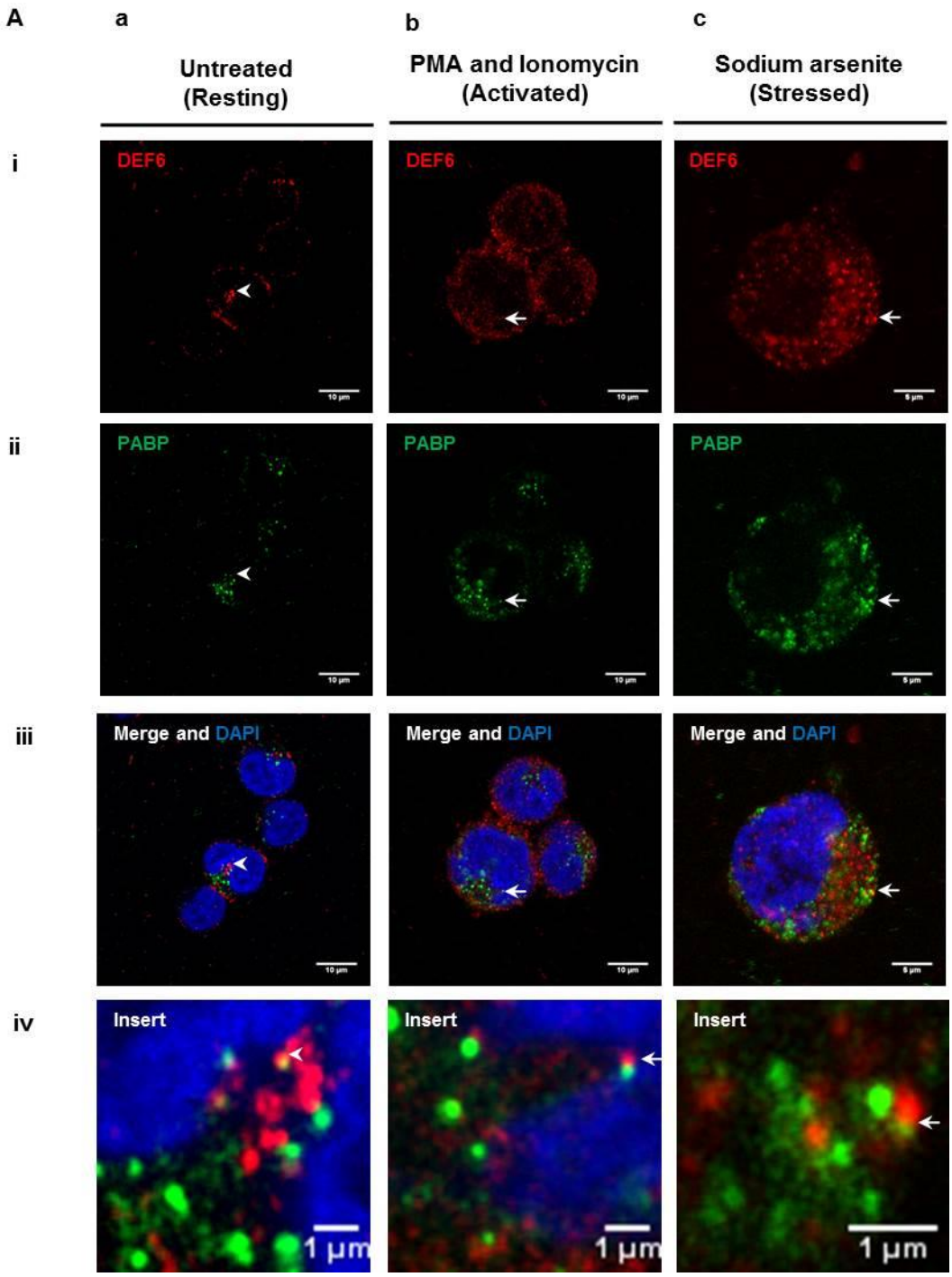
A
a
b
c
Untreated (Resting)
PMA and Ionomycin (Activated)
Sodium arsenite (Stressed)
i
DEF6
ii
PABP
iii
Merge and DAPI
iv
Insert
1 µm

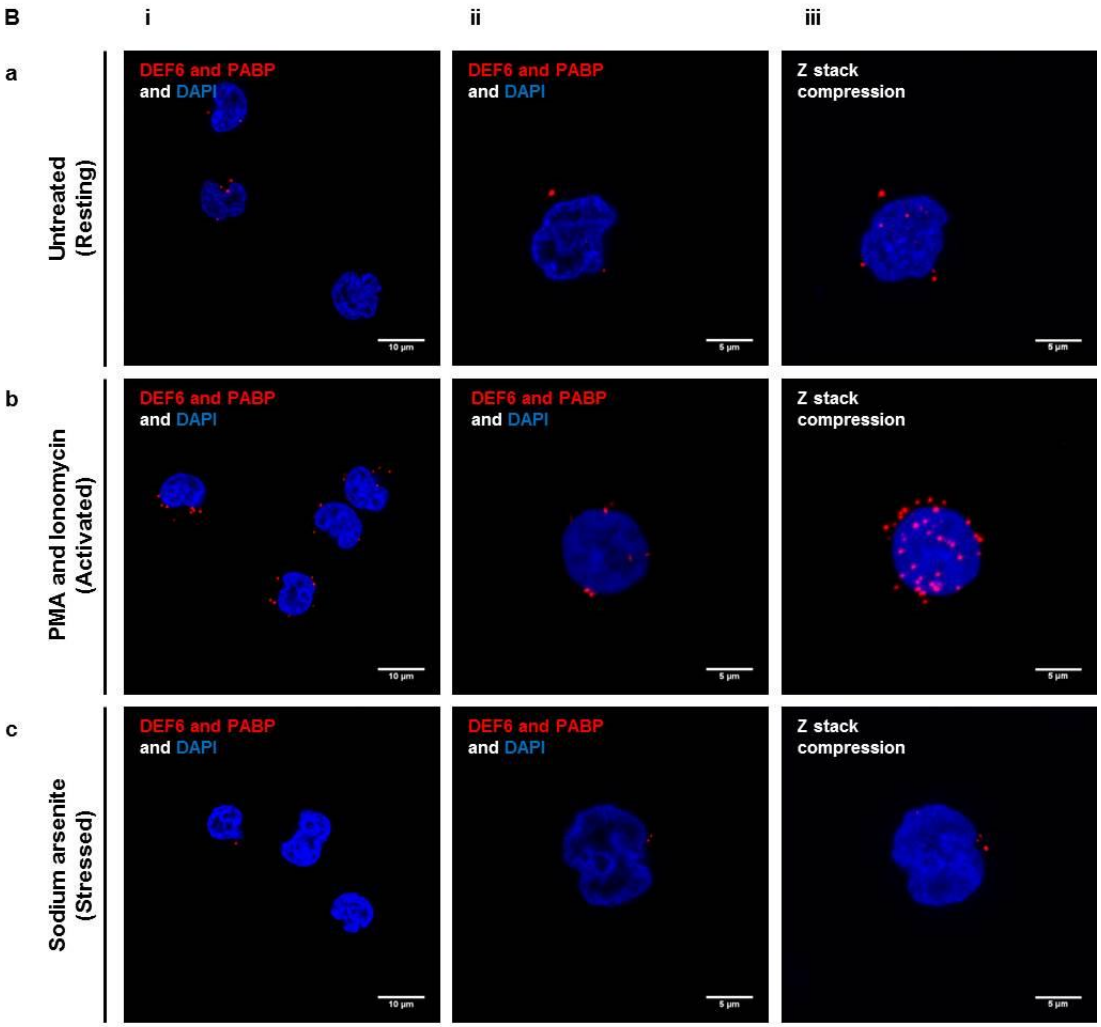
B
i
ii
iii
a
Untreated (Resting)
b
PMA and Ionomycin (Activated)
c
Sodium arsenite (Stressed)
DEF6 and PABP and DAPI
Z stack compression
10 µm
5 µm

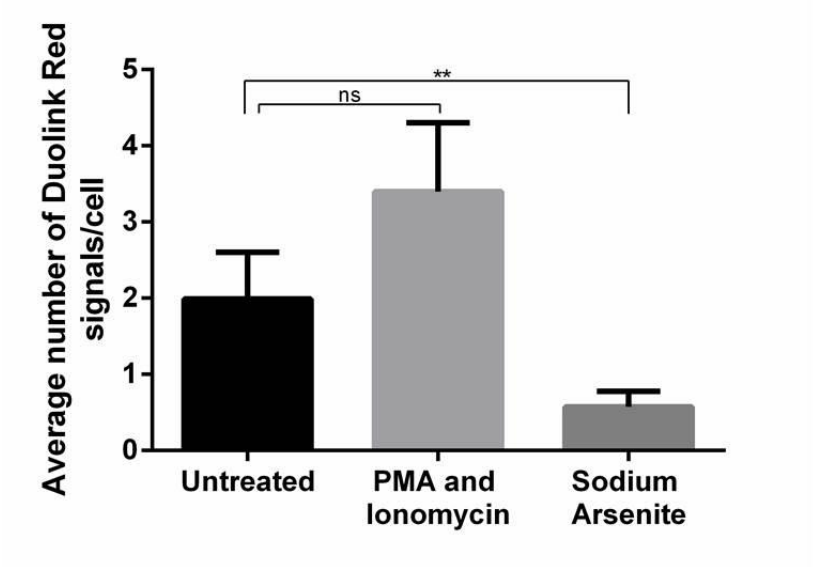
C
Average number of Duolink Red signals/cell
0
1
2
3
4
5
ns
**
Untreated
PMA and Ionomycin
Sodium Arsenite

Figure 3.2-5 DEF6 and PABP appear to co-localise at distinct aggregates in untreated cells whereas chemical activation and stress induces aggregate docking. Jurkat T cells were either left untreated, chemically activated using PMA and Ionomycin or stressed using sodium arsenite for 30 minutes at 37°C. **A** - Cells were then applied to Poly-L-Lysine coated coverslips, fixed, and stained using rabbit anti-DEF6 and mouse anti-PABP. Primary antibodies were then labelled using goat anti-rabbit 568 and goat anti-mouse 488 respectively. Images are of a single z plane at 63x magnification taken using a Zeiss LSM710 confocal microscope. White arrowheads indicate co-localisation and white arrows indicate granule docking. **B** - Cells were then applied to Poly-L-Lysine coated coverslips, fixed, and labelled using rabbit anti-DEF6 and mouse anti-PABP. Proteins in close proximity were detected using Duolink Red (Sigma) according to the manufacturer's instructions. Images are of a single z plane at a 63x magnification and either a 2x zoom (**i**) or a 4x zoom (**ii**). Images to the right represent the entire cell following compression of the corresponding z-stack into a single image (**iii**). The number of dots per cell for each of the 1x zoom images were counted using nuclei to define a single cell and the mean number of dots per cell was calculated. **C** - More DEF6 is in close proximity to PABP in untreated cells in comparison to sodium arsenite treated cells. PMA and ionomycin activation had no significant effect on DEF6 and PABP complex formation in comparison to untreated cells. The average number of Duolink Red signals per cell was calculated and compared using multiple t-tests using untreated as the comparative control. For each staining condition $20<n>40$ with 3 replicates. Error bars represent the standard deviation, ** $p \leq 0.01$ and ns is not significant.

Chemical activation and stressing of Jurkat T cells appears to result in granule docking between DEF6 and PABP as shown in figure 3.2-5A. In untreated, resting Jurkats, there appears to be co-localisation between DEF6 aggregates and PABP aggregates as indicated by the white arrow head (3.2-5Aa) However upon treatment with PMA and ionomycin, the PABP and DEF6 aggregates no longer overlap but are adjacent to one another (3.2-5b iv). Moreover, treatment with sodium arsenite also results in PABP and DEF6 aggregates being adjacent to one another with some co-localisation at the aggregate edge (3.2-5c iv).

The use of a PLA also shows that DEF6 is in close proximity to PABP in resting, chemically activated and stressed Jurkat T cells (3.2-5B). Comparison of the average number of PLA signals per cell between DEF6 and PABP shows that there is no significant difference between resting and chemically activated Jurkats (3.2-5C). Although, treatment of Jurkats using PMA and ionomycin to cause chemical activation does appear to increase the average number of PLA signals from around 2 signals per cell to 3.5 signals per cell. However, stressing of Jurkats using sodium arsenite significantly reduces the average number of PLA signals to around 0.5 signals per cell in comparison to resting Jurkats which have an average of around 2 signals per cell ($p \leq 0.01$).

A link between DEF6 and PABP was further investigated using emetine and puromycin to determine whether other methods of translation arrest had an effect on DEF6 and PABP co-localisation. Also, the use of puromycin and emetine was used to determine whether the preservation of active translation had a similar DEF6 and PABP distribution to that of DEF6 and puromycin.

Jurkat T cells were re-suspended in fresh RPMI 1640 and applied to poly-L-lysine coated coverslips. Cells either remained untreated or were treated with: puromycin; emetine; or puromycin and emetine; at 37°C for 30 minutes. Any active translation was maintained using polysome stabilisation buffers containing 3% PFA to fix the cells whilst on ice. DEF6 was stained using rabbit anti-DEF6 and goat anti-rabbit 568 whilst PABP was stained using mouse anti-PABP and goat anti-mouse 488. Nuclei were stained using Hoechst 33258 and cells were imaged by confocal microscopy.

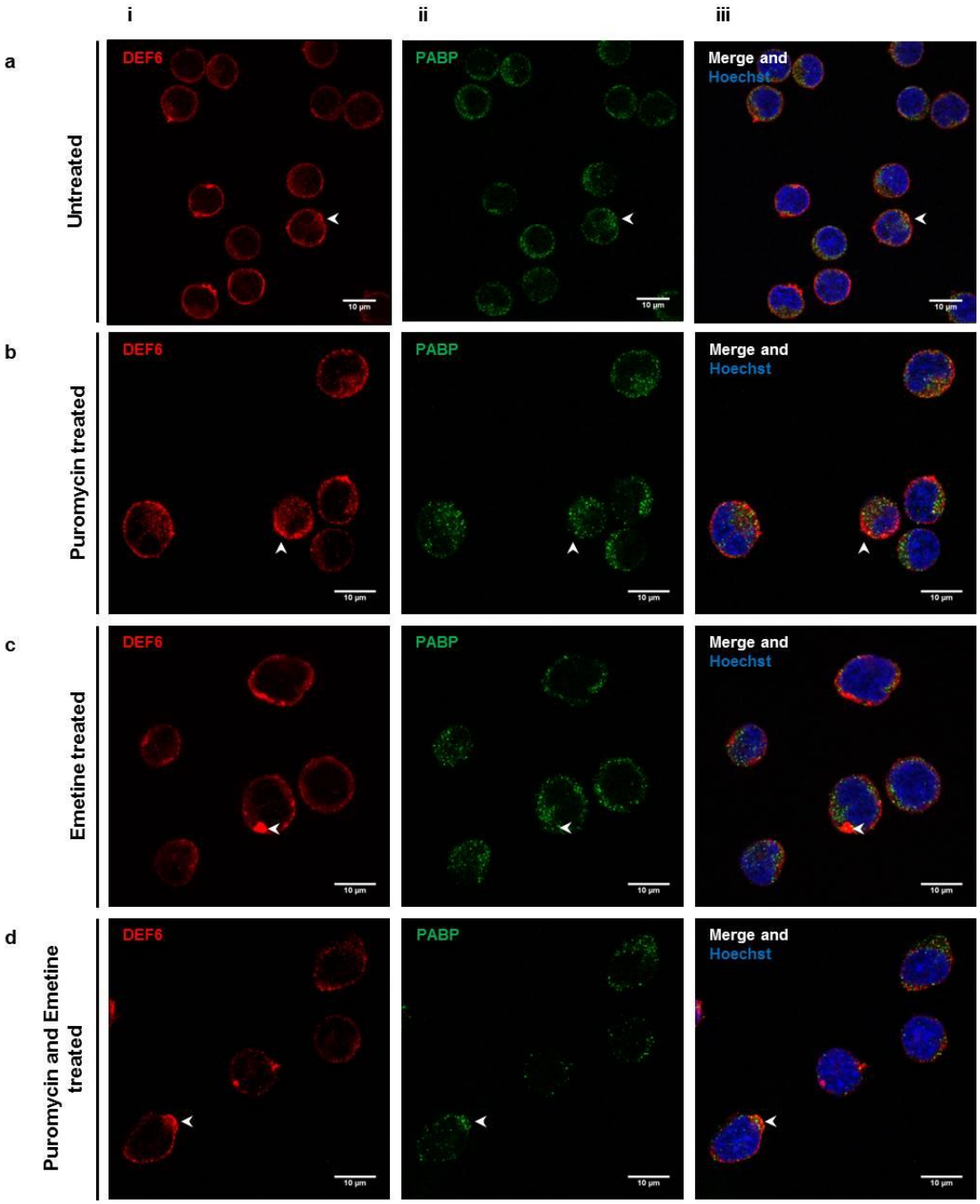

Figure 3.2-6 DEF6 co-localises with PABP in untreated and translationally inhibited Jurkat T cells. Cells were applied to Poly-L-Lysine coated coverslips and incubated with puromycin, emetine or puromycin and emetine at 37°C for 5 minutes. Cells were maintained on ice using polysome stabilisation buffer to preserve active translation and fix the cells. Staining buffer was used to permeabilise and block the cells. DEF6 and PABP were labelled using rabbit anti-DEF6 and mouse anti-PABP followed by goat anti-rabbit 568 and goat anti-mouse 488. Images are of a single z plane at a 63x magnification, 2x zoom and taken using a Zeiss LSM710 confocal microscope. Co-localisation between DEF6 and PABP is indicated by white arrowheads.

DEF6 appears to co-localise with PABP in all 4 treatment states as indicated by the white arrow heads in figure 3.2-6. In untreated Jurkat T cells there is co-localisation between DEF6 and PABP (a iii) whilst the use of emetine seems to increase the level of co-localisation seen (c iii and d iii). Upon puromycin treatment alone, there are a few PABP aggregates which co-localise with DEF6 at the plasma membrane as indicated by the white arrowhead in image b iii. The use of puromycin and emetine during the puromycylation method appears to have resulted in a PABP distribution similar to the puromycin staining pattern indicative of active translation as shown in figure 3.2-1.

To better compare the distribution of puromycin and PABP during active translation and the co-localisation with DEF6, inserts of images 3.2-6a iii; 3.2-6d iii; 3.2-1a iii have been arranged into a single figure.

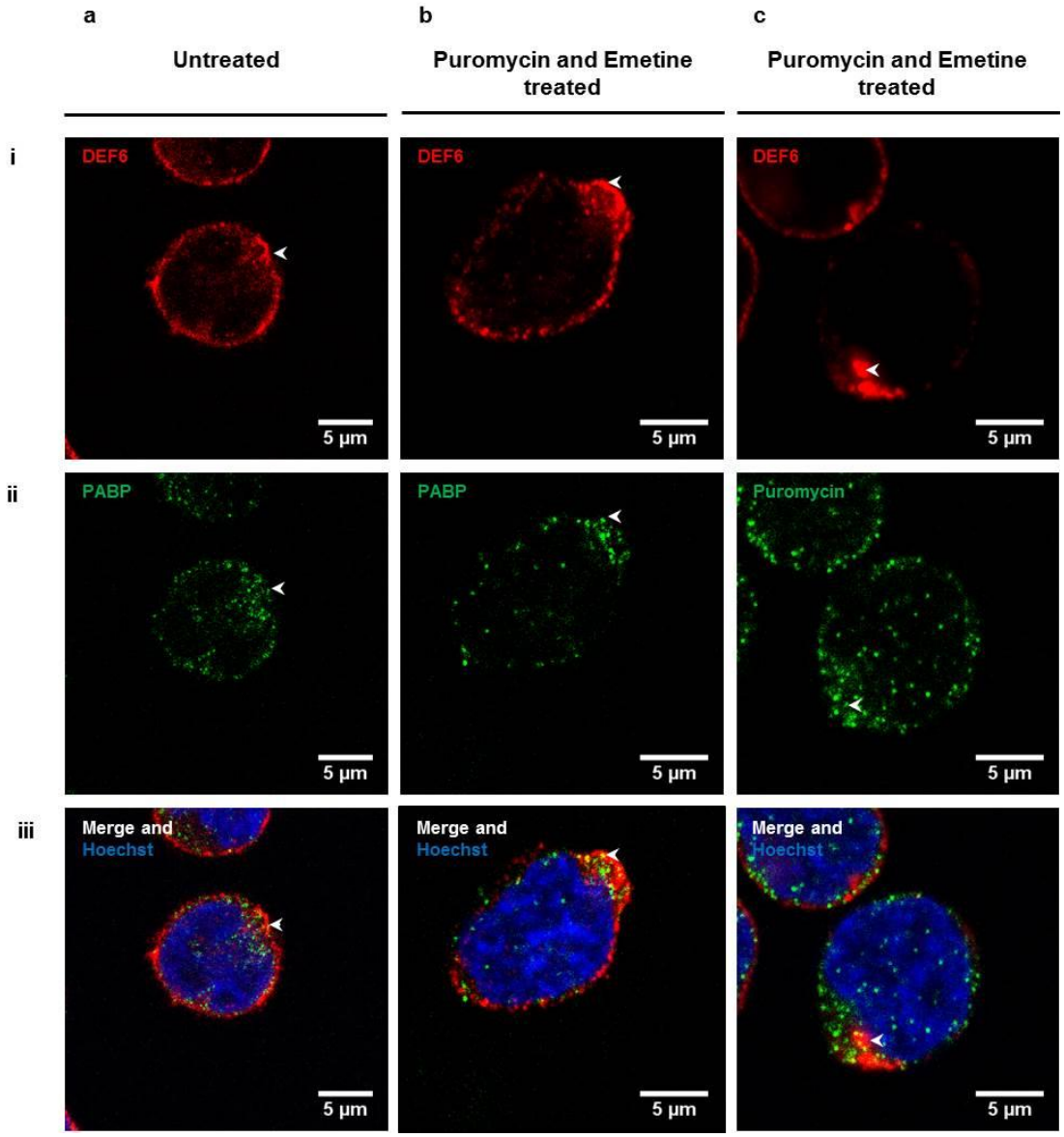

Figure 3.2-7 DEF6 co-localises with PABP in untreated cells as well as in puromycin and emetine treated cells. Cells were applied to Poly-L-Lysine coated coverslips and incubated with Puromycin and Emetine at 37°C for 5 minutes. Cells were maintained on ice using polysome stabilisation buffer to preserve active translation and fix the cells. Staining buffer was used to permeabilise and block the cells before incubation with rabbit anti-DEF6 and mouse anti-puromycin or mouse anti-PABP. Primary antibodies were labelled using goat anti-rabbit 568 and goat anti-mouse 488 respectively, and nuclei were stained using Hoechst 33258. Images are inserts of: 3.2-6a iii; 3.2-6d iii; 3.2-1a iii; and were acquired at a 63x magnification, 2x zoom using a Zeiss LSM710 confocal microscope and adapted using ImageJ.

As shown in figure 3.2-7, there is co-localisation between DEF6 and PABP in untreated resting Jurkat T cells (a). However, upon puromycin and emetine treatment and the use of the puromycylation method to preserve active translation, there is more co-localisation between DEF6 and PABP as indicated by the white arrow heads (biii). Furthermore, the distribution of PABP following the preservation of active translation is very similar to that of puromycin once incorporated into the elongating polypeptide chain (c). As a result, co-localisation between DEF6 and PABP appears to suggest that DEF6 is co-localising with PABP involved in active translation.

3.2.4 DEF6 co-localises with active translation at the immunological synapse

In response to TCR engagement, DEF6 is recruited to the IS and facilitates the rearrangement and formation of F-actin to stabilise the synapse (Fanzo et al., 2006). During the signal transduction cascade and the resulting T cell response, a number of different proteins are involved in a short space of time. Consequently, it is likely that proteins are produced locally at the immune synapse to facilitate the response. To establish if DEF6 distribution correlates with any active translation, the puromycylation method was applied to newly formed synapses between SEA/B loaded Raji B cells and Jurkat T cells and visualised by confocal microscopy.

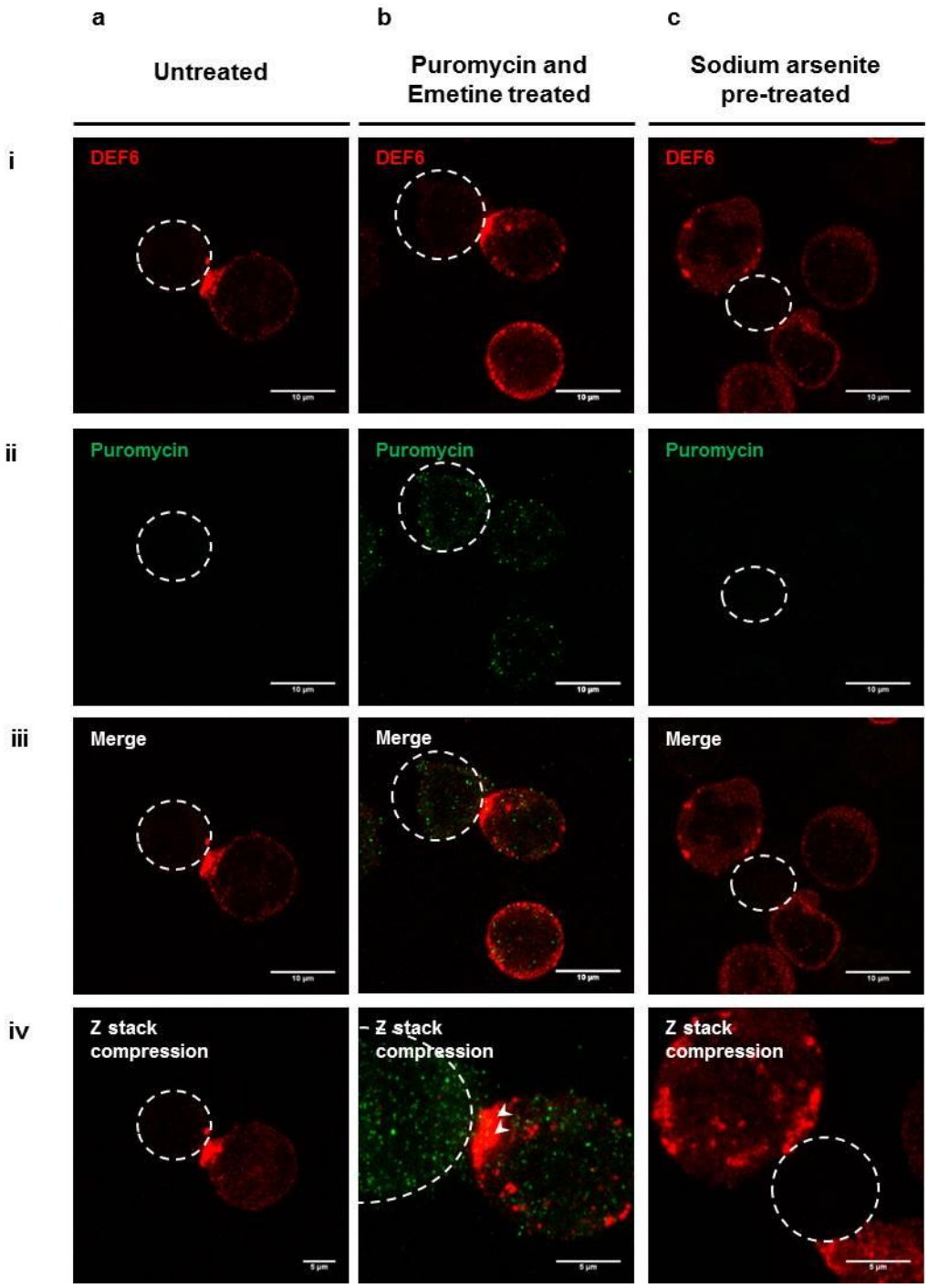
a
b
c
Untreated
Puromycin and Emetine treated
Sodium arsenite pre-treated
i
ii
iii
iv
DEF6
Puromycin
Merge
Z stack compression

Figure 3.2-8 Active translation is present at the immunological synapse. Jurkat T cells were incubated with SEA/B loaded Raji B cells and applied to Poly-L-Lysine coated coverslips. Cells were incubated with puromycin and emetine at 37 °C for 5 minutes. The negative control synapses were pre-incubated with sodium arsenite for 15 minutes prior to puromycin and emetine treatment. Cells were maintained on ice and active translation was preserved using polysome stabilisation buffer to fix the cells. Staining buffer was using to permeabilise and block the cells followed by incubation with rabbit anti-DEF6 and mouse anti-puromycin. Primary antibodies were labelled using goat anti-rabbit 568 and goat anti-mouse 488 respectively. Images are of a single z plane at a 63x magnification, 2x zoom and taken using a Zeiss LSM710 confocal microscope. The corresponding z-stack was acquired at a 100x magnification and compressed into a single image to represent the entire cell. The presence of Raji B cells is indicated by a faint DEF6 staining and the dotted white circle. White arrowheads indicate the presence of active translation at the immune synapse.

Figure 3.2-8 shows that activation of Jurkat T cells by SEA/B Raji B cells resulted in a high level of active translation throughout both cells (b ii). DEF6 translocated to the immune synapse as expected however a few DEF6 aggregates appear to have been fixed in transit (b i). Moreover, a second polarity appears to have formed at the opposite side of the T cell due to the presence of DEF6 enrichment at the plasma membrane opposite the IS (b i). Active translation is indeed present at the immune synapse and co-localises with DEF6 enrichment as indicated by white arrow heads in image b-iv however as active translation is present throughout the T cell further investigation is required to determine if DEF6 is directly involved with active translation at the synapse. Interestingly, prior treatment with sodium arsenite to inhibit active translation and prevent puromycin incorporation either resulted in a lack of DEF6 translocation to the immune synapse or inhibition of IS formation (c iv). Further investigation using another known IS marker would demonstrate whether the IS was able to form following translation inhibition or if a lack of DEF6 translocation has occurred.

3.2.5 Summary of main findings

- DEF6 aggregates co-localise with active translation in resting Jurkat T cells.
- DEF6 is in close proximity to active translation and as well PABP and eIF4E which are both translation factors.
- DEF6 co-localises with PABP in the same manner when puromycin and emetine is used alone or in conjunction with one another.
- Co-localisation between DEF6 and PABP is similar to puromycin labelled active translation and still occurs in untreated cells.
- Active translation is present at the immune synapse co-localising with DEF6 enrichment however active translation is also consistent through-out the Jurkat T cell and Raji B cell.

3.3 DEF6 is enriched at T-T cell junctions and is in close proximity to LFA-1

The current consensus in the literature suggests that DEF6 is involved in the TCR signal transduction cascade in response to APC antigen presentation (Singleton et al., 2011; Becart et al., 2008b). However, $CD4^+$ T cells are involved in many other signalling and adhesion events which require polymerisation of F-actin suggesting that other roles in general adhesion may not have been previously identified (Shimizu et al., 1991). In response to antigen presentation, T cells also prime one another to gauge whether a response is appropriate to reduce the risk of self-antigen responses. T-T cell adhesion is important in T cell priming to set an appropriate tolerance level reducing the number of responses to frequent low affinity antigens and reserving immune responses for high affinity antigens (Blair and Dustin, 2013). T cells also adhere to epithelial cells during extravasation allowing infiltration of inflamed tissue to coordinate a response to pathogens within the tissue itself (Muller, 2013).

3.3.1 DEF6 has varying patterns of enrichment in response to different activation methods

Jurkat T cells can be activated in a number of ways: chemical activation can be achieved using PMA and ionomycin; the addition of C305 anti-Jurkat TCR enables TCR engagement specific activation; and super antigen loaded Raji B cells can be used to mimic the full response to an APC including co-receptor signalling. Jurkat T cells were treated using the aforementioned conditions and prepared for confocal microscopy to compare the cellular location of DEF6 in response to the different activation methods.

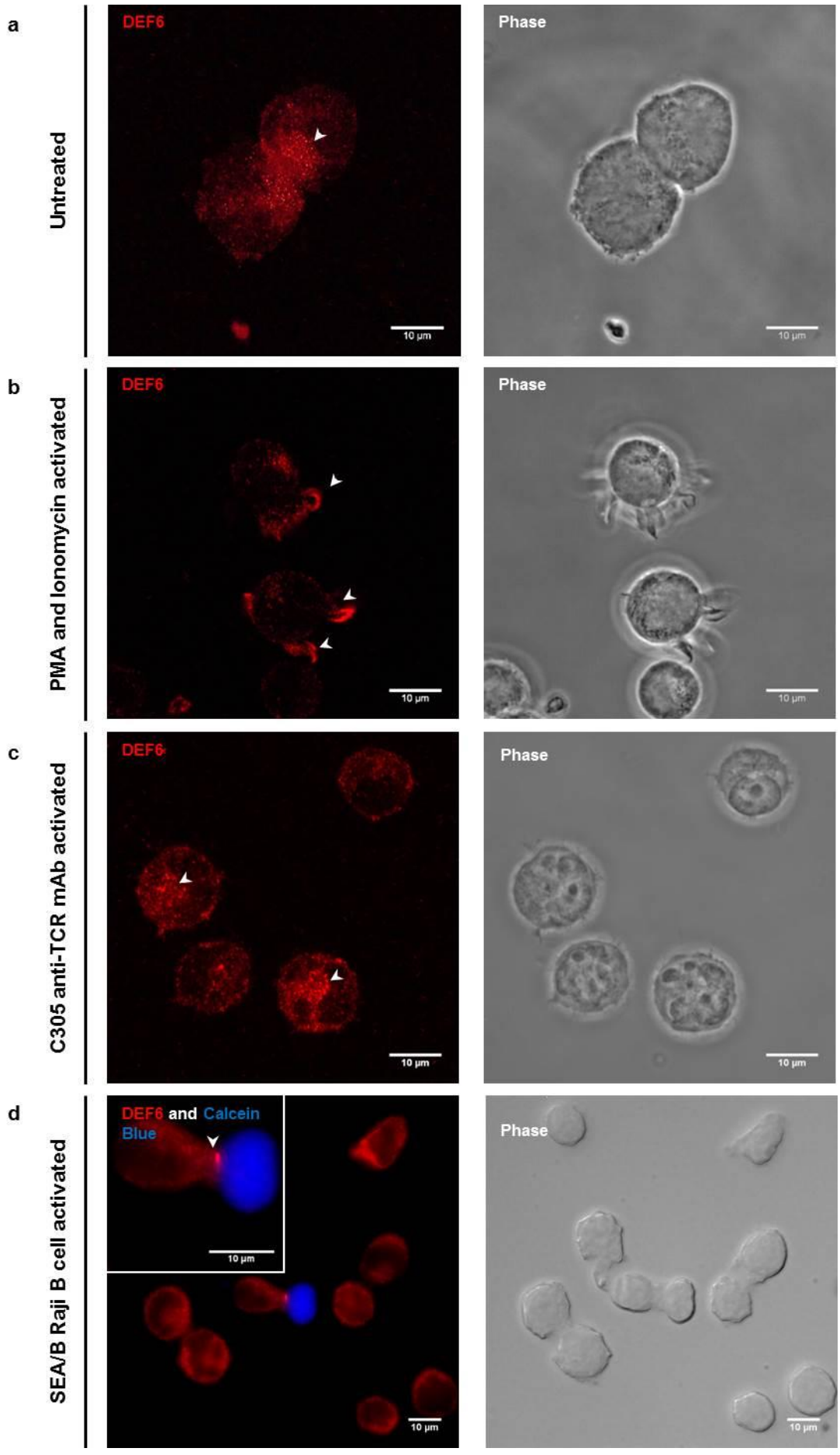
a
Untreated
DEF6
Phase
10 µm
b
PMA and Ionomycin activated
DEF6
Phase
10 µm
c
C305 anti-TCR mAb activated
DEF6
Phase
10 µm
d
SEA/B Raji B cell activated
DEF6 and Calcein Blue
Phase
10 µm

Figure 3.3-1 Artificial and *in vivo* simulating methods of activation affect DEF6 enrichment in Jurkat T cells. Jurkat T cells were either left untreated, chemically activated using PMA and ionomycin, activated by C305 mAb mediated engagement of the TCR or physiologically activated using SEA/B loaded Raji B cells. DEF6 was stained using rabbit anti-DEF6 and goat anti-rabbit 568 and Raji B cells were stained using calcein blue. Images of a single z plane were taken at a 63x magnification using confocal microscopy. Arrowheads indicate different DEF6 localisations dependent upon the treatment.

Figure 3.3-1 shows that in untreated Jurkat T cells, DEF6 remains largely diffuse however DEF6 aggregates are present in the cytoplasm (a). DEF6 also appears to be enriched between the two T cells although the cells do not appear to be adhering due to the absence of a non-specific synapse in the phase image. Chemical activation of the Jurkat T cells using PMA and ionomycin has resulted in the formation of filopodia as indicated by the white arrow heads in image b. In response to TCR stimulation alone, DEF6 does not translocate to the membrane as expected. Instead, DEF6 appears to form aggregates throughout the cytoplasm which suggests that TCR stimulation alone is insufficient for DEF6 translocation to the membrane and that additional co-receptor signalling may be required for the full response (c). Super antigen loaded Raji B cells mimic typical APC antigen presentation however they override the specificity and affinity requirements for usual activation due to the presence of *S. aureus* enterotoxin A and B. As a result, DEF6 does translocate to the immune synapse that has formed between the Raji B cell and Jurkat T cell which is visible in the phase image (d). This suggests that the full receptor network is indeed required for DEF6 translocation.

3.3.2 DEF6 translocates to T-T synapses

As TCR engagement alone was insufficient to cause DEF6 translocation to the membrane, investigation of whether translocation was specific to APC antigen presentation was required. PMA and ionomycin was again used to chemically activate the Jurkat T cells and sodium arsenite was used to induce stress in the cells to determine if adhesion would continue.

Jurkat T cells were re-suspended in fresh RPMI and either left untreated, or treated with PMA and ionomycin or sodium arsenite in suspension at 37°C for 30 minutes. Cells were applied to poly-L-lysine coated coverslips and DEF6 was stained using rabbit anti-DEF6 and goat anti-rabbit 568. Nuclei were stained using Hoechst 33258 and cells were imaged by confocal microscopy.

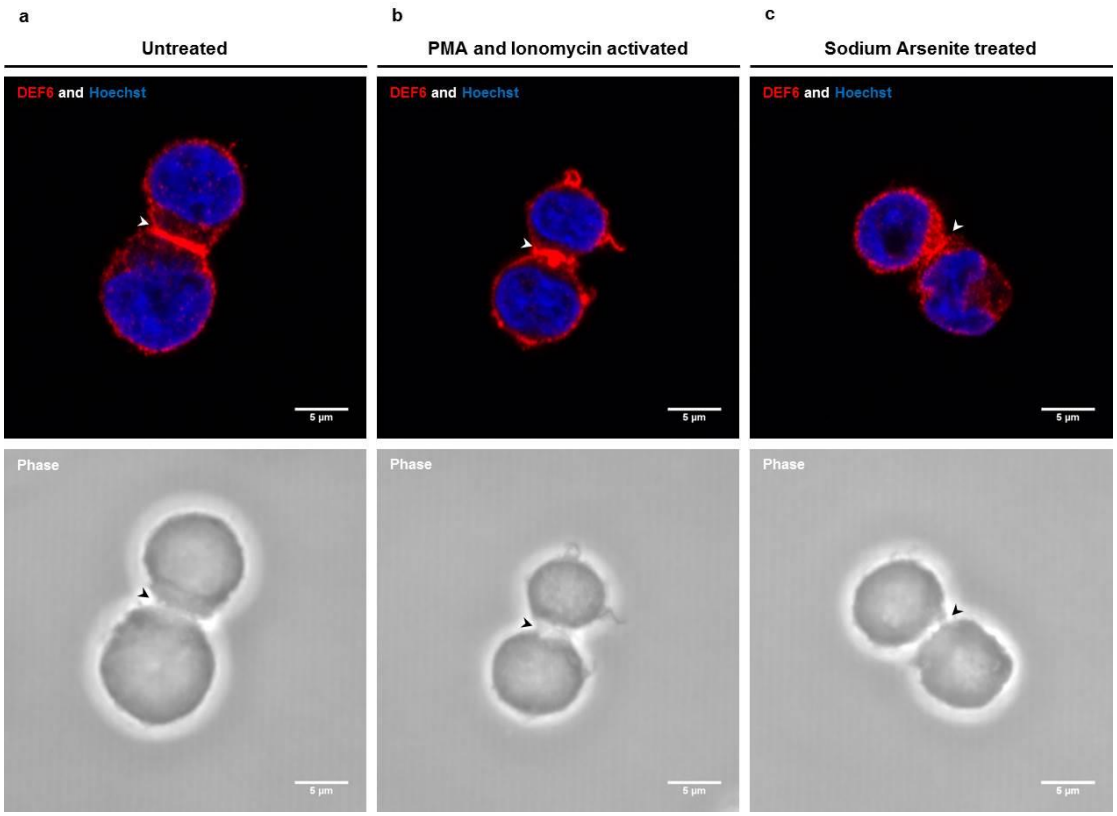

Figure 3.3-2 DEF6 is enriched during T-T cell adhesion. Activation of Jurkat T cells using PMA and ionomycin increased enrichment of DEF6 at the contact site where as stressing of the cells using Sodium arsenite reduced DEF6 enrichment as indicated by the white arrows. Black arrows indicate the formation of a synapse between the two T cells in the untreated and activated states. However, the formation of a complete synapse has been prevented upon stressing of the cells. Jurkat T cells were incubated with either RPMI 1640 alone, PMA and ionomycin or sodium arsenite for 30 minutes at 37°C. DEF6 was stained using rabbit anti-DEF6 and goat anti-rabbit 568 and nuclei were stained using Hoechst 33258. Images are of a single z plane at a 63x magnification and a 4x zoom obtained by confocal microscopy. Arrowheads indicate immune synapse formation.

In each of the phase images a clear T-T cell synapse can be seen indicating adhesion which is highlighted by the black arrow heads. In untreated Jurkat T cells DEF6 translocated to the synapse and is clearly enriched at the contact site (a). Chemical activation using PMA and ionomycin has also resulted in translocation to the synapse with the addition of filopodia formation which also demonstrates DEF6 enrichment (b). However, treatment with sodium arsenite to induce stress appears to reduce the enrichment of DEF6 at the synapse but does not fully prevent translocation to the contact site (c). This suggests that DEF6 translocation is not APC dependent indicating that the co-receptor involved in DEF6 translocation is present on the T cell membrane and may also be required for T-T cell priming.

3.3.3 CD81 and LFA-1 are candidates for targeting DEF6 to the membrane

The formation of the immune synapse results in the formation of a complex web of different receptors which interact and cross-link to result in transduction and amplification of the initial signal (Levy and Shoham, 2005). The protein receptors are organised and reside within lipid rafts within the plasma membrane to allow efficient response to signalling events. T cells have a number of different receptors however CD81, LFA-1 and ICAM1 are present on all T cells and are involved in integrin signalling and adhesion within the tetraspanin webs and lipid rafts (Yanez-Mo et al., 2009). Although ICAM1 is usually described as being present only on the APC, it is expressed by T cells but at a much lower level with LFA-1 being the predominant receptor that is expressed (Rocha-Perugini et al., 2013). The formation of DEF6 and receptor complexes was investigated using a PLA which enabled the visualisation of complexes *in vivo* and is more sensitive than other biochemical assays that may disrupt the association or require a larger number of associations to be visualised.

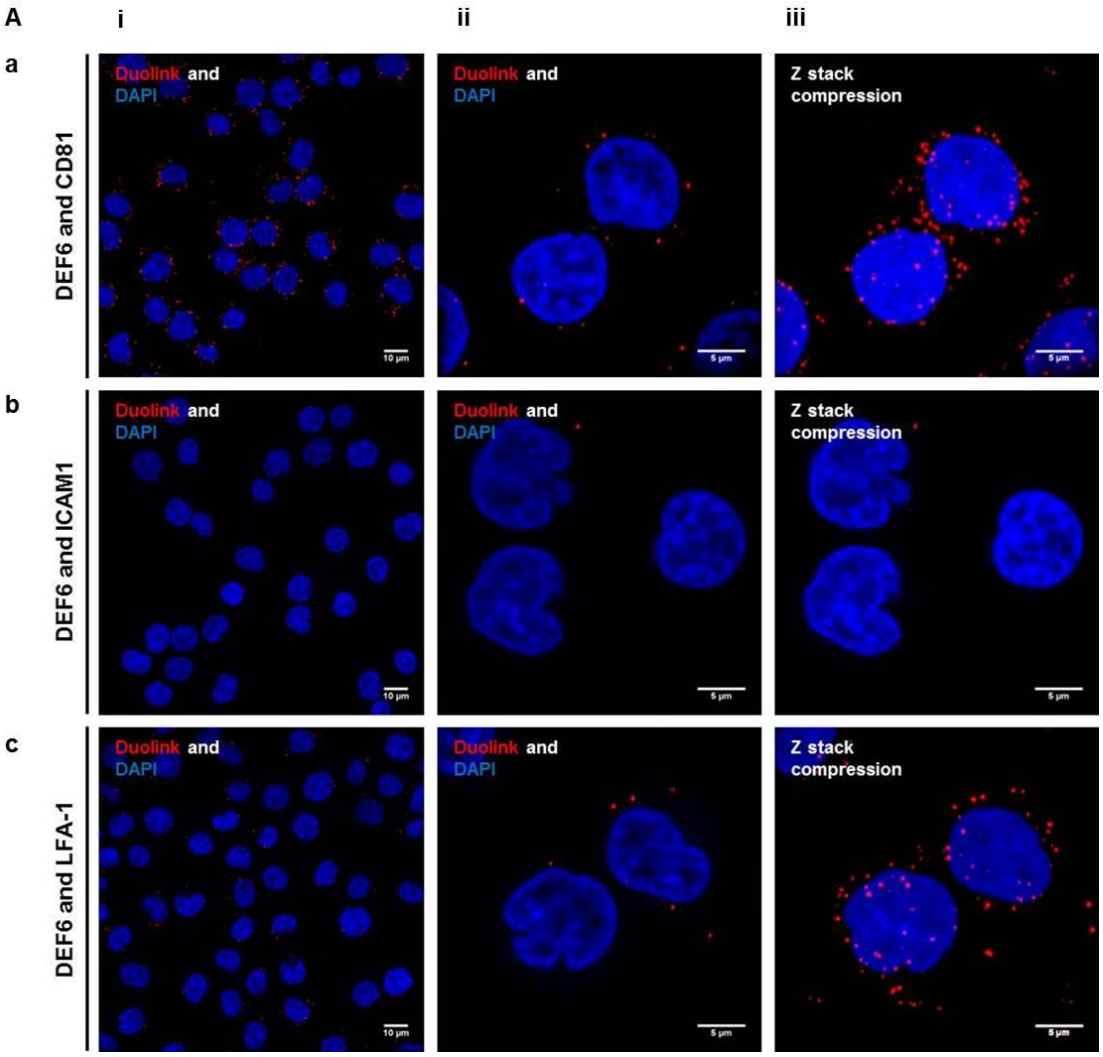
A
i
ii
iii
a
DEF6 and CD81
Duolink and DAPI
Duolink and DAPI
Z stack compression
b
DEF6 and ICAM1
Duolink and DAPI
Duolink and DAPI
Z stack compression
c
DEF6 and LFA-1
Duolink and DAPI
Duolink and DAPI
Z stack compression
10 µm
5 µm

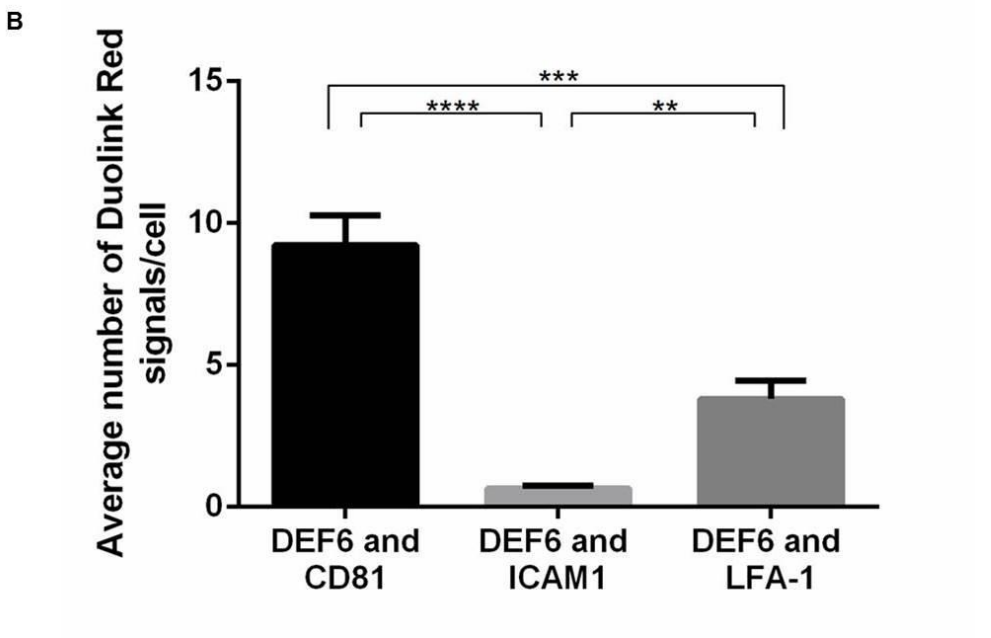
B
Average number of Duolink Red signals/cell
15
10
5
0
***
****
**
DEF6 and CD81
DEF6 and ICAM1
DEF6 and LFA-1

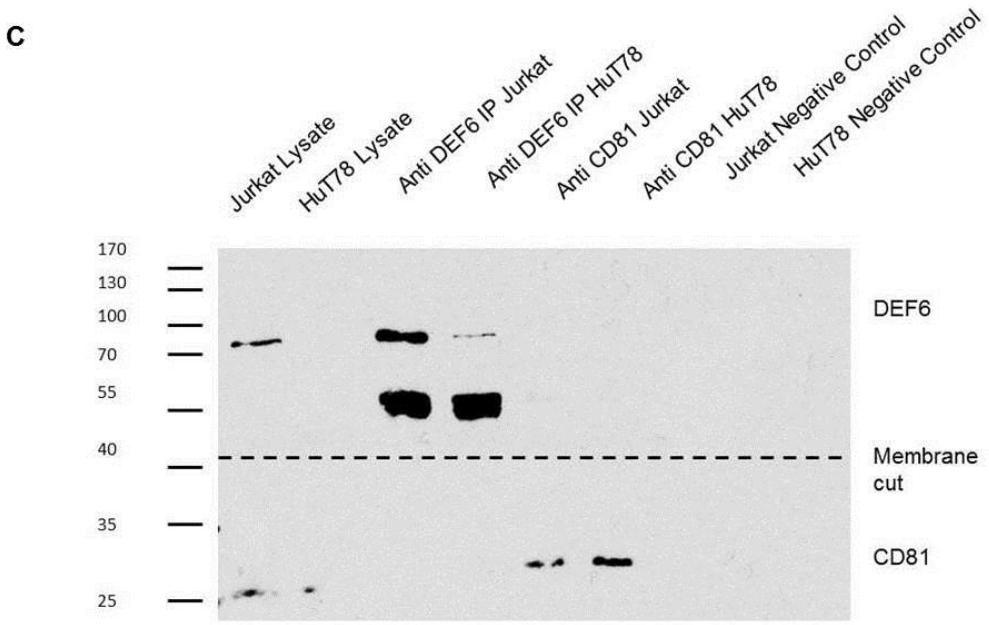

Figure 3.3-3 DEF6 is in close proximity to receptors involved in cell adhesion and the TCR signal transduction cascade. **A** - DEF6 and CD81, ICAM-1 or LFA-1 were labelled using their respective monoclonal antibodies. Proteins in close proximity were detected using a Duolink Red (Sigma) assay as per the manufacturer's instructions. Images are of a single z plane at a 63x magnification at either a 1x zoom (**i**) or a 4x zoom (**ii**). Images to the right represent the entire cell following compression of the corresponding z-stack into a single image (**iii**). The number of dots per cell for each of the 1x zoom images were counted using nuclei to define a single cell and the mean number of dots per cell was calculated. **B** - The mean number of Duolink Red signals per cell was calculated and compared using a one-way ANOVA and a multiple comparison. For each staining condition 20<n>50 with 3 replicates. Error bars represent the standard deviation and ** $p \leq 0.01$, *** $p \leq 0.001$ and **** $p \leq 0.0001$. **C** - Cell lysates were incubated with anti-DEF6 or anti-CD81 and complexes were precipitated using magnetic Dynabeads. Immunoprecipitates were separated by SDS-PAGE and the proteins were transferred to a PVDF membrane by semi-dry transfer. The membrane was cut above the 40kDa marker and the top half of the membrane was incubated with rabbit anti-DEF6 followed by goat anti-rabbit HRP. The bottom half of the membrane was incubated with mouse anti-CD81 followed by goat anti-mouse HRP. DEF6 is expressed more abundantly in Jurkats than in HuT78 resulting in no DEF6 signal in the HuT78 whole cell lysate but immunoprecipitation enriches DEF6 in the loaded sample resulting in a faint DEF6 signal.

As shown in 3.3-3A, DEF6 is in close proximity to all 3 membrane receptors in resting Jurkat T cells (aiii – ciii). However, significantly more DEF6 molecules are in close proximity to CD81 and LFA-1 in comparison to ICAM -1 as shown in figure 3.3-3B ($p \leq 0.0001$ and $p \leq 0.01$ respectively). As the protein expression of ICAM-1 on the surface of Jurkat T cells is lower in comparison to the surface of APCs, this result is not unexpected (Rocha-Perugini et al., 2013). Furthermore, figure 3.3-3B shows a significantly greater number of PLA signals between DEF6 and CD81 in comparison to DEF6 and LFA-1 ($p \leq 0.001$). As a result, an association between DEF6 and CD81 was investigated.

Figure 3.3-3C shows a western blot following co-immunoprecipitation of DEF6 and CD81 in Jurkat T cells and HuT78 T cells. HuT78 T cells were used as an alternative T cell as the DEF6 expression is much lower in comparison to Jurkat T cells as demonstrated by the whole cell lysates (3.3-3C). However, immunoprecipitation of DEF6 results in a DEF6 signal. The immunoprecipitation was carried using anti-DEF6 to determine if CD81 was also precipitated as well as in reverse using anti-CD81 to determine if DEF6 was co-precipitated. However, neither immunoprecipitation resulted in a positive association between DEF6 and CD81.

Consequently, it was hypothesised that DEF6 could be in close proximity to CD81 because trafficking of the DEF6 molecules had already occurred so they were in close proximity to the membrane. A general observation during puromycylation was that other temperature sensitive processes had also been preserved, such as what appeared to be vesicle trafficking of DEF6. As a result, the puromycylation method was used to determine whether stalling of

DEF6 trafficking altered the proximity pattern of DEF6 in relation to CD81, LFA-1 or ICAM-1.

3.3.4 Use of the Puromycylation method results in vesicle-like structure formation which is enriched in DEF6

Trafficking of receptors to the plasma membrane is a key component of receptor turnover and maintenance of a propagated signal. Therefore, CD81, ICAM1 and LFA-1 may also trafficked to the plasma membrane either in a vesicular dependent manner or as signalosomes. Consequently, investigation of whether DEF6 is in close proximity to any of the aforementioned receptors was necessary to determine whether DEF6 is truly in a complex with any of the candidates and to also give insight into how DEF6 is transported to the membrane. The puromycylation method stalls translation and preserves active translation at the ribosome. The use of fixation on ice and stabilisation of RNA complexes is particularly useful to visualise processes occurring within the cell which may be disrupted during normal fixation methods, such as vesicular transport. Puromycin, emetine and a combination of the two were individually used to treat Jurkat T cells to determine if the treatment method also had a significant effect on DEF6 enrichment and localisation.

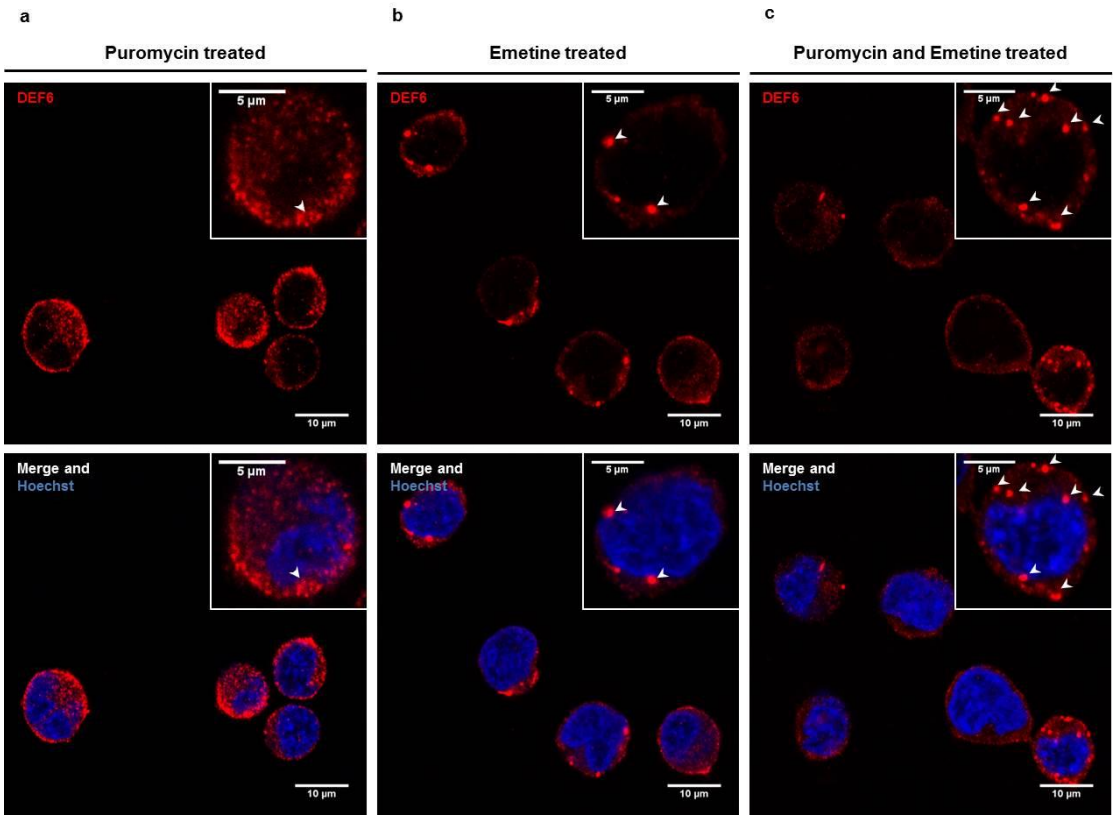

Figure 3.3-4 DEF6 is associated with what appears to be vesicle-like structures upon treatment with puromycin and emetine. Jurkat T cells were either treated with puromycin, emetine or both and stained using rabbit anti-DEF6 and goat anti-rabbit 568. Nuclei were stained using Hoechst 33258. Images are of a single z plane at a 63x magnification using confocal microscopy. Arrowheads indicate DEF6 localisation to vesicle-like structures.

The presence of emetine results in the formation of vesicle-like structures which are highly enriched in DEF6 as shown in figure 3.3-4 b and c. Puromycin treatment appears to result in aggregate formation which can follow a ring-like pattern however the vesicle-like structures are absent (3.3-4a). Puromycin is incorporated into the growing polypeptide chain during translation and causes stalling and dissociation of the ribosomal complex resulting in the formation of P-bodies which sequester and degrade the associated mRNA (Jimenez et al., 1977). Emetine prevents the disassociation of the ribosomal complex which reduces the formation of P-bodies as the mRNA is still within the ribosome (Jimenez et al., 1977). Consequently, the structures visible following emetine treatment are unlikely to be P-bodies and are much larger than the usual DEF6 aggregation pattern in response to stalled translation.

To investigate whether the vesicle-like structures contain lipids, Nile Red was used as marker to determine whether any lipids were of a neutral environment. This is because Nile Red is a non-specific marker of triacylglycerols, sphingolipids, cholesterol esters and phospholipids when it fluoresces in the green wavelength. Jurkat T cells were re-suspended in fresh RPMI 1640 and applied to poly-L-lysine coated coverslips. Cells were incubated with puromycin and emetine at 37°C for 5 minutes and fixed on ice using polysome stabilising buffers. A Nile Red solution was prepared and used to stain neutral lipids. Nuclei were stained using Hoechst 33258 and cells were imaged using fluorescence microscopy.

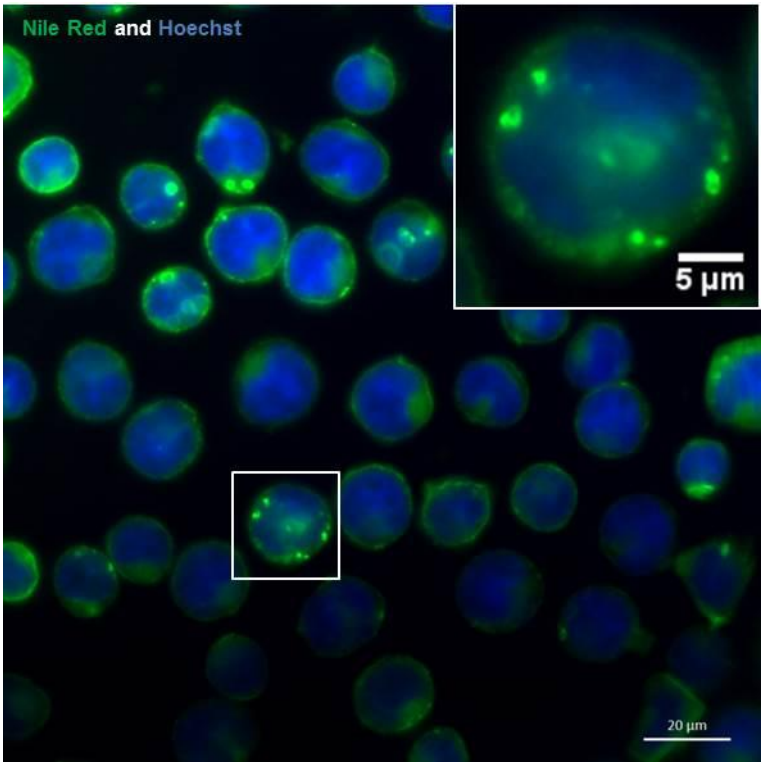

Figure 3.3-5 Vesicle-like structures formed during puromycin and emetine treatment stain using a lipid selective marker. Jurkat T cells were treated with puromycin and emetine and stained using Nile Red which fluoresces in a neutral lipid environment indicating the presence of triacylglycerols, sphingolipids, cholesterol esters and phospholipids. Images were taken using an Axioskop MOT and a 63x magnification.

Figure 3.3-5 shows that some Jurkat T cells display vesicle-like structures which fluoresce in the green wavelength once treated with puromycin and emetine and fixed using the puromycylation method. Interestingly, not all cells display these vesicle-like structures however some cells display multiple structures within the cell. Unfortunately Nile red is a non-specific marker of lipids and can fluoresce in the green and red wavelengths depending upon the type of lipid labelled. As a result, co-immunolabelling could not be carried out using anti-DEF6 and Nile red. Further investigation would be required using a specific lipid marker so that DEF6 could be stained simultaneously. The use of a detergent could be used to see whether the lipid staining disappears but if DEF6 staining remains then it would suggest that the structures are independent of lipids.

3.3.5 Sequestering of DEF6 to vesicle-like structures results in DEF6 being in close proximity to LFA-1

As DEF6 was shown to remain in the cytoplasm in vesicle-like structures following puromycin and emetine treatment, as shown in figure 3.3-4, the effect on the proximity to CD81, ICAM1 and LFA-1 was again investigated.

Jurkat T cells were re-suspended in fresh RPMI 1640, applied to poly-L-lysine coated coverslips and incubated with puromycin and emetine for 5 minutes at 37°C. Cells were fixed on ice using polysome stabilising buffers and DEF6 was labelled using rabbit anti-DEF6 whilst CD81, LFA-1 or ICAM-1 was labelled using mouse anti-CD81, anti-LFA-1 or anti-ICAM-1. Oligonucleotide coupled secondary antibodies were used to label their respective primary antibodies: donkey anti-rabbit plus labelled DEF6 whilst donkey anti-mouse minus labelled CD81, LFA-1 or ICAM-1. If the oligonucleotide probes were within 40nm, a ligase reaction was used to ligate the oligonucleotides and the signal was amplified using a polymerase and red amplification buffer. Nuclei were stained using DAPI within the mountant and cells were imaged by fluorescent microscopy. The mean number of PLA signals per cell was calculated and preliminary data was compared using a one-way ANOVA.

A

a

DEF6 and CD81

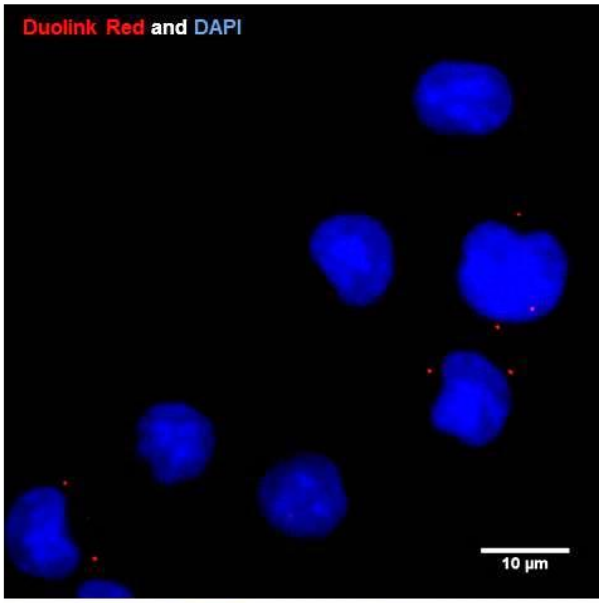

b

DEF6 and ICAM1

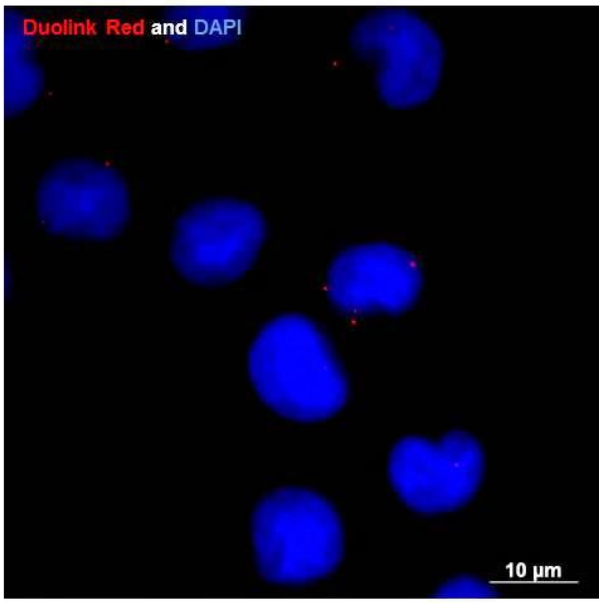

c

DEF6 and LFA-1

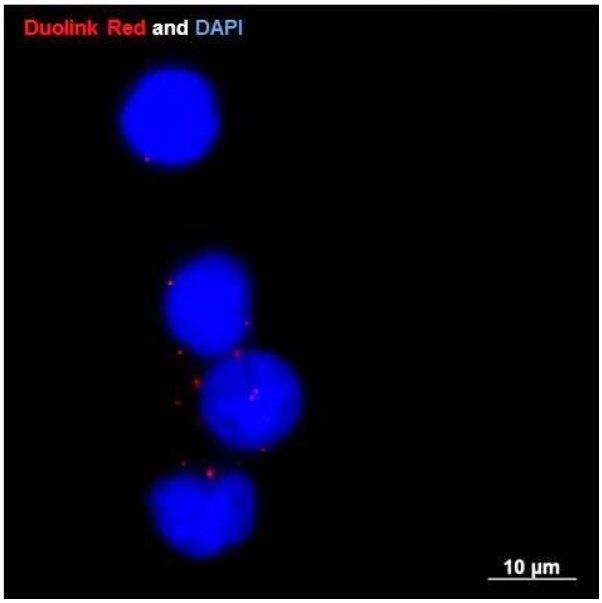

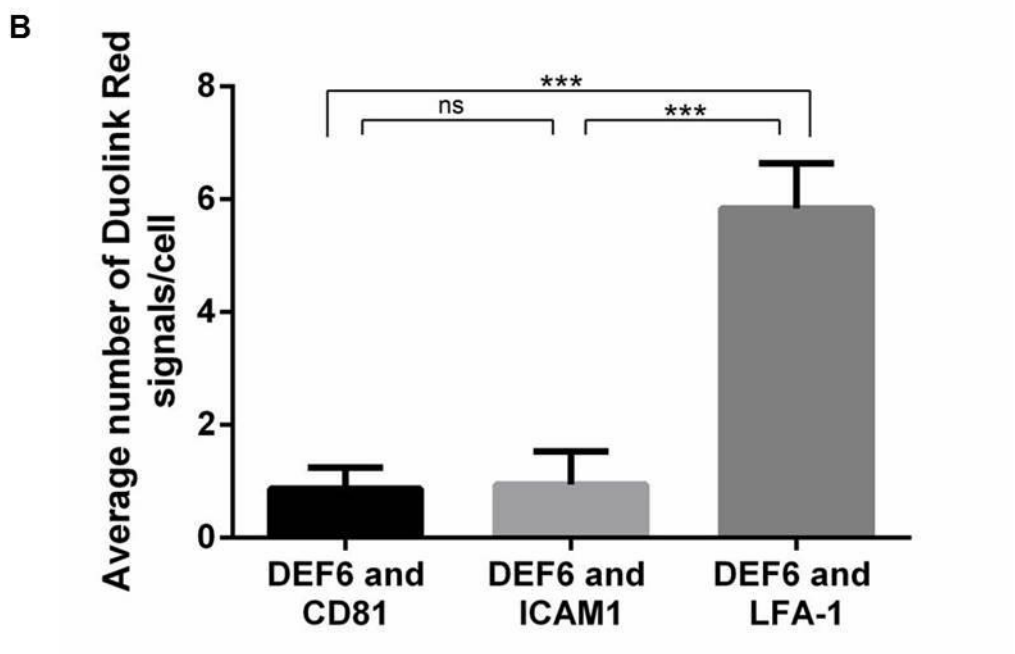

Figure 3.3-6 Redirection of DEF6 to vesicle-like structures greatly reduces the amount of DEF6 which is in close proximity to CD81. Jurkat T cells were treated using puromycin and emetine. DEF6 and CD81, ICAM-1 or LFA-1 were labelled using their respective monoclonal antibodies. Proteins in close proximity were detected using a Duolink Red (Sigma) assay as per the manufacturer's instructions. Images are of multiple z planes at a 63x magnification using an Axio imager M2. The mean number of Duolink Red signals per cell was calculated and compared using a one-way ANOVA and a multiple comparison. For each staining condition $2 \leq n > 10$ with 3 replicates. Error bars represent the standard deviation, *** $p \leq 0.001$ and ns is not significant.

As shown in figure 3.3-6A, DEF6 is still in close proximity to all three membrane receptors in resting Jurkat T cells. However the average number of PLA signals between DEF6 and CD81 has reduced from around 9 signals per cell to 1 signal per cell (3.3-3B and 3.3-6B). Moreover, the average number of PLA signals between DEF6 and LFA-1 has increased from around 4 signals per cell to 6 signals per cell (3.3-3B and 3.3-6B). The number of a PLA signals between DEF6 and ICAM-1 has remained the same at around 1 signal per cell (3.3-3B and 3.3-6B). The average number of DEF6 and LFA-1 PLA signals is also significantly greater than the average number of DEF6 and CD81 PLA signals as shown in figure 3.3-6B ($p \leq 0.001$). Moreover, the reduction in the average number of DEF6 and CD81 PLA signals has resulted in a non-significant difference in comparison to DEF6 and ICAM-1 suggesting that DEF6 is indeed further from CD81 when Jurkats are treated with puromycin and emetine (3.3-6B).

An association between DEF6 and LFA-1 was investigated however the anti-LFA-1 antibody could not be optimised for the use of co-immunoprecipitation so further work would be required to determine if there is an association between DEF6 and LFA-1. Furthermore, it is assumed that LFA-1 is also within vesicle-like structures following puromycin and emetine treatment however immunofluorescence could be used to identify the LFA-1 distribution following treatment to determine if LFA-1 is within these structures.

3.3.6 Summary of main findings

- Jurkat T cell activation results in DEF6 aggregation and enrichment at filopodia.
- Engagement of the TCR alone is insufficient for DEF6 translocation to the plasma membrane.
- DEF6 is able to translocate to the T-T cell synapse and is enriched further upon chemical activation of the T cells.
- CD81 and LFA-1 are both likely candidates to facilitate DEF6 movement to the plasma membrane.
- DEF6 does not appear to be associated with CD81 in resting Jurkat T cells.
- The use of the puromycylation method to preserve fixation sensitive processes results in DEF6 enrichment at vesicle-like structures and highlights that DEF6 is likely to be transported in close proximity to LFA-1 rather than CD81.

3.4 Discussion of Results

3.4.1 DEF6 forms an aggregate which co-localises with mRNA and is in close proximity to 4E-T

Hey et al. (2012) determined that DEF6 aggregation was in response to ITK phosphorylation and that exogenous DEF6 granules co-localise with DCP1, a P-body marker. However, investigation of endogenous DEF6 aggregates and mRNA regulatory granules was not carried out. In COS-7 cells, exogenous WT-DEF6 remained diffuse within the COS-7 cytoplasm but this may be due to the absence of the T cell signalling machinery. Moreover, the ITK phosphomimic DEF6 mutant, Y210EY222E-DEF6, formed cytoplasmic granules regardless of external treatment. Upon treatment with sodium arsenite, WT-DEF6 formed cytoplasmic aggregates indicating that cellular stress is sufficient for DEF6 aggregation. Figure 3.1-1 demonstrates that endogenous DEF6 is able to aggregate in Jurkat T cells regardless of the T cell state suggesting that DEF6 aggregation is a normal cellular response as well as occurring in response to stress. Investigation of DEF6 protein expression in response to chemical activation and stress showed that relative DEF6 protein levels increased in comparison to untreated Jurkat T cells as shown in figure 3.1-2. This suggests that DEF6 protein expression increases in response to activation and may be linked to the role of DEF6 in F-actin polymerisation at the IS in response to activation (Fanzo et al., 2006). To further investigate the effect of activation and stress upon DEF6 aggregation, flow cytometry could be used to measure granulation and protein expression more accurately than the use of confocal microscopy and western blot analysis.

To determine whether DEF6 aggregates co-localise with endogenous P-bodies, a PLA was used to identify close proximity with 4E-T, a P-body specific marker that transports eIF4E to P-bodies (Ferraiuolo et al., 2005). As shown in figure 3.1-4, DEF6 is in close proximity to 4E-T in untreated and stressed Jurkat T cells however activation of the T cells results in complete abolishment of DEF6 and 4E-T proximal signals. Figure 3.1-5 shows that P-bodies are still likely to be present as DDX6 and 4E-T proximal signals remain following chemical activation of the T cells. Stressing of the T cells using sodium arsenite resulted in fewer proximal signals between DDX6 and 4E-T suggesting that DEF6 aggregates that are in close proximity to 4E-T following stress may be absent of DDX6. A large scale proteome-map study was completed and published at a similar time which identified a direct DEF6-4E-T interaction using a yeast 2-hybrid assay (Rolland et al., 2014). The study described a reliable direct interaction if the yeast 2-hybrid assay provided a positive interaction at least 3 out of 4 attempts. These data corroborate the findings of Hey et al. (2012) and show that DEF6 aggregates co-localise with an endogenous P-body marker.

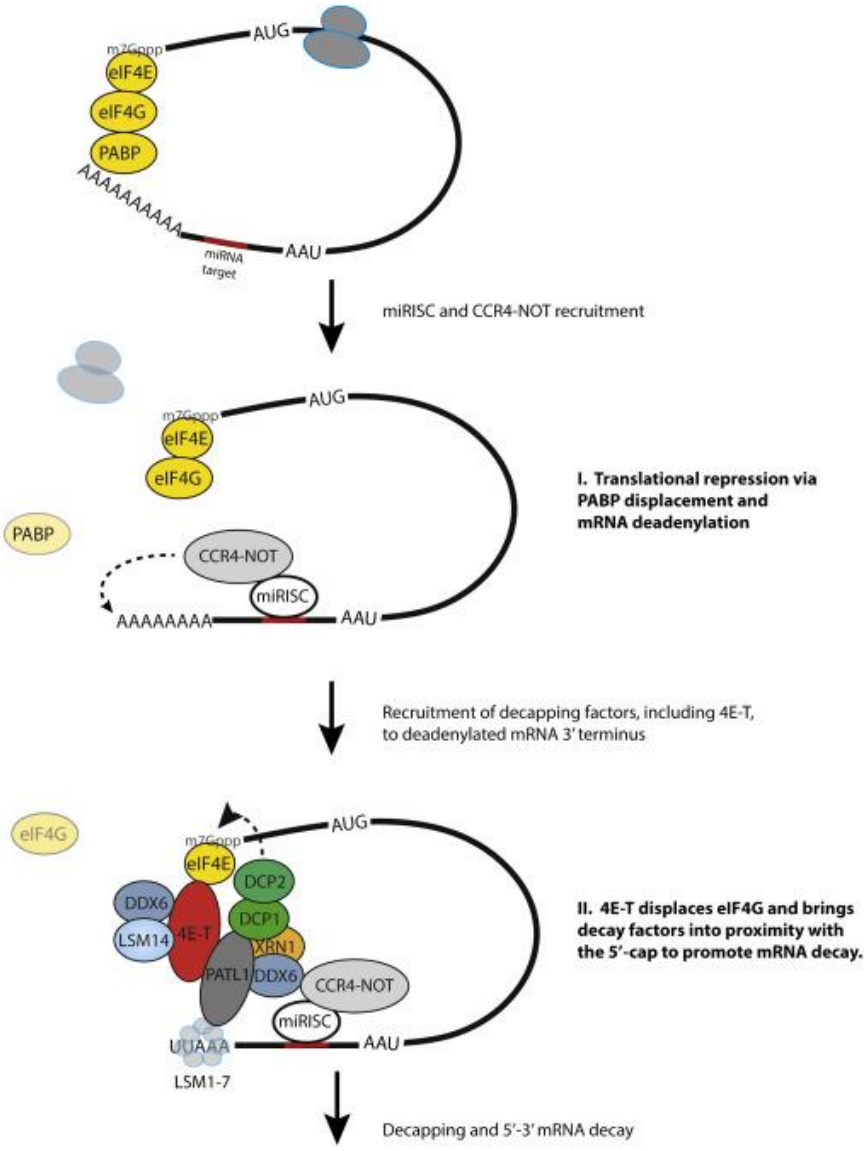

Figure 3.4-1 The proposed model for the role of 4E-T in the deadenylation and decapping of mRNA. During translation initiation the mRNA is circularised due to the association of eIF4E, eIF4G and PABP. However, binding of a miRNA target by the RISC complex causes recruitment of CCR4-NOT and displaces PABP leading to linearization. CCR4-NOT then deadenylates the PolyA tail to produce an oligoadenylated sequence which recruits the decapping machinery and the mRNA is circularise once more by the interaction of 4E-T with eIF4E and PATL1. Following decapping of the mRNA by DCP1 and DCP2, the 5'-3' exonuclease XRN1 is able to hydrolyse the mRNA residues, completing degradation (Nishimura et al., 2015).

As shown in figure 3.4-1, mRNA silencing via degradation is closely linked to translation initiation. The mRNA remains circularised whilst eIF4E, eIF4G and PABP are associated on the mRNA. Formation of the RISC complex on the target miRNA recognition sequence results in the recruitment of the CCR4-NOT complex and causes displacement of PABP. The CCR4-NOT complex facilitates deadenylation of the 3' to form an oligoadenylated sequence which causes recruitment of the decapping and degradation machinery. 4E-T is proposed to maintain mRNA circularity by binding eIF4E and PATL1 to allow the recruited DCP1 and DCP2 to remove the mRNA cap. This allows the 5'-3' exonuclease XRN1 to begin hydrolysis of the mRNA residues to complete degradation (Nishimura et al., 2015).

As a result, eIF4E is retained during the formation of the decapping complex and is associated with 4E-T. Moreover, PABP is involved in the early stages of degradation until becoming displaced by the CCR4-NOT complex. Consequently, a potential link between DEF6, mRNA stability and 4E-T-mediated degradation may be an ideal area for future investigation.

As the DEF6 aggregates appear to associate with 4E-T, the granules were investigated to determine whether they contain mRNA. Figure 3.1-6 shows that the exogenous phosphomimic Y210EY222E-DEF6 granules expressed in COS-7 cells do in fact co-localise with mRNA labelled with a Cy5 coupled Oligod(T). The phosphomimic granules mimic ITK phosphorylation at Y210 and Y222 which Hey et al. (2012) determined caused DEF6 aggregation in COS-7 cells and co-localisation with a P-body marker. Endogenous DEF6 granules were also investigated for the presence of mRNA using the Cy5-oligod(T) method as well as the non-specific acridine orange however the presence of mRNA in endogenous granules could not be detected by confocal microscopy due to a lack of sensitivity. Moreover, a method to detect a direct association between mRNA and DEF6 was proposed but could not be established due to the absence of a known RNA binding sequence as well as a lack of sensitivity using mRNA loaded oligod(T) beads and pooled mRNA. An alternative method would be to use an individual nucleotide resolution cross-linking and immunoprecipitation method, known as iCLIP, to selectively precipitate DEF6 using antibodies and sequence any potential mRNA that was co-precipitated. This would briefly involve cross-linking *in vivo* protein-RNA interactions using UV and precipitating the interactions using an antibody specific to the protein of interest during RNA preserving immunoprecipitation. RNA is dephosphorylated at the 3' end and an adapter linker is ligated: the 5' end is also radiolabelled. Free RNA is removed using SDS-PAGE and bound RNA is isolated following membrane transfer of the protein-RNA complex. The RNA is reverse transcribed to produce cDNA which is separated by electrophoresis. The cDNA is then linearised and

amplified by PCR followed by high-throughput sequencing to identify sequences which are bound by the protein of interest (Huppertz et al., 2014). However this method would require significant optimisation and time which unfortunately could not be carried out during this work.

As a result, RNAbindR was used to predict whether DEF6 contained an RNA binding domain to corroborate whether the finding was reliable. The amino acid sequence of DEF6 is highly conserved across multiple species so the DEF6 sequence was aligned using human, mouse, zebrafish and xenopus sequences (Mavrakis et al., 2004). Once aligned using T-Coffee, RNAbindR predicted two RNA binding sequences within DEF6, one within the proposed EF hand and the other within the PH domain. Interestingly, the second proposed RNA binding sequence begins with Y222 which may suggest that the phosphorylation of Y222 by ITK is involved with mRNA binding.

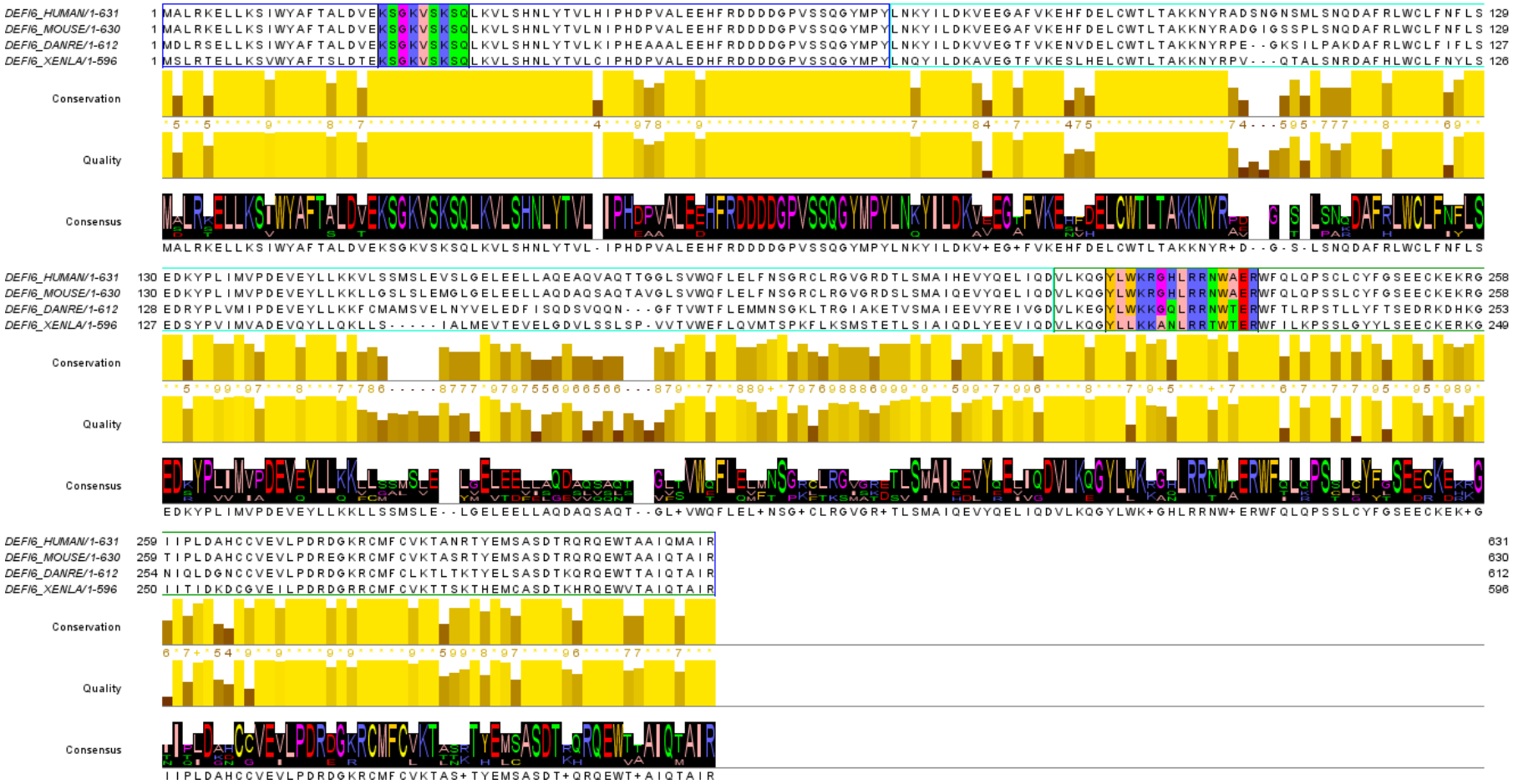
DEFI6_HUMAN/1-631
DEFI6_MOUSE/1-630
DEFI6_DANRE/1-612
DEFI6_XENLA/1-596
Conservation
Quality
Consensus

Figure 3.4-2 DEF6 is predicted to have two mRNA binding sequences that are conserved amongst the main experimental species. The DEF6 protein sequences for Homo sapien, Mus musculus, Danio rerio and Xenopus laevis were aligned using T-Coffee and the output was used in Jalview. Sequence conservation and the quality of the sequence alignment are displayed by the height of the corresponding bar and the colour, with the conserved amino acid displayed underneath. The predicted RNA binding sites are coloured using Zappo which demonstrates the properties of the corresponding amino acid: salmon pink – hydrophobic; orange – aromatic; blue – positive; red – negative; green – hydrophilic; Pink – conformationally special; yellow – cysteine. The domain corresponding to the protein sequence is depicted by the coloured border: dark blue – EF hand; light blue; ITAM-like motif; green – PH domain.

Recent studies have also identified other proteins with known metabolic roles that are now being implicated in RNA binding and regulation (Beckmann et al., 2015; Beckmann et al., 2016). For example, Beckmann et al. (2015) determined that many of the glycolytic enzymes were capable of binding RNA, despite lacking conventional RNA binding motifs, and this ability to bind RNA was present in both *Saccharomyces cerevisiae* and human HuH-H7 hepatocytes. As DEF6 lacks a conventional RNA binding motif, it may facilitate RNA binding in association to other metabolic proteins as suggested by Beckmann et al. (2016).

3.4.2 DEF6 is in close proximity to active translation in naïve and activated T cells and co-localises with PABP and eIF4E

The puromycylation method allowed accurate visualisation of active translation *in vivo* using confocal microscopy. Figures 3.2-1 and 3.2-2 show that DEF6 aggregates do co-localise with active translation which is further corroborated by a PLA as shown in figure 3.2-3. Furthermore, investigation of a link between DEF6 and translation factors showed that DEF6 is in close-proximity to eIF4E and PABP.

Figure 3.2-4A showed co-localisation between DEF6 and eIF4E, including within a filopodium which formed in response to chemical activation by PMA and ionomycin. This was further corroborated by figure 3.2-4B which shows close proximity between DEF6 and eIF4E in untreated, chemically activated and stressed T cells. Stressing of the Jurkat T cells led to a significant reduction in the number of PLA signals between DEF6 and eIF4E ($p \leq 0.05$) as shown in figure 3.2-4C.

Interestingly, it has been suggested that eIF4E is a key regulator of translation in $CD4^+$ T cells in response to activation (Bjur et al., 2013). As eIF4E cap binding is required for translation initiation, the level of eIF4E expression is a rate limiting step during translation. Consequently, eIF4E expression increased in response to activation and the translation of cell cycle proteins and proliferation mediators also increased. Moreover, inhibition of eIF4E expression resulted in a drive towards $FOXP3^+$ T cell differentiation indicating that eIF4E mediates the differentiation of $FOXP3^-$ T cells towards the regulatory lineage (Bjur et al., 2013).

An association between DEF6 and the mRNA cap has been investigated by Ms Maha Alsayegh (unpublished) within the laboratory using co-immunoprecipitation, however an association has failed to be seen. A complex which may form between DEF6 and the mRNA cap may be sensitive to cell lysis and precipitation conditions causing disassociation. Another potential way to determine an association may be to use Jurkat T cell lysates and incubate them with mRNA cap loaded beads and precipitate any associated proteins. Those proteins could be separated by SDS-PAGE and digested for identification by mass spectroscopy. The control sample would require the beads minus the loaded mRNA cap to identify non-specific interactions between proteins and the beads themselves.

Figure 3.2-5 also appears to show an association between DEF6 and PABP. DEF6 aggregates and PABP co-localise in untreated cells whilst chemical activation and stressing appear to cause DEF6 granule docking with PABP (3.2-5A). The PLA showed that the average number of PLA signals significantly decrease in response to treatment with sodium arsenite ($p \leq 0.01$) which corroborates the results of DEF6 and eIF4E proximity in response to stress.

Investigation of whether the use of puromycin and/or emetine affected PABP distribution demonstrated that PABP was not affected and had a similar distribution pattern to active translation further corroborating the idea that DEF6 is in close proximity to active translation (3.2-7). However, simultaneous labelling of puromycin and PABP was not possible due to the availability of only mouse mAbs.

Localised translation is fundamental to neuronal synapse formation and maintenance as it facilitates the ability to produce proteins where they are locally required rather than transporting the proteins across the cell. This method is highly efficient and allows the cell to coordinate a response to signalling at the synapse (Bassell and Warren, 2008). As a result, a similar model could be present during IS formation and signalling to maintain the complex SMAC and the following response. Figure 3.2-8 shows that active translation is present at the IS but it also present throughout the T cell. The active translation does co-localise with enriched DEF6 at the IS and it is important to note that it is not excluded suggesting that proteins are being synthesised at the IS which may be fundamental to the immunological response. Interestingly, pre-treatment of the cells with sodium arsenite inhibited DEF6 translocation to the IS suggesting that DEF6 translocation may be dependent upon active translation or the formation of the IS itself may be dependent upon active translation. Further work will be required to identify whether DEF6 or the IS formation is the dependent factor by using another IS marker, such as PLCθ, to determine whether the IS was actually able to form.

3.4.3 DEF6 translocation to the membrane occurs in close proximity to LFA-1

Current literature has established that DEF6 translocation to the IS is in response to LCK phosphorylation and it is hypothesised that this translocation results in the activation of $NFAT_{C1/2}$ (Gupta et al., 2003a; Becart et al., 2008b). Gupta et al. (2003a) also proposed that DEF6 was phosphorylated at Tyr210 by LCK, however, DEF6 is phosphorylated at Tyr210 and Tyr222 by ITK and results in aggregation (Hey et al., 2012). Furthermore, Singleton et al. (2011) determined that ITK regulates the spatiotemporal pattern of DEF6 at the IS to regulate the position of Cdc42 during F-actin polymerisation and IS stabilisation.

However, the actual mode of DEF6 transport in response to antigen presentation had not been fully investigated, for example, does DEF6 translocate as an aggregate or within a larger complex? Figure 3.3-1b suggests that DEF6 translocation to filopodia may be dependent upon calcium release as ionomycin treatment results in the release of calcium from intracellular stores. Calcium dependent localisation has been attributed to the potential presence of a calcium binding EF hand and it is proposed that DEF6 anchoring to the membrane is facilitated by the PH domain associating with PIP_3 (Gupta et al., 2003a; Tanaka et al., 2003). Fos et al. (2014) have recently suggested that the two EF hands within the DEF6 N-terminus do in fact bind calcium and were able to demonstrate a faint signal by autoradiography following binding of ^{45}Ca. However, deletion of both proposed EF hands, Δ19-30 and Δ57-68, reduced the binding capability of DEF6 but it was not significantly different to WT DEF6. This does suggest that

DEF6 translocation could be in fact independent of an external signal as long as intracellular calcium is released.

Figure 3.3-1 also highlights the requirement for a full receptor network to induce DEF6 translocation to the plasma membrane. SEA/B loaded Raji B cell resulted in DEF6 translocation to the IS however TCR engagement alone did not. TCR engagement actually resulted in DEF6 aggregation, a response attributed to ITK phosphorylation (Hey et al., 2012). This suggests that another co-factor associated with the TCR may in fact induce translocation removing the specificity and high affinity requirement of a TCR-MHC II association.

Figure 3.3-2 also demonstrated that DEF6 is able to translocate to T-T cell junctions which suggests the receptor signal required for DEF6 movement is not APC specific. Integrin signalling is primarily attributed to the binding of the ECM and anchoring the intracellular cytoskeleton to the plasma membrane (Hynes, 2002). However, integrins are also essential for binding their corresponding receptor on the recipient cell to promote inside-out signalling and suggests that DEF6 may be involved in various methods of cell communication which are not specific to IS signal transduction (Hynes, 2002). Samson et al. (2007) have previously determined that Def6 associates with α7A, a splice isoform of the alpha chain of $\alpha7\beta1$. The integrin $\alpha7\beta1$ is expressed by skeletal myocytes and facilitates laminin binding to the membrane. Interaction between Def6 and α7A was determined by a yeast two-hybrid assay and only full length Def6 interacted with α7A.

Investigation of DEF6 transport using sensitive preservation methods highlighted that DEF6 may in fact be transported to the membrane in vesicle-like structures. Core components of the TCR signalling network have previously been shown to translocate to the membrane within sub-synaptic vesicles, e.g. TCRζ, LAT, ZAP70 and SLP76, and their recruitment and organisation at the plasma membrane is dependent upon LCK phosphorylation (Soares et al., 2013). These sub-synaptic vesicles are pre-packaged receptor complexes which are able to fuse with the membrane at the IS to form distinct nano-domains. Upon TCR activation, the distinct nano-domains aggregate within the plasma membrane to maintain the propagated signal more efficiently (Dinic et al., 2015). Following engagement of the TCR and subsequent TCR nano-domain patching, the T cell-APC interaction is stabilised via integrin binding. Therefore, it is essential for LFA-1 to be trafficked to the leading edge of the plasma membrane to facilitate the association of LFA-1 to ICAM-1. This is achieved by Rab proteins, small GTPases which promote vesicle formation and trafficking via the cytoskeleton, and LFA-1 trafficking may be regulated by Rab13 (Nishikimi et al., 2014). As a result, LFA-1 trafficking is likely to involve small vesicle formation and translocation along the actin cytoskeleton which appears to corroborate the findings shown by figures 3.3-4 and 3.3-5.

Preliminary data suggests that DEF6 is in close proximity to LFA-1 following sensitive cell preservation methods and DEF6 may be transported to the cell membrane in close proximity to LFA-1. As DEF6 is involved in the rearrangement of F-actin via activation of Rac1 and Cdc42, DEF6 may also be involved in the trafficking of LFA-1 along the cytoskeleton. Once DEF6 has been transported, fusion of the vesicle-like structure with the T cell membrane results in DEF6 being in close proximity to CD81 and LFA-1 as shown in figure 3.3-3. This suggests that at the membrane, DEF6 is in close proximity to the tetraspanin web which is instrumental to preserving the stability of the IS and anchoring the T and B cell during signal propagation and the response (Rocha-Perugini et al., 2013).

However, further work will be required to determine if DEF6 is truly complexed with LFA-1 and to determine if there is a direct interaction. For example, the puromycylation method could be carried out to determine if LFA-1 also localises to the vesicle-like structures to visualise the cellular structure in conjunction with the PLA results. Moreover, a binding assay could be carried out using a DEF6 loaded column to determine if LFA-1 binds to DEF6. However, if the association is indirect then the assay conditions are unlikely to replicate the *in vivo* complex. As sub-synaptic vesicles contain other key components, as described above, antibodies directed against these proteins could be used to identify the vesicle-like structures using co-localisation studies and confocal-microscopy.

Cote et al. (2015) also suggested that DEF6 associates with LFA-1 in $CD4^+$ T cells. $Def6^{-/-}$ knockout $CD4^+$ T cells showed a reduced ability to associate with ICAM-1 via LFA-1 without a decrease in CD11a or CD18 expression, the two molecules that together form LFA-1. A direct association was also shown between DEF6 and GTP bound Rap1, a small GTPase which is associated with LFA-1, and that they are independently recruited to the IS in response to antigen presentation. The direct association was described to be mediated by the PH domain of DEF6 and exogenous expression of a DEF6-ΔPH mutant in Jurkat T cells resulted in a dose-dependent reduction in the ability to bind ICAM-1. This was attributed to a reduction in the affinity maturation of LFA-1 as it remained in a low-affinity conformation. Treatment with magnesium chloride chemically induced affinity maturation causing LFA to change to a high-affinity conformation and rescued the ability to bind ICAM-1 (Cote et al., 2015). As a result, these data appear to corroborate the finding that DEF6 is in close proximity to LFA-1, however, the study did not investigate whether DEF6 is transported to the IS along with LFA-1.

T-T cell priming has been suggested as a fundamental component of the immune response. T-T cell priming is required to reduce the number of motile $CD4^+$ T cells that have already experienced a high affinity antigen which will increase the likelihood that a naïve T cell will encounter the circulating antigen presented by an APC (Helft et al., 2008). The translocation of DEF6 to the T cell membrane in response to other T cells as well as APCs suggests that DEF6 is involved in T-T cell association. Using current models for DEF6 involvement in the IS, DEF6 could facilitate F-actin polymerisation to stabilise the T-T cell junction in a similar manner described to that of the IS (Fanzo et al., 2006).

Chapter 4 Discussion

4.1 Structure of DEF6 and its Relation to mRNA Regulation and Turnover

Proteins associated with P-bodies and mRNA turnover often have a regulatory feature to prevent continuous aggregation, degradation or association with a target. Hey (2011) proposed a closed loop regulation model for DEF6 in which the C-terminus binds the PH domain to prevent auto-aggregation, and phosphorylation of DEF6 by ITK at Y210 and Y222 causes dissociation of the C-terminus from the PH domain. The DEF6 protein is then freely able to form the intended tertiary structure, which is hypothesised to be a donut arrangement, and aggregate to form granules. The closed loop model of regulation may also affect the ability of DEF6 to associate with mRNA or 4E-T due to the possibility of an mRNA binding domain beginning with tyrosine residue 222. If the C-terminus is associated with the PH domain of DEF6, tyrosine residue 210 may be available for ITK phosphorylation triggering dissociation and freeing Y222 for phosphorylation allowing aggregation.

The presence of a NLS and NES signal is also an interesting feature for a GEF. It allows DEF6 to translocate within the nucleus and also back to the cytoplasm which is a characteristic that currently does not coincide with its role in the literature. DEF6 is attributed to Cdc42 and Rac1 phosphorylation at the IS which would suggest a primarily plasma membrane localisation (Mavrakis et al., 2004; Gupta et al., 2003a). However, DEF6 is present throughout the cytoplasm and smaller DEF6 signals and aggregates are visible within the nucleus. This suggests that DEF6 does have a deliberate function within the nucleus which may link to a role in mRNA regulation and turnover. DEF6 may demonstrate an auto-regulatory function by binding its

own mRNA transcripts within the nucleus and preventing further protein expression of DEF6 until a suitable external stimulus requires an increased level of DEF6, such as the formation of the IS and activation of LCK or ITK. DEF6 may bind other mRNA transcripts encoding related proteins which have a role downstream of DEF6 in the TCR signal transduction cascade, for example NFAT or perhaps Rac1, Cdc42 and RhoA. Or alternatively, DEF6 may bind the transcripts of proteins which facilitate the full T cell response following differentiation and proliferation, such as IL-2, IL-10, TGFβ, IFNγ etc. As a result, nuclear export of DEF6 and subsequent phosphorylation of DEF6 by LCK and/or ITK may cause the dissociation of the C-terminus from the PH domain, allowing DEF6 to fold into the functional tertiary structure. This may result in direct dissociation from the target mRNA transcripts or indirect dissociation from an interacting mRNA binding protein and cause DEF6 to aggregate or catalyse the GDP-GTP exchange for Rac1, Cdc42 and RhoA.

FMRP is a well-known example of a protein which translocates to the nucleus of the neurone to associate with target mRNA transcripts and shuttle the transcripts to the synapse upon activation. Dephosphorylated FMRP is transported as aggregates by retrograde and anterograde motors along the axon and phosphorylated FMRP-mRNA aggregates represses the expression of the associated transcripts (Bassell and Warren, 2008).

SWAP-70 is a similar protein to DEF6 which is primarily expressed in B cells, although the requirement for a similar protein in a different cell type has not yet been established. SWAP-70 also has an NLS and NES which allow the nuclear transport of SWAP-70 to facilitate B cell class switching (Masat et al., 2000). Although T cells do not have a similar process, DEF6 may be involved

with differentiation and proliferation as activation of DEF6 leads to nuclear translocation of NFAT in response to Cdc42 activation (Becart et al., 2007). This again links to the proposed idea that DEF6 may bind mRNA transcripts which would promote differentiation and proliferation such as interleukin and cytokine transcripts.

4.2 Importance of a Guanine Nucleotide Exchange Factor Interacting with Active Translation

The proposed idea that DEF6 may have an auto-regulatory role in its own expression may also extend to translation of the corresponding mRNA. For example, shuttling of DEF6 to the nucleus to bind DEF6 encoded transcripts and export of DEF6-mRNA aggregates out of the nucleus may allow DEF6 to associate with polysomes in preparation for DEF6 dissociation in response to TCR activation and LCK and/or ITK phosphorylation. As a result, the protein expression of DEF6 would increase in response to activation and may facilitate an increased rate of cytoskeletal remodelling at the IS as DEF6 would activate Rac1 and Cdc42 leading to F-actin polymerisation (Mavrakis et al., 2004; Gupta et al., 2003a).

An alternative link between DEF6 and active translation may be a structural role, promoting anchorage of polysomes to the actin cytoskeleton. Remodelling of the cytoskeleton may allow transport of active translation as required creating a cellular polarity in the production of particular proteins which may be essential during IS formation and maintenance. Polysomes are often either membrane associated or cytosolic so this would relate to polysomes that are not associated with the rough endoplasmic reticulum but may perhaps require an anchorage point close to the plasma membrane.

A role in F-actin polymerisation may also relate to a potential function as a transporting chaperone protein allowing DEF6 to associate with translation factors and promoting translocation of these factors to sites of active translation. It may also relate to the transport of translation factors from sites of active translation to established stress granules in response to an external stressor.

The rate of translation and the availability of eIF4E also has an effect on T cell differentiation and proliferation. Naïve T cells are able to differentiate into effector T cells or T regulatory cells: effector T cells include T helper 1 cells; T helper 2 cells; follicular T helper cells; and T helper 17 cells. Treg cells differ due to their expression of FOXP3 and altered cytokine profile which enables the Treg cells to regulate effector T cells (Bjur et al., 2013). If the cell environment results in stressor stimuli, such as: hypoxia; glucose deprivation; heat shock or UV exposure; then eIF4E is sequestered by eIF4E binding proteins which drive eIF4E towards stress granules and P-bodies. This reduces the availability of eIF4E for the formation of translation initiation complexes and reduces the rate of translation in a $CD4^+$ T cell. This has been shown to promote the expression of FOXP3 in $CD4^+$ T cells and promotes a Treg cell lineage which results in an increase in effector T cell regulation (Bjur et al., 2013).

Activation of $CD4^+$ T cells via TCR stimulation increases the rate of translation due to the activation of PI3K which activates AKT. AKT subsequently phosphorylates mTOR which results in the phosphorylation of eIF4E binding proteins and the dissociation from eIF4E resulting in an increase in translation (Istomine et al., 2016). As DEF6 is suggested to associate with 4E-T, an eIF4E binding protein, DEF6 may be involved in regulating the availability of eIF4E at the IS and the subsequent rate of translation which would determine the differentiation of the naïve T cell in response to TCR stimulation (Kamenska et al., 2014; Bjur et al., 2013).

4.3 The Potential Role of a Guanine Nucleotide Exchange Factor in the Posttranscriptional Regulation of mRNA in T cells

During the immune response, the T cell has a distinct polarity which ensures that proteins involved in the TCR signal transduction cascade are targeted towards the IS and proteins which are involved in dampening or completing this response are targeted to the distal side of the T cell. In each case specific mRNA transcripts would be required for translation and the production of the respective proteins, suggesting that changes in the cellular response would require changes in the availability of mRNA transcripts. This may be achieved by increasing mRNA degradation or induction or inhibition of miRNA silencing to achieve the desired protein expression. To maintain the cell polarity, mRNA turnover is likely to require the cytoskeleton to provide anchorage points and maintain the cytoplasmic location during changes to mRNA regulation and degradation. As a result, DEF6 may provide a key link between the actin cytoskeleton and anchorage of mRNPs during changes to mRNA expression and turnover.

The average T cell response requires changes to protein expression in a shorter time span than is probable following an increase or decrease in gene expression. Therefore, storage of pre-produced mRNA transcripts within P-bodies or stress granules is likely an efficient way to respond to a desired change in protein expression (Kafasla et al., 2014). Engagement of the TCR by a pMHCII molecule will induce the signal transduction cascade resulting in phosphorylation of DEF6 by LCK and/or ITK which may provide a link between TCR activation and changes to mRNA availability. Phosphorylation of DEF6 by LCK may lead to the dissociation of DEF6 from 4E-T and P-bodies causing translocation of DEF6 to the IS to facilitate the production of F-actin and stabilisation of the IS. An alternative result may be that DEF6 is phosphorylated by LCK and results in DEF6 and 4E-T translocating to the IS. As 4E-T is an eIF4E binding protein, it may be possible that eIF4E is also chaperoned to the IS and may help to promote translation at the IS. Alternatively eIF4E may be sequestered within P-bodies via 4E-T association to prevent translation (Kamenska et al., 2014).

Treg cells also regulate the target effector T cell via posttranscriptional regulation of mRNA and protein expression by secreting exosomes containing miRNAs (Okoye et al., 2014). Exosomes are a fundamental method for the $CD4^+$ T cell to communicate with the recipient APC and alter the posttranscriptional regulation within that cell. It has been suggested that Cdc42 activation is critical for exosomal delivery and that whilst the translocation of the MTOC facilitates secretion, it is not essential for continued exosomal delivery (Chemin et al., 2012). On the other hand, Cdc42 activation and F-actin polymerisation is required. Interestingly, DEF6 and 4E-T have

been identified as components of exosomes that have been secreted during communication. This may suggest a role in altering the protein expression profile of the recipient cell by directly binding mRNA or indirectly affecting mRNA via 4E-T and eIF4E (Mittelbrunn et al., 2011; Perez-Hernandez et al., 2013).

4.4 The Effect of a DEF6 Knockout Genotype on the Posttranscriptional Regulation of mRNA in T cells

A Def6$^{-/-}$ phenoptype has previously been described to promote the onset of SLE in C57BL/6 mice as well as causing large vessel vasculitis and rheumatoid arthritis (Fanzo et al., 2006; Chen et al., 2008). Def6$^{-/-}$ CD4^{+} T cells were also described as having a reduced ability to produce IL-2 and IFNγ leading to a reduction in proliferation (Canonigo-Balancio et al., 2009). The production and secretion of interleukins and cytokines is posttranscriptionally regulated by miRNA mediated silencing (Istomine et al., 2016). As a result, a lack of DEF6 expression may result in a dysregulation of miRNA and the ability of miRNA to bind their corresponding mRNA transcripts.

A reduction in DEF6 expression may also affect eIF4E localisation as 4E-T may be free to sequester eIF4E and will not translocate to the IS in response to DEF6 activation by LCK or ITK. A potential effect may be an enrichment of eIF4E within P-bodies as it is sequestered and chaperoned by 4E-T. Consequently, active translation may be absent from the IS leading to a failure to establish a translational polarity in response to TCR engagement.

As Vav1 and DEF6 appear to have a redundant role in terms of their GEF activity and the activation of Cdc42 and Rac1, a DEF6$^{-/-}$ phenotype could potentially highlight a redundancy in terms of mRNA association and 4E-T binding as well. Would Vav1 display mRNP characteristics as well, or perhaps the activation of Cdc42 is critical in terms of vesicular communication with the recipient cell and that role is maintained in the absence of DEF6. A potential effect of a DEF6$^{-/-}$ phenotype may be changes to the contents of exosomes targeted to the recipient APC as Vav1 could continue to activate Cdc42 but a lack of DEF6 would result in the absence or inclusion of unintended mRNA transcripts.

4.5 Conclusions

In conclusion, DEF6 appears to be linked to mRNA turnover and translation in T cells. This novel role may be distinct from the GEF role, or the GEF activity may facilitate any potential activity DEF6 has during mRNA turnover and translation. Moreover, the link to mRNA turnover and translation appears to be in response to an extracellular signal, such as TCR-pMHC and/or LFA-1 and ICAM-1 signalling. The activation of DEF6 in response to this extracellular signal is mediated by LCK and ITK and the two kinases may induce separate DEF6 roles, or may sequentially activate DEF6 to result in efficient localisation and switching between GEF activity, regulation of translation and regulation of mRNA turnover. A schematic representation of the conclusions drawn during this work is shown below in figure 4.4-1.

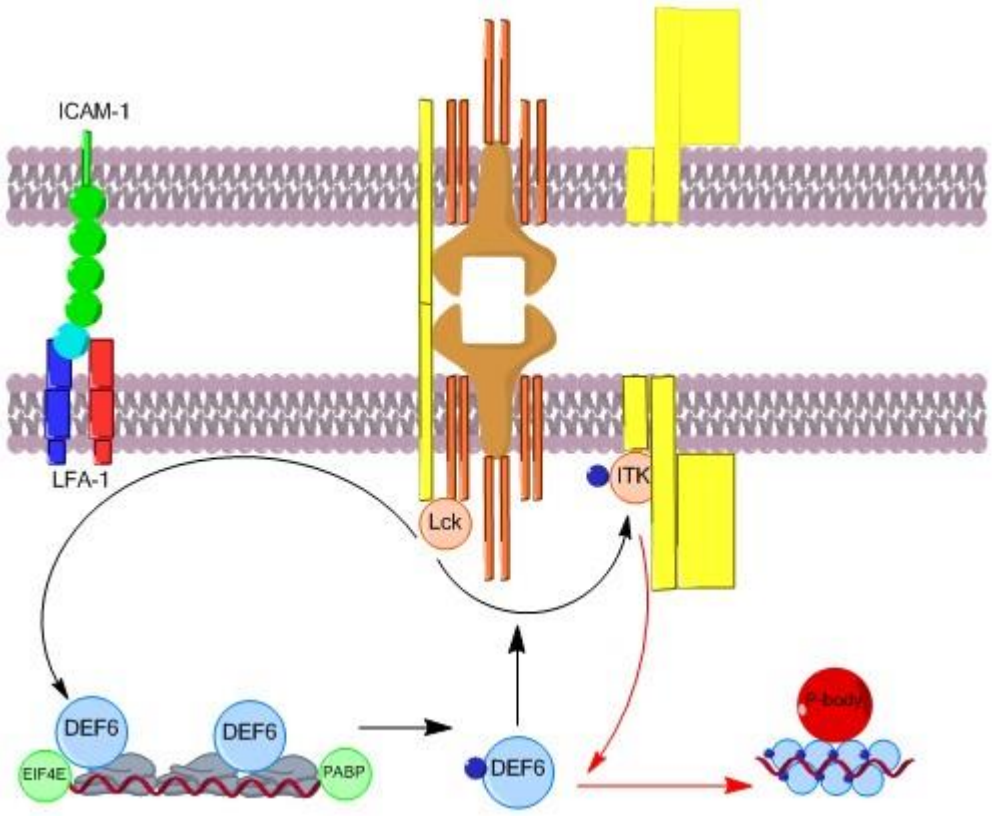

Figure 4.4-1 Proposed role of DEF6 in T cells. DEF6 is in close proximity to active translation, eIF4E and PABP in resting and activated cells. Phosphorylation of DEF6 by LCK in response to antigenic presentation and/or non-specific T cell co-receptor signalling results in DEF6 translocation to the synapse and may possibly chaperone translating complexes to the synapse. Whilst translocating, DEF6 is in close proximity to LFA-1 whose engagement may be the non-specific inside-out signal required for translocation. Finally, phosphorylation of DEF6 by ITK results in aggregation and co-localisation with mRNA and P-bodies and may be involved with miRNA mediated silencing via 4E-T.

Chapter 5 Appendix

5.1 Primary and Secondary Antibodies

Table 5.1-1 List of antibodies used, species of origin and supplier.

Antibody	Host	Clonality	Isotype	Supplier	Cat. Number	Use	Dilution	MW (kDa)
DEF6	Rabbit	Monoclonal (EPR7492)	IgG	Abcam	Rabmab 5619-1	WB IF	1/5000 1/250	74
4e-T	Goat	Polyclonal (N-18)	IgG	Santa Cruz Biotechnology	Sc-13453	IF	1/500	140
PABP	Mouse	Monoclonal (10E10)	IgG1	Santa Cruz Biotechnology	Sc-32318	WB IF	1/1000 1/250	70
Phosphoserine	Mouse	Monoclonal (4A4)	IgG1	Millipore	05-1000	WB	1/2000	Dependent on protein
CD81	Mouse	Monoclonal (5A6)	IgG1	Santa Cruz Biotechnology	Sc-23962	WB IF	1/500 1/250	22-26
Puromycin	Mouse	Monoclonal (12D10)	IgG2a	Millipore	MABE343	IF	1/10,000	
GW182	Mouse	Monoclonal (4B6)	IgG1	Santa Cruz Biotechnology	Sc-56314	IF IP WB	1/100	
T cell receptor	Mouse	Monoclonal (C305)	IgM	Millipore	05-919	Activation	1/100	
Xrn1	Rabbit	Polyclonal	IgG	Abcam	Ab70259	IF	1/200	
DDX6	Rabbit	Polyclonal	IgG	Abcam	Ab40684	IF	1/1000	
eIF4E	Mouse	Monoclonal (P-2)	IgG1	Santa Cruz Biotechnology	Sc-9976	IF		

Antibody	Host	Clonality	Isotype	Supplier	Cat. Number	Use	Dilution	Visual Colour
6x His Tag	Mouse	Monoclonal (HIS.H8)	IgG2b	Abcam	Ab18184	WB	1/1000	
Integrin αL	Mouse	Monoclonal (27)	IgG1	Santa Cruz Biotechnology	Sc-135951	IF		
ICAM-1	Mouse	Monoclonal (15.2)	IgG1	Santa Cruz Biotechnology	Sc-107	IF		
Rabbit IgG (H+L) Alexafluor 568	Goat			Molecular probes	A11011	IF	1/500	Red
Rabbit IgG (H+L) Alexafluor 488	Goat			Molecular probes	A11008	IF	1/500	Green
Mouse IgG (H+L) Alexafluor 488	Goat			Molecular probes	A11001	IF	1/500	Green
Rabbit IgG (H+L) Alexafluor 568	Donkey			Molecular probes	A10042	IF	1/500	Red
Mouse IgG (H+L) Alexafluor 594	Goat			Molecular probes	A11005	IF	1/500	Red
Goat IgG (H+L) Alexafluor 488	Donkey			Molecular probes	A11055	IF	1/500	Green
Rabbit IgG H+L HRP linked	Goat			Cell Signaling Technology	7074	WB	1/2000	

Antibody	Host	Clonality	Isotype	Supplier	Cat. Number	Use	Dilution	MW (kDa)
Mouse IgG H+L HRP linked	Horse			Cell Signaling Technology	7076	WB	1/2000	

5.2 Cell Stains

Table 5.2-1 List of cell stains used and the supplier.

Stain	Supplier	Cat. Number	Use	Dilution
Phalloidin Atto Alexafluor 488	Sigma Aldrich	49409	IF	1/1000
Calcein blue	Life technologies	C1429	IF	1µg/ml

5.3 References

ANDERSON, J. S. J. & PARKER, R. 1998. The 3 ' to 5 ' degradation of yeast mRNAs is a general mechanism for mRNA turnover that requires the SKI2 DEVH box protein and 3 ' to 5 ' exonucleases of the exosome complex. *Embo Journal,* 17**,** 1497-1506.

ANDERSON, P. & KEDERSHA, N. 2002. Visibly stressed: the role of eIF2, TIA-1, and stress granules in protein translation. *Cell Stress & Chaperones,* 7**,** 213-221.

ANDERSON, P. & KEDERSHA, N. 2006. RNA granules. *Journal of Cell Biology,* 172**,** 803-808.

ANDREI, M. A., INGELFINGER, D., HEINTZMANN, R., ACHSEL, T., RIVERA-POMAR, R. & LUHRMANN, R. 2005. A role for eIF4E and eIF4E-transporter in targeting mRNPs to mammalian processing bodies. *Rna-a Publication of the Rna Society,* 11**,** 717-727.

ANGUS, K. L. & GRIFFITHS, G. M. 2013. Cell polarisation and the immunological synapse. *Curr Opin Cell Biol,* 25**,** 85-91.

ARCHER, S. K., SHIROKIKH, N. E., HALLWIRTH, C. V., BEILHARZ, T. H. & PREISS, T. 2015. Probing the closed-loop model of mRNA translation in living cells. *RNA Biol,* 12**,** 248-54.

BACHMANN, M. F., MCKALL-FAIENZA, K., SCHMITS, R., BOUCHARD, D., BEACH, J., SPEISER, D. E., MAK, T. W. & OHASHI, P. S. 1997. Distinct roles for LFA-1 and CD28 during activation of naive T cells: adhesion versus costimulation. *Immunity,* 7**,** 549-57.

BASHKIROV, V. I., SCHERTHAN, H., SOLINGER, J. A., BUERSTEDDE, J. M. & HEYER, W. D. 1997. A mouse cytoplasmic exoribonuclease (mXRN1p) with preference for G4 tetraplex substrates. *Journal of Cell Biology,* 136**,** 761-773.

BASSELL, G. J. & WARREN, S. T. 2008. Fragile X syndrome: loss of local mRNA regulation alters synaptic development and function. *Neuron,* 60**,** 201-14.

BECART, S., BALANCIO, A. J., CHARVET, C., FEAU, S., SEDWICK, C. E. & ALTMAN, A. 2008a. Tyrosine-phosphorylation-dependent translocation of the SLAT protein to the immunological synapse is required for NFAT transcription factor activation. *Immunity,* 29**,** 704-19.

BECART, S., CHARVET, C., BALANCIO, A. J. C., DE TREZ, C., TANAKA, Y., DUAN, W., WARE, C., CROFT, M. & ALTMAN, A. 2007. SLAT regulates Th1 and Th2 inflammatory responses by controlling Ca2+/NFAT signaling. *Journal of Clinical Investigation,* 117**,** 2164-2175.

BECART, S., CHARVET, C., CANONIGO, A. J. & ALTMAN, A. 2008b. Antigen-induced translocation of SLAT to immunological synapse is required for NFAT activation and Th1/Th2 immune responses. *Faseb Journal,* 22.

BECKMANN, B. M., CASTELLO, A. & MEDENBACH, J. 2016. The expanding universe of ribonucleoproteins: of novel RNA-binding proteins and unconventional interactions. *Pflugers Arch,* 468**,** 1029-40.

BECKMANN, B. M., HOROS, R., FISCHER, B., CASTELLO, A., EICHELBAUM, K., ALLEAUME, A. M., SCHWARZL, T., CURK, T.,

FOEHR, S., HUBER, W., KRIJGSVELD, J. & HENTZE, M. W. 2015. The RNA-binding proteomes from yeast to man harbour conserved enigmRBPs. *Nat Commun,* 6**,** 10127.

BILLADEAU, D. D., NOLZ, J. C. & GOMEZ, T. S. 2007. Regulation of T-cell activation by the cytoskeleton. *Nat Rev Immunol,* 7**,** 131-43.

BISWAS, P. S., GUPTA, S., CHANG, E., SONG, L., STIRZAKER, R. A., LIAO, J. K., BHAGAT, G. & PERNIS, A. B. 2010. Phosphorylation of IRF4 by ROCK2 regulates IL-17 and IL-21 production and the development of autoimmunity in mice. *Journal of Clinical Investigation,* 120**,** 3280-3295.

BJUR, E., LARSSON, O., YURCHENKO, E., ZHENG, L., GANDIN, V., TOPISIROVIC, I., LI, S., WAGNER, C. R., SONENBERG, N. & PICCIRILLO, C. A. 2013. Distinct translational control in CD4+ T cell subsets. *PLoS Genet,* 9**,** e1003494.

BLAIR, D. A. & DUSTIN, M. L. 2013. T cell priming goes through a new phase. *Nat Immunol,* 14**,** 311-312.

BUCHAN, J. R. & PARKER, R. 2009. Eukaryotic stress granules: the ins and outs of translation. *Mol Cell,* 36**,** 932-41.

CANONIGO-BALANCIO, A. J., FOS, C., PROD'HOMME, T., BECART, S. & ALTMAN, A. 2009. SLAT/Def6 plays a critical role in the development of Th17 cell-mediated experimental autoimmune encephalomyelitis. *J Immunol,* 183**,** 7259-67.

CHEMIN, K., BOHINEUST, A., DOGNIAUX, S., TOURRET, M., GUEGAN, S., MIRO, F. & HIVROZ, C. 2012. Cytokine secretion by CD4+ T cells at the immunological synapse requires Cdc42-dependent local actin remodeling but not microtubule organizing center polarity. *J Immunol,* 189**,** 2159-68.

CHEN, Q., YANG, W., GUPTA, S., BISWAS, P., SMITH, P., BHAGAT, G. & PERNIS, A. B. 2008. IRF-4-binding protein inhibits interleukin-17 and interleukin-21 production by controlling the activity of IRF-4 transcription factor. *Immunity,* 29**,** 899-911.

COTE, M., FOS, C., CANONIGO-BALANCIO, A. J., LEY, K., BECART, S. & ALTMAN, A. 2015. SLAT promotes TCR-mediated, Rap1-dependent LFA-1 activation and adhesion through interaction of its PH domain with Rap1. *J Cell Sci,* 128**,** 4341-52.

DAVID, A., DOLAN, B. P., HICKMAN, H. D., KNOWLTON, J. J., CLAVARINO, G., PIERRE, P., BENNINK, J. R. & YEWDELL, J. W. 2012. Nuclear translation visualized by ribosome-bound nascent chain puromycylation. *J Cell Biol,* 197**,** 45-57.

DE LA ROCHE, M., RITTER, A. T., ANGUS, K. L., DINSMORE, C., EARNSHAW, C. H., REITER, J. F. & GRIFFITHS, G. M. 2013. Hedgehog signaling controls T cell killing at the immunological synapse. *Science,* 342**,** 1247-50.

DECKER, C. J. & PARKER, R. 2012. P-Bodies and Stress Granules: Possible Roles in the Control of Translation and mRNA Degradation. *Cold Spring Harbor Perspectives in Biology,* 4**,** a012286.

DECKER, C. J., TEIXEIRA, D. & PARKER, R. 2007. Edc3p and a glutamine/asparagine-rich domain of Lsm4p function in processing body assembly in Saccharomyces cerevisiae. *J Cell Biol,* 179**,** 437-49.

DIECKMANN, N. M., FRAZER, G. L., ASANO, Y., STINCHCOMBE, J. C. & GRIFFITHS, G. M. 2016. The cytotoxic T lymphocyte immune synapse at a glance. *J Cell Sci,* 129**,** 2881-6.

DINIC, J., RIEHL, A., ADLER, J. & PARMRYD, I. 2015. The T cell receptor resides in ordered plasma membrane nanodomains that aggregate upon patching of the receptor. *Sci Rep,* 5**,** 10082.

DUSTIN, M. L. 2008. Visualization of Cell-Cell Interaction Contacts-Synapses and Kinapses. *Multichain Immune Recognition Receptor Signaling: From Spatiotemporal Organization to Human Disease,* 640**,** 164-182.

DUSTIN, M. L. 2009. The cellular context of T cell signaling. *Immunity,* 30**,** 482-92.

DUSTIN, M. L. & SPRINGER, T. A. 1989. T-Cell Receptor Cross-Linking Transiently Stimulates Adhesiveness through Lfa-1. *Nature,* 341**,** 619-624.

EULALIO, A., BEHM-ANSMANT, I. & IZAURRALDE, E. 2007a. P bodies: at the crossroads of post-transcriptional pathways. *Nature Reviews Molecular Cell Biology,* 8**,** 9-22.

EULALIO, A., BEHM-ANSMANT, I., SCHWEIZER, D. & IZAURRALDE, E. 2007b. P-body formation is a consequence, not the cause, of RNA-mediated gene silencing. *Molecular and Cellular Biology,* 27**,** 3970-3981.

EULALIO, A., HELMS, S., FRITZSCH, C., FAUSER, M. & IZAURRALDE, E. 2009. A C-terminal silencing domain in GW182 is essential for miRNA function. *RNA,* 15**,** 1067-77.

FANZO, J. C., YANG, W., JANG, S. Y., GUPTA, S., CHEN, Q., SIDDIQ, A., GREENBERG, S. & PERNIS, A. B. 2006. Loss of IRF-4-binding protein leads to the spontaneous development of systemic autoimmunity. *J Clin Invest,* 116**,** 703-14.

FERRAIUOLO, M. A., BASAK, S., DOSTIE, J., MURRAY, E. L., SCHOENBERG, D. R. & SONENBERG, N. 2005. A role for the eIF4E-binding protein 4E-T in P-body formation and mRNA decay. *J Cell Biol,* 170**,** 913-24.

FIUMARA, F., FIORITI, L., KANDEL, E. R. & HENDRICKSON, W. A. 2010. Essential role of coiled coils for aggregation and activity of Q/N-rich prions and PolyQ proteins. *Cell,* 143**,** 1121-35.

FOS, C., BECART, S., CANONIGO BALANCIO, A. J., BOEHNING, D. & ALTMAN, A. 2014. Association of the EF-hand and PH domains of the guanine nucleotide exchange factor SLAT with IP(3) receptor 1 promotes Ca(2)(+) signaling in T cells. *Sci Signal,* 7**,** ra93.

FRIEDL, P. & GUNZER, M. 2001. Interaction of T cells with APCs: the serial encounter model. *Trends in Immunology,* 22**,** 187-191.

GARNEAU, N. L., WILUSZ, J. & WILUSZ, C. J. 2007. The highways and byways of mRNA decay. *Nat Rev Mol Cell Biol,* 8**,** 113-126.

GLADDING, C. M., FITZJOHN, S. M. & MOLNÁR, E. 2009. Metabotropic Glutamate Receptor-Mediated Long-Term Depression: Molecular Mechanisms. *Pharmacological Reviews,* 61**,** 395-412.

GOMEZ, T. S., MCCARNEY, S. D., CARRIZOSA, E., LABNO, C. M., COMISKEY, E. O., NOLZ, J. C., ZHU, P., FREEDMAN, B. D., CLARK, M. R., RAWLINGS, D. J., BILLADEAU, D. D. & BURKHARDT, J. K.

2006. HS1 functions as an essential actin-regulatory adaptor protein at the immune synapse. *Immunity,* 24**,** 741-52.

GUPTA, S., FANZO, J. C., HU, C., COX, D., JANG, S. Y., LEE, A. E., GREENBERG, S. & PERNIS, A. B. 2003a. T cell receptor engagement leads to the recruitment of IBP, a novel guanine nucleotide exchange factor, to the immunological synapse. *J Biol Chem,* 278**,** 43541-9.

GUPTA, S., LEE, A., HU, C., FANZO, J., GOLDBERG, I., CATTORETTI, G. & PERNIS, A. B. 2003b. Molecular cloning of IBP, a SWAP-70 homologous GEF, which is highly expressed in the immune system. *Human Immunology,* 64**,** 389-401.

HELFT, J., JACQUET, A., JONCKER, N. T., GRANDJEAN, I., DOROTHEE, G., KISSENPFENNIG, A., MALISSEN, B., MATZINGER, P. & LANTZ, O. 2008. Antigen-specific T-T interactions regulate CD4 T-cell expansion. *Blood,* 112**,** 1249-58.

HEY, F. 2011. DEF6 is phosphorylated by the TEC-Family Kinase ITK and forms inducible cytoplasmic granules.

HEY, F., CZYZEWICZ, N., JONES, P. & SABLITZKY, F. 2012. DEF6, a novel substrate for the Tec kinase ITK, contains a glutamine-rich aggregation-prone region and forms cytoplasmic granules that co-localize with P-bodies. *J Biol Chem,* 287**,** 31073-84.

HILGERS, V., TEIXEIRA, D. & PARKER, R. 2006. Translation-independent inhibition of mRNA deadenylation during stress in Saccharomyces cerevisiae. *Rna-a Publication of the Rna Society,* 12**,** 1835-1845.

HOTFILDER, M., BAXENDALE, S., CROSS, M. A. & SABLITZKY, F. 1999. Def-2,-3,-6 and-8, novel mouse genes differentially expressed in the haemopoietic system. *British Journal of Haematology,* 106**,** 335-344.

HUPPERTZ, I., ATTIG, J., D'AMBROGIO, A., EASTON, L. E., SIBLEY, C. R., SUGIMOTO, Y., TAJNIK, M., KÖNIG, J. & ULE, J. 2014. iCLIP: Protein–RNA interactions at nucleotide resolution. *Methods,* 65**,** 274-287.

HYNES, R. O. 2002. Integrins: bidirectional, allosteric signaling machines. *Cell,* 110**,** 673-87.

INGELFINGER, D., ARNDT-JOVIN, D. J., LUHRMANN, R. & ACHSEL, T. 2002. The human LSm1-7 proteins colocalize with the mRNA-degrading enzymes Dcp1/2 and Xrnl in distinct cytoplasmic foci. *RNA,* 8**,** 1489-501.

ISGRO, J., GUPTA, S., JACEK, E., PAVRI, T., DUCULAN, R., KIM, M., KIROU, K. A., SALMON, J. E. & PERNIS, A. B. 2013. Enhanced rho-associated protein kinase activation in patients with systemic lupus erythematosus. *Arthritis Rheum,* 65**,** 1592-602.

ISTOMINE, R., PAVEY, N. & PICCIRILLO, C. A. 2016. Posttranscriptional and Translational Control of Gene Regulation in CD4⁺ T Cell Subsets. *The Journal of Immunology,* 196**,** 533.

JACKSON, R. J., HELLEN, C. U. T. & PESTOVA, T. V. 2010. The mechanism of eukaryotic translation initiation and principles of its regulation. *Nat Rev Mol Cell Biol,* 11**,** 113-127.

JAIN, S. & PARKER, R. 2013. The discovery and analysis of P Bodies. *Adv Exp Med Biol,* 768**,** 23-43.

JIANG, S., LI, C., OLIVE, V., LYKKEN, E., FENG, F., SEVILLA, J., WAN, Y., HE, L. & LI, Q.-J. 2011. Molecular dissection of the miR-17-92 cluster's critical dual roles in promoting Th1 responses and preventing inducible Treg differentiation. *Blood,* 118**,** 5487.

JIMENEZ, A., CARRASCO, L. & VAZQUEZ, D. 1977. Enzymic and nonenzymic translocation by yeast polysomes. Site of action of a number of inhibitors. *Biochemistry,* 16**,** 4727-30.

KAFASLA, P., SKLIRIS, A. & KONTOYIANNIS, D. L. 2014. Post-transcriptional coordination of immunological responses by RNA-binding proteins. *Nat Immunol,* 15**,** 492-502.

KAHVEJIAN, A., ROY, G. & SONENBERG, N. 2001. The mRNA closed-loop model: the function of PABP and PABP-interacting proteins in mRNA translation. *Cold Spring Harb Symp Quant Biol,* 66**,** 293-300.

KAIZUKA, Y., DOUGLASS, A. D., VARMA, R., DUSTIN, M. L. & VALE, R. D. 2007. Mechanisms for segregating T cell receptor and adhesion molecules during immunological synapse formation in Jurkat T cells. *Proc Natl Acad Sci U S A,* 104**,** 20296-301.

KAMENSKA, A., LU, W. T., KUBACKA, D., BROOMHEAD, H., MINSHALL, N., BUSHELL, M. & STANDART, N. 2014. Human 4E-T represses translation of bound mRNAs and enhances microRNA-mediated silencing. *Nucleic Acids Res,* 42**,** 3298-313.

KATO, M., HAN, T. W., XIE, S., SHI, K., DU, X., WU, L. C., MIRZAEI, H., GOLDSMITH, E. J., LONGGOOD, J., PEI, J., GRISHIN, N. V., FRANTZ, D. E., SCHNEIDER, J. W., CHEN, S., LI, L., SAWAYA, M. R., EISENBERG, D., TYCKO, R. & MCKNIGHT, S. L. 2012. Cell-free formation of RNA granules: low complexity sequence domains form dynamic fibers within hydrogels. *Cell,* 149**,** 753-67.

KAWAKAMI, A., TIAN, Q., DUAN, X., STREULI, M., SCHLOSSMAN, S. F. & ANDERSON, P. 1992. Identification and functional characterization of a TIA-1-related nucleolysin. *Proc Natl Acad Sci U S A,* 89**,** 8681-5.

KEDERSHA, N. & ANDERSON, P. 2002. Stress granules: sites of mRNA triage that regulate mRNA stability and translatability. *Biochemical Society Transactions,* 30**,** 963-969.

KEDERSHA, N., CHO, M. R., LI, W., YACONO, P. W., CHEN, S., GILKS, N., GOLAN, D. E. & ANDERSON, P. 2000. Dynamic shuttling of TIA-1 accompanies the recruitment of mRNA to mammalian stress granules. *Journal of Cell Biology,* 151**,** 1257-1268.

KEDERSHA, N. L., GUPTA, M., MILLER, I. J., STREULI, M. & ANDERSON, P. 1999. Phosphorylation of eIF-2 alpha promotes the recruitment of untranslated mRNAs to TIA-1/R+ stress granules. *Molecular Biology of the Cell,* 10**,** 293a-293a.

KIM, S. T., SHIN, Y., BRAZIN, K., MALLIS, R. J., SUN, Z. Y., WAGNER, G., LANG, M. J. & REINHERZ, E. L. 2012. TCR Mechanobiology: Torques and Tunable Structures Linked to Early T Cell Signaling. *Front Immunol,* 3**,** 76.

LARIMER, F. W., HSU, C. L., MAUPIN, M. K. & STEVENS, A. 1992. Characterization of the XRN1 gene encoding a 5'-->3' exoribonuclease: sequence data and analysis of disparate protein and mRNA levels of gene-disrupted yeast cells. *Gene,* 120**,** 51-7.

LEVY, S. & SHOHAM, T. 2005. The tetraspanin web modulates immune-signalling complexes. *Nat Rev Immunol,* 5**,** 136-48.

LI, Z., WU, F., BRANT, S. R. & KWON, J. H. 2011. IL-23 Receptor Regulation by Let-7f in Human CD4⁺ Memory T Cells. *The Journal of Immunology,* 186**,** 6182.

MA, F., LIU, X., LI, D., WANG, P., LI, N., LU, L. & CAO, X. 2010. MicroRNA-466l Upregulates IL-10 Expression in TLR-Triggered Macrophages by Antagonizing RNA-Binding Protein Tristetraprolin-Mediated IL-10 mRNA Degradation. *The Journal of Immunology,* 184**,** 6053.

MASAT, L., CALDWELL, J., ARMSTRONG, R., KHOSHNEVISAN, H., JESSBERGER, R., HERNDIER, B., WABL, M. & FERRICK, D. 2000. Association of SWAP-70 with the B cell antigen receptor complex. *Proc. Natl. Acad. Sci. USA,* 97**,** 2180-4.

MAVRAKIS, K. J., MCKINLAY, K. J., JONES, P. & SABLITZKY, F. 2004. DEF6, a novel PH-DH-like domain protein, is an upstream activator of the Rho GTPases Rac1, Cdc42, and RhoA. *Exp Cell Res,* 294**,** 335-44.

MICHELITSCH, M. D. & WEISSMAN, J. S. 2000. A census of glutamine/asparagine-rich regions: Implications for their conserved function and the prediction of novel prions. *Proceedings of the National Academy of Sciences of the United States of America,* 97**,** 11910-11915.

MITTELBRUNN, M., GUTIERREZ-VAZQUEZ, C., VILLARROYA-BELTRI, C., GONZALEZ, S., SANCHEZ-CABO, F., GONZALEZ, M. A., BERNAD, A. & SANCHEZ-MADRID, F. 2011. Unidirectional transfer of microRNA-loaded exosomes from T cells to antigen-presenting cells. *Nat Commun,* 2**,** 282.

MOLLETT, E. 2014. A study of DEF6 granule formation using biophysical and cellular methods.

MORETTI, S., ARMOUGOM, F., WALLACE, I. M., HIGGINS, D. G., JONGENEEL, C. V. & NOTREDAME, C. 2007. The M-Coffee web server: a meta-method for computing multiple sequence alignments by combining alternative alignment methods. *Nucleic Acids Research,* 35**,** W645-W648.

MUHLRAD, D., DECKER, C. J. & PARKER, R. 1994. Deadenylation of the unstable mRNA encoded by the yeast MFA2 gene leads to decapping followed by 5'-->3' digestion of the transcript. *Genes Dev,* 8**,** 855-66.

MULLER, W. A. 2013. Getting Leukocytes to the Site of Inflammation. *Veterinary pathology,* 50**,** 7-22.

MURUGAIYAN, G., DA CUNHA, A. P., AJAY, A. K., JOLLER, N., GARO, L. P., KUMARADEVAN, S., YOSEF, N., VAIDYA, V. S. & WEINER, H. L. 2015. MicroRNA-21 promotes Th17 differentiation and mediates experimental autoimmune encephalomyelitis. *J Clin Invest,* 125**,** 1069-80.

NISHIKIMI, A., ISHIHARA, S., OZAWA, M., ETOH, K., FUKUDA, M., KINASHI, T. & KATAGIRI, K. 2014. Rab13 acts downstream of the kinase Mst1 to deliver the integrin LFA-1 to the cell surface for lymphocyte trafficking. *Sci Signal,* 7**,** ra72.

NISHIMURA, T., PADAMSI, Z., FAKIM, H., MILETTE, S., DUNHAM, W. H., GINGRAS, A. C. & FABIAN, M. R. 2015. The eIF4E-Binding Protein

4E-T Is a Component of the mRNA Decay Machinery that Bridges the 5' and 3' Termini of Target mRNAs. *Cell Rep,* 11**,** 1425-36.

NISWENDER, C. M. & CONN, P. J. 2010. Metabotropic Glutamate Receptors: Physiology, Pharmacology, and Disease. *Annual review of pharmacology and toxicology,* 50**,** 295-322.

NOLZ, J. C., GOMEZ, T. S., ZHU, P., LI, S., MEDEIROS, R. B., SHIMIZU, Y., BURKHARDT, J. K., FREEDMAN, B. D. & BILLADEAU, D. D. 2006. The WAVE2 complex regulates actin cytoskeletal reorganization and CRAC-mediated calcium entry during T cell activation. *Curr Biol,* 16**,** 24-34.

NOTREDAME, C., HIGGINS, D. G. & HERINGA, J. 2000. T-coffee: a novel method for fast and accurate multiple sequence alignment1. *Journal of Molecular Biology,* 302**,** 205-217.

OKOYE, I. S., COOMES, S. M., PELLY, V. S., CZIESO, S., PAPAYANNOPOULOS, V., TOLMACHOVA, T., SEABRA, M. C. & WILSON, M. S. 2014. MicroRNA-containing T-regulatory-cell-derived exosomes suppress pathogenic T helper 1 cells. *Immunity,* 41**,** 89-103.

PEREZ-HERNANDEZ, D., GUTIERREZ-VAZQUEZ, C., JORGE, I., LOPEZ-MARTIN, S., URSA, A., SANCHEZ-MADRID, F., VAZQUEZ, J. & YANEZ-MO, M. 2013. The intracellular interactome of tetraspanin-enriched microdomains reveals their function as sorting machineries toward exosomes. *J Biol Chem,* 288**,** 11649-61.

ROCHA-PERUGINI, V., ZAMAI, M., GONZALEZ-GRANADO, J. M., BARREIRO, O., TEJERA, E., YANEZ-MO, M., CAIOLFA, V. R. & SANCHEZ-MADRID, F. 2013. CD81 controls sustained T cell activation signaling and defines the maturation stages of cognate immunological synapses. *Mol Cell Biol,* 33**,** 3644-58.

ROLLAND, T., TASAN, M., CHARLOTEAUX, B., PEVZNER, S. J., ZHONG, Q., SAHNI, N., YI, S., LEMMENS, I., FONTANILLO, C., MOSCA, R., KAMBUROV, A., GHIASSIAN, S. D., YANG, X., GHAMSARI, L., BALCHA, D., BEGG, B. E., BRAUN, P., BREHME, M., BROLY, M. P., CARVUNIS, A. R., CONVERY-ZUPAN, D., COROMINAS, R., COULOMBE-HUNTINGTON, J., DANN, E., DREZE, M., DRICOT, A., FAN, C., FRANZOSA, E., GEBREAB, F., GUTIERREZ, B. J., HARDY, M. F., JIN, M., KANG, S., KIROS, R., LIN, G. N., LUCK, K., MACWILLIAMS, A., MENCHE, J., MURRAY, R. R., PALAGI, A., POULIN, M. M., RAMBOUT, X., RASLA, J., REICHERT, P., ROMERO, V., RUYSSINCK, E., SAHALIE, J. M., SCHOLZ, A., SHAH, A. A., SHARMA, A., SHEN, Y., SPIROHN, K., TAM, S., TEJEDA, A. O., TRIGG, S. A., TWIZERE, J. C., VEGA, K., WALSH, J., CUSICK, M. E., XIA, Y., BARABASI, A. L., IAKOUCHEVA, L. M., ALOY, P., DE LAS RIVAS, J., TAVERNIER, J., CALDERWOOD, M. A., HILL, D. E., HAO, T., ROTH, F. P. & VIDAL, M. 2014. A proteome-scale map of the human interactome network. *Cell,* 159**,** 1212-26.

SAGE, P. T., VARGHESE, L. M., MARTINELLI, R., SCIUTO, T. E., KAMEI, M., DVORAK, A. M., SPRINGER, T. A., SHARPE, A. H. & CARMAN, C. V. 2012. Antigen Recognition Is Facilitated by Invadosome-like Protrusions Formed by Memory/Effector T Cells. *Journal of Immunology,* 188**,** 3686-3699.

SAMSON, T., WILL, C., KNOBLAUCH, A., SHAREK, L., VON DER MARK, K., BURRIDGE, K. & WIXLER, V. 2007. Def-6, a guanine nucleotide exchange factor for Rac1, interacts with the skeletal muscle integrin chain alpha7A and influences myoblast differentiation. *J Biol Chem,* 282**,** 15730-42.

SCHINDELIN, J., ARGANDA-CARRERAS, I., FRISE, E., KAYNIG, V., LONGAIR, M., PIETZSCH, T., PREIBISCH, S., RUEDEN, C., SAALFELD, S., SCHMID, B., TINEVEZ, J. Y., WHITE, D. J., HARTENSTEIN, V., ELICEIRI, K., TOMANCAK, P. & CARDONA, A. 2012. Fiji: an open-source platform for biological-image analysis. *Nat Methods,* 9**,** 676-82.

SHETH, U. & PARKER, R. 2003. Decapping and decay of messenger RNA occur in cytoplasmic processing bodies. *Science,* 300**,** 805-808.

SHETH, U. & PARKER, R. 2006. Targeting of aberrant mRNAs to cytoplasmic processing bodies. *Cell,* 125**,** 1095-1109.

SHIMIZU, Y., NEWMAN, W., GOPAL, T. V., HORGAN, K. J., GRABER, N., BEALL, L. D., VAN SEVENTER, G. A. & SHAW, S. 1991. Four molecular pathways of T cell adhesion to endothelial cells: roles of LFA-1, VCAM-1, and ELAM-1 and changes in pathway hierarchy under different activation conditions. *J Cell Biol,* 113**,** 1203-12.

SINGLETON, K. L., GOSH, M., DANDEKAR, R. D., AU-YEUNG, B. B., KSIONDA, O., TYBULEWICZ, V. L., ALTMAN, A., FOWELL, D. J. & WULFING, C. 2011. Itk controls the spatiotemporal organization of T cell activation. *Sci Signal,* 4**,** ra66.

SOARES, H., HENRIQUES, R., SACHSE, M., VENTIMIGLIA, L., ALONSO, M. A., ZIMMER, C., THOULOUZE, M. I. & ALCOVER, A. 2013. Regulated vesicle fusion generates signaling nanoterritories that control T cell activation at the immunological synapse. *J Exp Med,* 210**,** 2415-33.

SODERBERG, O., GULLBERG, M., JARVIUS, M., RIDDERSTRALE, K., LEUCHOWIUS, K. J., JARVIUS, J., WESTER, K., HYDBRING, P., BAHRAM, F., LARSSON, L. G. & LANDEGREN, U. 2006. Direct observation of individual endogenous protein complexes in situ by proximity ligation. *Nat Methods,* 3**,** 995-1000.

STEWART, M. P., CABANAS, C. & HOGG, N. 1996. T cell adhesion to intercellular adhesion molecule-1 (ICAM-1) is controlled by cell spreading and the activation of integrin LFA-1. *J Immunol,* 156**,** 1810-7.

SUN, C., MOLINEROS, J. E., LOOGER, L. L., ZHOU, X. J., KIM, K., OKADA, Y., MA, J., QI, Y. Y., KIM-HOWARD, X., MOTGHARE, P., BHATTARAI, K., ADLER, A., BANG, S. Y., LEE, H. S., KIM, T. H., KANG, Y. M., SUH, C. H., CHUNG, W. T., PARK, Y. B., CHOE, J. Y., SHIM, S. C., KOCHI, Y., SUZUKI, A., KUBO, M., SUMIDA, T., YAMAMOTO, K., LEE, S. S., KIM, Y. J., HAN, B. G., DOZMOROV, M., KAUFMAN, K. M., WREN, J. D., HARLEY, J. B., SHEN, N., CHUA, K. H., ZHANG, H., BAE, S. C. & NATH, S. K. 2016. High-density genotyping of immune-related loci identifies new SLE risk variants in individuals with Asian ancestry. *Nat Genet*.

TANAKA, Y., BI, K., KITAMURA, R., HONG, S. J., ALTMAN, Y., MATSUMOTO, A., TABATA, H., LEBEDEVA, S., BUSHWAY, P. J. & ALTMAN, A. 2003. SWAP-70-like adapter of T cells, an adapter protein

that regulates early TCR-initiated signaling in Th2 lineage cells. *Immunity,* 18**,** 403-414.

TEIXEIRA, D., SHETH, U., VALENCIA-SANCHEZ, M. A., BRENGUES, M. & PARKER, R. 2005. Processing bodies require RNA for assembly and contain nontranslating mRNAs. *Rna-a Publication of the Rna Society,* 11**,** 371-382.

TERRIBILINI, M., SANDER, J. D., LEE, J.-H., ZABACK, P., JERNIGAN, R. L., HONAVAR, V. & DOBBS, D. 2007. RNABindR: a server for analyzing and predicting RNA-binding sites in proteins. *Nucleic Acids Research,* 35**,** W578-W584.

TIAN, Q., STREULI, M., SAITO, H., SCHLOSSMAN, S. F. & ANDERSON, P. 1991. A polyadenylate binding protein localized to the granules of cytolytic lymphocytes induces DNA fragmentation in target cells. *Cell,* 67**,** 629-39.

TYBULEWICZ, V. L. 2005. Vav-family proteins in T-cell signalling. *Current Opinion in Immunology,* 17**,** 267-274.

TYBULEWICZ, V. L. & HENDERSON, R. B. 2009. Rho family GTPases and their regulators in lymphocytes. *Nat Rev Immunol,* 9**,** 630-44.

UCHIUMI, T., TERAO, K. & OGATA, K. 1980. Identification of neighboring protein pairs in rat liver 60S ribosomal subunits cross-linked with dimethyl suberimidate or dimethyl 3,3'-dithiobispropionimidate. *J Biochem,* 88**,** 1033-44.

VALITUTTI, S., DESSING, M., AKTORIES, K., GALLATI, H. & LANZAVECCHIA, A. 1995. Sustained signaling leading to T cell activation results from prolonged T cell receptor occupancy. Role of T cell actin cytoskeleton. *J Exp Med,* 181**,** 577-84.

VAN DIJK, E., COUGOT, N., MEYER, S., BABAJKO, S., WAHLE, E. & SERAPHIN, B. 2002. Human Dcp2: a catalytically active mRNA decapping enzyme located in specific cytoplasmic structures. *EMBO J,* 21**,** 6915-24.

WALLACE, I. M., O'SULLIVAN, O., HIGGINS, D. G. & NOTREDAME, C. 2006. M-Coffee: combining multiple sequence alignment methods with T-Coffee. *Nucleic Acids Research,* 34**,** 1692-1699.

WELLS, S. E., HILLNER, P. E., VALE, R. D. & SACHS, A. B. 1998. Circularization of mRNA by eukaryotic translation initiation factors. *Mol Cell,* 2**,** 135-40.

YANEZ-MO, M., BARREIRO, O., GORDON-ALONSO, M., SALA-VALDES, M. & SANCHEZ-MADRID, F. 2009. Tetraspanin-enriched microdomains: a functional unit in cell plasma membranes. *Trends Cell Biol,* 19**,** 434-46.

YI, J., WU, X. F. S., CRITES, T. & HAMMER, J. A. 2012. Actin retrograde flow and actomyosin II arc contraction drive receptor cluster dynamics at the immunological synapse in Jurkat T cells. *Molecular Biology of the Cell,* 23**,** 834-852.

ZEHN, D. & BEVAN, M. J. 2006. T cells with low avidity for a tissue-restricted antigen routinely evade central and peripheral tolerance and cause autoimmunity. *Immunity,* 25**,** 261-270.

ZENG, R., CANNON, J. L., ABRAHAM, R. T., WAY, M., BILLADEAU, D. D., BUBECK-WARDENBERG, J. & BURKHARDT, J. K. 2003. SLP-76 coordinates Nck-dependent Wiskott-Aldrich syndrome protein

recruitment with Vav-1/Cdc42-dependent Wiskott-Aldrich syndrome protein activation at the T cell-APC contact site. *J Immunol,* 171**,** 1360-8.